To the Graduate Council:

I am submitting herewith a dissertation written by Jack Douglas Galloway entitled “Boiling Water Reactor Core Simulation with Generalized Isotopic Inventory Tracking for Actinide Management” I have examined the final electronic copy of this dissertation for form and content and recommend that it be accepted in partial fulfillment of the requirements for the degree of Doctor of Philosophy, with a major in Nuclear Engineering.

G. Ivan Maldonado, Major Professor

We have read this dissertation
and recommend its acceptance:

Kevin T. Clarno

Lee L. Riedinger

Arthur E. Ruggles

Accepted for the Council:

Carolyn R. Hodges
Vice Provost and Dean of the Graduate School

(Original signatures are on file with official student records.)

Boiling Water Reactor Core Simulation with Generalized Isotopic Inventory Tracking for Actinide Management

A Dissertation Presented for
the Doctor of Philosophy
Degree
The University of Tennessee, Knoxville

Jack 5ƻʣƎʈl·ǎ Galloway
August 2010

Acknowledgments

In this short space I would like to thank all the people who have worked to be a support to me throughout this endeavor. First off, I would like to thank my advisor Dr. G. Ivan Maldonado, who years ago pursued and encouraged me to enroll in graduate school and who has been an invaluable technical advisor as well as friend through these years.

The number of people who have served as encouragements, technical support, and fellowship are too numerous to mention, but those who have stood out will be mentioned. Dr. Matthew Jessee as both friend and technical mentor, Dr. Kevin Clarno who is also serving on my committee, Dr. Ian Gauld who always had his door open to help, David Dixon who's friendship has been a joy for years, Hermilo Hernandez, the number of collaborators at Oak Ridge National Laboratory who have worked to keep me both funded and serving on a truly enjoyable project. In addition I would like to thank Julie and Jon, my sister and brother, for their emotional support and encouragement. I want to thank my wife, Becky, for the support and encouragement she has provided throughout this journey. As I look at the people who have surrounded me and been my support through these years I am both humbled and thankful.

The most influential people in my life are my parents Gary and Jennie Galloway. I am so thankful for Mom's constant encouragement and affirming words. I also thank my Dad; as a mentor in Christ, as a Father figure, as a nuclear engineer. I only hope I can garner the respect of my peers in technical prowess and more importantly in strength of character and humility that he has over his years as a nuclear engineer.

Finally, and most importantly, I want to thank Christ Jesus, to whom I gave my life over to many years ago, and who has never failed. As I look back through this journey, I see how He has fulfilled his promise to never leave; especially in the most difficult times. May this document serve as a witness to me and those who read, testifying to Christ's faithfulness.

Abstract

The computational ability to accurately simulate boiling water reactor operation under the full range of standard steady-state operation, along with the capability to fully track the isotopic distribution of any fueled region in any location in the core has been developed. This new three-dimensional node-by-node capability can help designers track, for example, a full suite of minor and major actinides, fission products, and even light elements that result from depletion, decay, or transmutations. This isotopic tracking capability is not restricted to BWRs and can be employed in the modeling of PWRs, CANDUs, and other reactor types that can be modeled with the NESTLE code, the base core simulator employed in this research.

To accurately simulate boiling water reactor operation, a major thermal-hydraulics upgrade was performed which involved the implementation of a drift-flux solution scheme to model steady-state boiling water flow. Sub-cooled boiling and bulk boiling are accurately modeled and a scheme for computing the correct flow distribution has been implemented. In addition, the incorporation of a nodal ORIGEN-based microscopic depletion solution has been included which allows for exceptional detail in tracking a large number of elements in every node of a core design, thus accounting for spectral dependencies such as moderator density effects, moderator temperature effects, fuel temperature effects, as well as controlled or uncontrolled conditions.

The results of this study show the excellent fidelity of the two-phase solution for accurately predicting the boiling of water when compared to experimental results. Likewise, the isotopic inventory results show near-identical agreement with the well-established and validated ORIGEN-based SCALE/TRITON isotopic depletion sequence. The aim of these developments is to eventually produce a publicly available three-dimensional core simulator capable of assessing detailed isotopic inventories, a capability particularly valuable for the evaluation of recycling scenarios and actinide management in a variety of reactor types and fuel designs.

Table of Contents

List of Figures

List of Tables

Abbreviations and Symbols

BOC	Beginning of cycle
BWR	Boiling water reactor
CFD	Computational fluid dynamics
CPR	Critical power ratio
CPU	Central processing unit
DRBL	Diskless remote boot Linux
EOC	End of cycle
EPRI	Electric power research institute
GWD	Giga-watt days
LWR	Light water reactor
MOC	Middle of cycle
MOX	Mixed-oxide fuel
MTU	Metric ton of uranium
NRC	Nuclear regulatory commission
OECD	Organization for economic cooperation and development
PWR	Pressurized water reactor
SDM	Shutdown margin
SNF	Spent nuclear fuel
T2N	Triton to NESTLE
TIP	Travelling in-core probe
X_{nvg}	Quality of net vapor generation
G	Mass flux
A_x	Cross-sectional area
k_∞	k-infinity
k_{eff}	k-effective
α	Void fraction
ρ	Density
ϕ	Flux
u	Internal energy

1 Introduction

1.1 Background

While nuclear energy continues to prove to be a major player as an electricity source in the world and in the United States, one of the main outstanding controversies in public perception continues to be the handling of spent nuclear fuel, often referred to as nuclear *waste* despite the fact it is generally an untapped and valuable resource. Accordingly, several options to deal with spent nuclear fuel have been proposed ranging from full recycling, to separations and recycling of certain components, to long-term storage of all constituents. Most recently, however, multi-billion dollar efforts originally directed toward the long-term storage of US nuclear waste in facilities such as Yucca Mountain have apparently dwindled to a halt while the current administration and the US Department of Energy devise a new strategy toward nuclear waste disposal. In principle, this change in direction promotes a more careful evaluation of recycling options.

When discussing potential recycling scenarios, much effort has been put forth recently into recycling in fast reactors, while there has been a less concerted effort invested into the potential of using the existing fleet of light water reactors (LWRs) as drivers for recycling of spent fuel waste components. The main underlying assumption is that higher energy (fast) neutrons are more efficient at transmuting a larger variety of transuranic isotopes. However, in practice, operating fast reactors do not exist in the US and the likelihood of such facilities being built anytime soon is quite low and surrounded by large uncertainties. Meanwhile, our country successfully operates 104 LWRs that could realistically be employed to help mitigate some of the problems associated with nuclear waste.

As seen in Figure 1.1, in the 1 to 100 year time frame after the discharge of spent fuel, fission product activity is the dominating contributor to heat generation and radiotoxicity from spent fuel while the contribution due to actinide decay becomes the dominating contributor during the 100 to 1000 year period and beyond. The greatest contributor to actinide activity during this 100 to 1000 year time frame is americium-241 (^{241}Am).

Several options exist for managing fission products, given their relatively short half-lives in comparison to those of the actinides, separation and storage can be an adequate path. Alternatively, transmutation in fast reactors has also been proposed. Likewise, dealing with plutonium isotopes via recycling in thermal or fast reactors or as mixed oxide (MOX) fuel are technically mature areas in which much research has been invested over the years.

Among several objectives, this project originated by proposing the incineration of the most active and long-lived minor actinide, ^{241}Am, by employing the existing fleet of operating boiling water reactors (BWRs). One of the underlying hypotheses was to try to exploit the significant boiling in the upper region of a BWR core. Although a BWR exhibits a standard thermal neutron spectrum in the lower portion of the core, it promotes a harder neutron spectrum in the upper region of the core. This spectral shift could potentially be utilized to preferentially load americium or other actinides at the appropriate axial levels for optimum spectral utilization for incineration.

Accordingly, via collaboration with the Westinghouse Electric Co., this research project provides substantial proof-of-principle of the ability to efficiently incinerate recycled minor actinides such as ^{241}Am (as heterogeneous targets) in a BWR by employing commercial-grade three-dimensional (3-D) core design simulation tools for the analysis. This first-of-its-kind study is described in detail in Chapter 2.

Next, while in the process of assessing available tools and their various constraints, this project also addresses a major hurdle encountered while evaluating the viability of recycling scenarios in a BWR, which is the lack of available 3-D BWR core simulation codes with the capability to provide detailed isotopic information for a wide variety of isotopes, including the

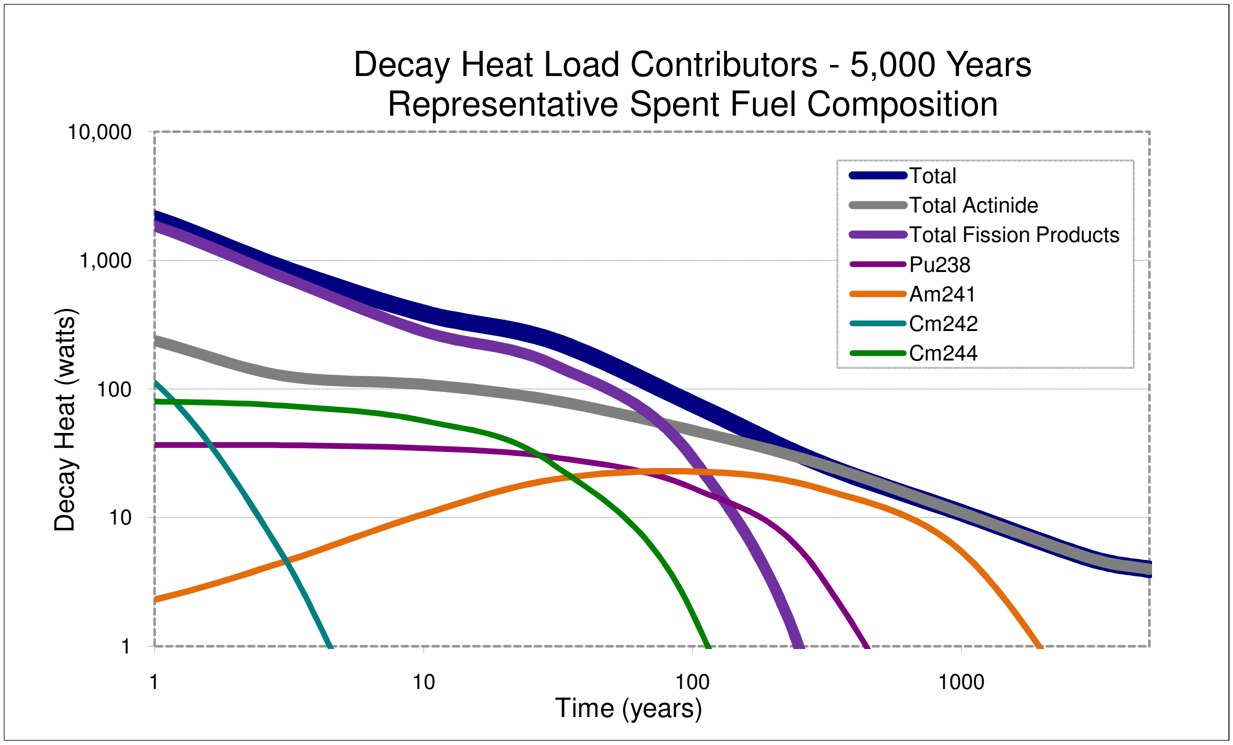

Figure 1.1 Contribution to Heat Load in Spent Nuclear Fuel

full suite of transuranics: neptunium, plutonium, americium, curium, and potentially any of the higher trace elements as well as detailed fission products. In fact, the typical core simulators available for performing such a study tend to contain a very limited output of isotopic information only reporting a select number of plutonium, neptunium and americium isotopes (with no curium isotopes generally available or tracked) as well as typically lumping fission products. Due to the lack of a viable tool for this type of analysis, the development of software capable of modeling a BWR while also tracking a complete description of node-by-node isotopics became the major focus of this project following the proof of principle studies.

Through collaboration with North Carolina State University and under sponsorship by Oak Ridge National Laboratory this project also became linked to the integration of the NESTLE 3-D PWR core simulation software [34] to the SCALE/TRITON lattice physics and core depletion sequences [21] In fact, this collaboration provided a perfect platform to pursue the development of a BWR simulator, and to ultimately seek its integration to the world-renowned ORIGEN depletion capabilities on a node-by-node basis. This work required two major components: First, the development of a thermal-hydraulic module capable of capturing sub-cooled void fraction, as well as accurately modeling the void fraction in the bulk boiling phase. Secondly, the implementation of a scheme for tracking a wide number of isotopes on a nodal basis, within the scope of a "traditional" 3-D core simulator.

The thermal-hydraulic developments to upgrade the NESTLE code from a reliable pressurized water reactor (PWR) simulator to a BWR simulator are discussed in Chapters 3, while the validation of the BWR simulator is presented in Chapter 4. Finally, the work related to the integration of NESTLE to ORIGEN is discussed in Chapter 5.

1.2 Literature Review

1.2.1 Transmutation

For several decades the nuclear industry in the United States has marched forward with the expectation that the spent nuclear fuel, which is currently stored on-site at power plant locations, would end up permanently stored in the Yucca Mountain nuclear waste disposal site which, until recently, was still under construction. Due to a combination of political struggles, environmental concerns, and the potential for recovering energy from the spent nuclear fuel, this expectation has been waning somewhat. Due to this, the investigations of alternate routes for handling spent nuclear fuel have gained momentum in recent times. Therefore, understanding the details of transmutation environments continues to be of growing importance, including but not restricted to fast reactors, thermal reactors and sub-critical accelerator driven transmutation.

While researching the literature surrounding actinide transmutation, several studies were found assessing the viability of actinide transmutation using both LWRs and fast reactors. The majority of these studies focused on point-reactor models or two-dimensional simulations performed with codes akin to lattice-physics codes, or by using MCNP based simulations. These studies have been beneficial for determining which isotopes are well suited for incineration in a fast spectrum and which are well suited to incineration in a thermal spectrum, but leave significant uncertainties surrounding the viability of in-core and multi-cycle fuel management and the practical implementation within modern day LWRs. Not surprisingly, for a number of valid reasons, it was also observed that there is a strong research base in this area from outside the United States, although several excellent resources were found originating in the U.S.

According to Varaine and Zaetta [35] recycling in LWRs is a possibility for a limited number of isotopes, due to the thermal cross-sections of various actinides. However, this study was confined to studying PWR transmutation models, and the spectral shift characteristic of a BWR was not investigated. Promising results were obtained and a feasibility study for actinide transmutation was based in France, where the PWR is the nuclear reactor of choice, and where France has been a leader in separations and transmutation of mixed-oxide (MOX) fuels for decades. Irrelevant of the background, that research illustrated that thermal reactor transmutation is technically feasible in PWRs, while the effects in BWRs and via 3-D nuclear fuel management evaluations were not part of that study.

Considerable experience exists in the recycling of plutonium in LWRs, primarily in Europe and Japan. In the United States, the recycle of weapons-grade material into LWRs in the form of MOX fuel is planned and lead-test assemblies with MOX fuel have been loaded in the Duke Power Catawba nuclear reactor. Thus, the use of MOX fuel for burning plutonium has been demonstrated. The introduction of other actinides such as Np, Am, and Cm into LWR fuel, however, has not yet been established and presents several challenges in manufacturing, handling, and transportation aspects in addition to impacts upon reactor performance.

Several studies have been performed to evaluate homogeneous and heterogeneous recycling options. Much of that work is well summarized in a compendium report by Taiwo and Hill [33] which provides additional references to a number of detailed reports on the CORAIL, CONFU, Inert-Matrix, and various other heterogeneous and homogenous recycling strategies. The research performed so far provides an excellent overview of the potential of LWR recycling strategies. Most of the prior research, however, does not typically include full-core analyses and does not focus upon BWRs, which are key emphases of the research herein reported, in particular research which pertains to americium-spiked lattices and bundles.

With regard to the potential for using BWRs in this capacity, as it was earlier shown by Erighin and Maldonado [7] with the MCNP and MONTEBURNS codes, François and Guzman [9] have shown some promising studies at the lattice level, using the lattice physics code HELIOS with the intention of developing a fuel design intended to use minor actinide loading to supplant traditional burnable absorbers. Clearly observed in these research studies is that the behavior of k_∞ as a function of burnup is dramatically different relative to the typical behavior seen in a lattice loaded with gadolinium as the burnable absorber, the beginning of life reactivity is much higher due to the significant differences in thermal absorption cross-sections. Despite these differences, the potential to incinerate long-lived actinides was illustrated. However, the next step of accommodating actinide loaded bundles into core loading patterns and the impact on core behavior needs to be understood. Likewise, it is important to note that while these prior studies showed promise at the lattice level, they lacked a comprehensive tool to study the impact upon core-wide thermal and reactivity limits as well as the corresponding 3-D transmutation effects.

Similarly, Hernandez and Maldonado [14] and [15] have demonstrated success in designing BWR lattices and tools for optimizing actinide transmutation. However, the process of optimizing fuel bundles and core reload designs for actinide transmutation, while satisfying operational constraints is still a non-existent capability. Additionally, Raitses, et al. [26] have also performed studies pertaining to the feasibility of using BWRs as transmutation drivers; among other things investigating the effect that void fraction has on the transmutation effect. While this study did not focus particularly on ^{241}Am, the dominant contributor to the heat load from 100-1000 years, it demonstrated the feasibility of using BWR cores for such transmutation. As seen throughout these studies, the lack of a robust and available tool to perform 3-D in-core and multi-cycle fuel analysis, as well as the lack of generalized isotopic tracking capability is evident. While many studies are performed at the lattice level, or using an extension of lattice results to potential core-wide results, the lack of a tool capable of simulating in-core fuel behavior as well as isotopic changes is clear.

While discussing a thermal neutron spectrum as an avenue for the transmutation of ^{241}Am, it is helpful to point out how this occurs. ^{241}Am is transmuted via capture through one of the two following reactions:

$$^{241}_{95}Am + ^{1}_{0}n \rightarrow ^{242}_{95}Am_{gs}, \qquad t_{1/2} = 16\ hours$$

$$^{241}_{95}Am + ^{1}_{0}n \rightarrow ^{242}_{95}Am_{m}, \qquad t_{1/2} = 141\ years$$

Fortunately, the fission cross-section for both states of ^{242}Am is favorable for incineration. At 0.0253 eV the total fission cross-section for the ground state is ~2100 barns, whereas at the same conditions, the total fission-cross section for the meta stable state is ~6700 barns [16] . Given these high values of the thermal fission cross-section, relative to that of ^{235}U at 582 barns, the ability to incinerate this high heat-load component of spent fuel in a thermal spectrum appears quite viable. While in the past there was varying nuclear data surrounding the ground state fission cross-section, due to its short half-life, the various nuclear data files have come into close agreement regarding the cross-section of ^{242gs}Am, which is of fundamental importance for any nuclear computer simulation. Fioni, et al. [8] have demonstrated the ability to incinerate ^{241}Am with thermal neutrons, with success, leading them to the conclusion: "the ^{242gs}Am capture cross section keeps the option [open] to transmute ^{241}Am together with the minor actinides issued from multi-recycling of a MOX fuel by an intense flux of moderated neutrons". This provides the key requirement for transmutation, as there are numerous reactors worldwide capable of providing an intense flux of moderated neutrons, and since ^{242gs}Am readily fissions in this environment the potential is evident.

With respect to transmutation of various isotopes in a thermal environment, one major factor is the inventory of the highly transmutable isotopes. For instance, ^{241}Am is advantageous for transmutation in a thermal environment through the capture reaction, followed by the fission of ^{242}Am. Other isotopes are not nearly as favorable, such as ^{241}Pu. When placed in a thermal environment, ^{241}Pu will capture a neutron, becoming ^{242}Pu which does not have an advantageous path towards incineration or transmutation, but rather tends to lead to higher and heavier actinides, which are unfavorable. One way to treat this is to leave spent nuclear fuel (SNF) to "cool" for 30 years or more after being used in-core. In this way, given the 14 year half life of ^{241}Pu which beta decays to ^{241}Am, approximately 75% of the original inventory of ^{241}Pu has converted to the transmutable ^{241}Am, while the initial inventory of ^{241}Am is relatively unchanged given its long half-life on the order of 430 years. Collins, Renier, DelCul and Spencer [4] have performed calculations detailing and investigating the effect of this cooling time, using two simulations; one simulation performed with a 30 year cooling time, and another simulation with a five year cooling time. In addition, a comparison of the production and destruction rates of several of the key transuranics was performed when using an ABR (advanced burner reactor) versus a LWR. The results of this study again showed promising results for the potential incineration of various minor actinides, in particular ^{241}Am, in a thermal flux environment.

Studies, such as the aforementioned study, as well as the work done by Collins and Renier [5] Zaetta [38] as well as numerous other sources have discussed the potential need for a two-fold transmutation system, comprised of recycling in both fast reactor and thermal reactor environments. As mentioned before, this appears to be a potentially advantageous scenario as it takes advantage of, at least in part, the infrastructure already in place as well as allowing for the recovery of much of the unused energy still present in spent nuclear fuel. The lack of a capability for simulating actinide loaded bundles burned in BWR core loading patterns that satisfy thermal and safety limits (shut down margin for instance) and represent appropriate conditions for several cycles as well as accurately evaluating the transmutation of actinides is again encountered.

Of particular interest, and observed in the literature, are the conflicting approaches regarding the most effective reactor type for the incineration of various plutonium isotopes. Historically, the practice of loading MOX bundles in LWR cores has been carried out, thus many reports point to recycling plutonium in the LWR while recommending the other actinides be transmuted in a fast reactor. That said, however, several other reports comment that the most efficient process may be a partial inversion of this, whereby plutonium isotopes end up in a fast reactor while some of the higher actinides (such as ^{241}Am) are best transmuted in a thermal reactor. This indicates that more detailed evaluation tools are needed to study the inherent changes due to loading new materials in nuclear fuel, the different in-core behavior, and the practical limitations on the volume of new materials that can be safely loaded in a core while satisfying operational limits. Thus, an available, efficient, and accurate tool for analyzing BWR core behavior with a generalized tracking of isotopic inventories provides a new and significant contribution to the newly emerging field of LWR recycling and actinide management.

1.2.2 Thermal-Hydraulics

In order to develop a code capable of solving representative steady-state BWR operating conditions, one essential component is a robust steady-state two-phase flow solution scheme. Several options exist for solving two-phase flow conditions. RELAP5-3D [28] uses a model described as follows:

> "The RELAP5-3D hydrodynamic model is a transient, two-fluid model for flow of a two-phase vapor/gas-liquid mixture that can contain noncondensable components in the vapor/gas phase and/or a soluble component in the liquid phase. A one-dimensional as well as a multi-dimensional hydrodynamic model is included in the code."

While the RELAP5-3D approach is certainly among the state of the art methods in two-phase flow analysis, the desired thermal-hydraulic solution for this BWR core design application need not be a robust solver applicable to transient conditions, but rather one that handles steady-state flow characteristics accurately and quickly. Another influencing factor was the lack of need for a multi-dimensional solution. Given the boxed (fuel channel) design in BWR bundles, the flow is essentially a vertical flow, thus a one-dimensional capability is sufficient. Finally, the time requirements for achieving convergence in a RELAP5-3D solution scheme can be high, and since each channel needs to be modeled independently leading to upwards of 800 channel solutions, an alternate solution algorithm was pursued in contrast to the current wave of coupled neutronic and thermal-hydraulic efforts [36] .

Numerous modern industrial BWR simulation codes utilize the drift-flux model as their approach to two-phase flow computation within their core simulators. The accuracy of steady-state solutions has been well documented, as well as the speed of convergence when compared to distinct two-fluid models. In addition, in the development of the BWR analysis and optimization tool FORMOSA-B, Moore [22] utilized the drift-flux solution scheme as the thermal-hydraulic solution algorithm of choice, yielding good results with relatively short computational time requirements. While no doubt a valuable tool for BWR analysis, FORMOSA-B is neither publicly available, nor capable of tracking the necessary number of isotopes needed for transmutation analyses. In addition to FORMOSA-B, many other private companies utilize the drift-flux method as their solution algorithm of choice for steady-state conditions such as GE's PANACEA code, Studsvik's SIMULATE code [32] , and Westinghouse's POLCA code, as a few examples. However all of these methodologies are company proprietary and unavailable to the public. In essence, if one wants to have a two-phase flow drift-flux model embedded into a core simulator, one has to develop, implement and validate it.

1.2.3 Isotopics

Public or open-source simulation tools that can perform a detailed 3-D actinide management and analysis of a BWR are not available. While codes such as MONTEBURNS [25] added the capability of ORIGEN-caliber isotopic tracking to the MCNP code, attempting to analyze a large BWR core (700-800 bundles) with these tools is computationally daunting, not to mention that these tools do not include the capability of modeling thermal-hydraulic feedbacks. While MONTEBURNS may not be the computational tool to use for developing and analyzing BWR core loading patterns the employment of ORIGEN as the computational tool for isotopic evaluations is an insightful and helpful approach. Thus, applying a similar approach to utilize the latest available version of ORIGEN [12] on a nodal basis within the paradigm of a traditional BWR core simulator is herein pursued as a unique objective, as in fact, no such capability exists within modern 3-D LWR simulators.

The usage of ORIGEN as the main depletion tool has been utilized and demonstrated to show excellent agreement within the SCALE suite of codes, primarily in the TRITON depletion sequence [30] . ORIGEN has been coupled with various two-dimensional neutronics solvers, NEWT as the discrete-ordinates solver, or KENO as a Monte Carlo based solver. In these applications ORIGEN is called after each subsequent burnup step, as well as intermittently as part of the predictor-corrector step, to predict the isotopic distribution. Numerous verifications of this have been performed; Bowman and Gill [2] illustrated the accuracy and fidelity for LWR fuels, and Dehart and Ulses [6] have shown the various lattice physics capabilities of TRITON, including their capability to track isotopes extensively. However, as observed with other studies herein cited, the lack of a 3-D "full reactor" operational environment with spatially dependent thermal-hydraulic feedback is a common theme.

2 Proof of Principle Studies

Initial studies on the feasibility of the transmutation of ^{241}Am in the thermal neutron spectrum of a BWR yielded positive results. The first step of a proof of principle study incorporated using the 3-D core simulator POLCA-7, a product of Westinghouse Electric Co. Using an initial core loading pattern provided with the code as a starting point, four bundles spiked with ^{241}Am were loaded into a central location of the core. The four bundles loaded in the core were generated via the lattice physics optimization code FORMOSA-L, which had been adapted to include an optimization option for americium transmutation, [14] [15] An overview of this process, including core loading is shown in Figure 2.1, which is intended to illustrate the process by which the lattice to bundle design was developed as well as the locations in the core to which the bundles were loaded. In the first graph, the optimization process is depicted, which is comprised of an optimization routine designed to determine the optimum loading pattern for maximizing ^{241}Am transmutation, while keeping certain fuel performance characteristics (power peaking and end of life reactivity) within prescribed constraints. The second picture depicts the lattice loading pattern developed, which is intended to illustrate the optimized loading which resulted in the ^{241}Am concentrated on the lattice periphery. The third picture of the sequence shows the four central locations into which these optimized, spiked lattices were loaded.

In order to simulate pseudo-equilibrium conditions three cycles were simulated whereby the entire core of non-spiked bundles was removed and reloaded, while the four spiked bundles remained in their noted positions. Simulations with burnups higher than 30 GWD/MTU showed promising results with respect to americium transmutation.

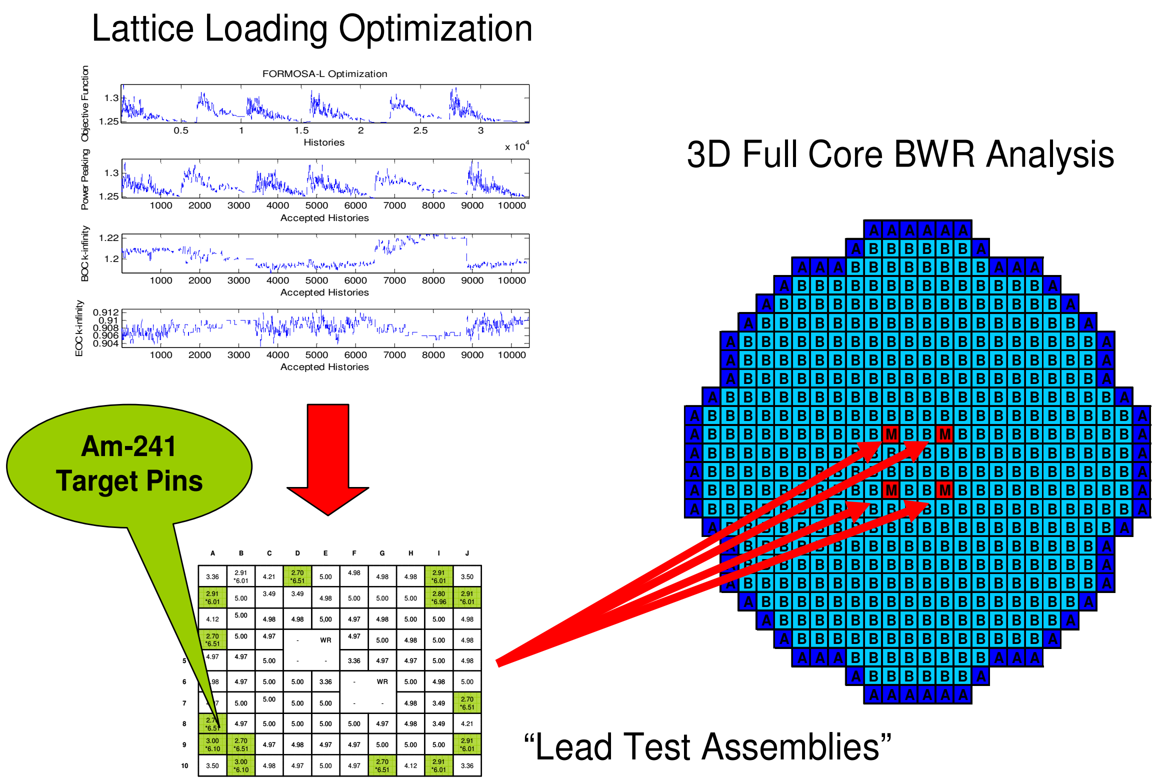

Figure 2.1 Lattice to Core Process

During the simulations using the initial core loading pattern given and inserting spiked bundles, several unfavorable thermal margin results were observed located primarily in the neighborhood of the four spiked bundles, where severe power peaking was observed. In practice, this was the result of loading much higher ^{235}U enriched bundles (>4% enriched) in central locations in a core where every other bundle was enriched to 1.94% in ^{235}U (characteristic of an initial core). Thus, it was determined that a more representative core loading pattern was needed to accurately assess the level of transmutation that could be achieved in a modern BWR core, as well as to model a more realistic impact upon reactivity margins.

No publicly available core loading strategies were found that suited the purpose, as these are generally tightly controlled and proprietary to vendors and utilities, therefore, a realistic core loading pattern that could be led to an equilibrium state was created. The fuel bundle used was created in-house, which compared very favorably against an industry standard bundle used as a benchmark. The following Figure 2.2 shows a quarter core slice of the loading pattern and the burnup values of the bundles in-core at the beginning of the equilibrium cycle.

The bundle used for this simulation was comprised of four major zones. The bottom axial zone containing natural uranium (characteristic of modern fuel designs), followed by a dominant zone featuring gadolinium loaded pins for reactivity suppression, followed by a vanishing zone where part-length rods end, finally a natural uranium top, also with vanished rods; shown in Figure 2.3. In practice natural uranium lattices are loaded at the top and bottom locations of a bundle due to the high neutron leakage at the points. A slightly more reactive core would be achieved if enriched uranium was utilized at the top and bottom, but the economic penalty associated with the manufacturing of these enriched lattices more than offsets the reactivity gain, thus modern designs use natural uranium as the lattices at the top and bottom of the bundle and have been coined as the term “axial blankets”.

Once loaded with fuel, the core was driven to an equilibrium state using a representative standard bundle, by performing nine fuel burn and shuffle sequences. Once demonstrating equilibrium behavior, the spiked bundles were then loaded into two or four locations, referencing quarter core symmetry (thus eight or sixteen total bundles in-core). ^{241}Am transmutation was evaluated, as well as initial studies into possible effects on shutdown margin. For the first study using the equilibrium core design, the spiked bundles were loaded into fresh fuel locations and then another equilibrium analysis was done, loading and shuffling for somewhere between seven to nine fuel burn and reshuffle sequences before equilibrium behavior was exhibited, inserting the spiked bundles into the same fresh location at the beginning of each reload. The loading positions for the spiked bundles throughout the cycle are illustrated in Figure 2.4.

Two independent simulations were performed for the fourth burnt spiked bundles, occupied by positions “C4” or “C4 Alt”. The difference between “C4” and C4 Alt” is a contrast between what industry would typically do with these high burnup bundles, as opposed to what would be best for transmutation. Utilities typically move the least reactive bundles to the core periphery, to maximize cycle length, hence where the “C4” bundles are placed. This would cause a limitation on the amount of ^{241}Am transmuted though, as the neutron flux is much lower on the periphery. Typically these bundles are placed on the periphery, due to the same effect as observed in the axial blankets described above. In order to have the longest cycle and most efficient usage of fuel, the radial neutron leakage is minimized by loading the least reactive bundles on the periphery and the more reactive bundles internally. This allows the highest fraction of neutrons produced to be absorbed in fuel elements as opposed to leaking out of the core periphery. As a sensitivity study, these bundles were also placed in more central core locations to observe the difference in ^{241}Am transmutation as a result of bundle locations at high burnup positions. Predictably the bundles in the “C4 Alt” positions encountered greater ^{241}Am transmutation. The difference was on the order of ~3-4% transmutation in the standard “C4” location as opposed to the “C4 Alt” position. The further discussion of where to place the bundles, as well as the economic penalty associated, would undoubtedly lie between the operating utility and those responsible for waste disposal.

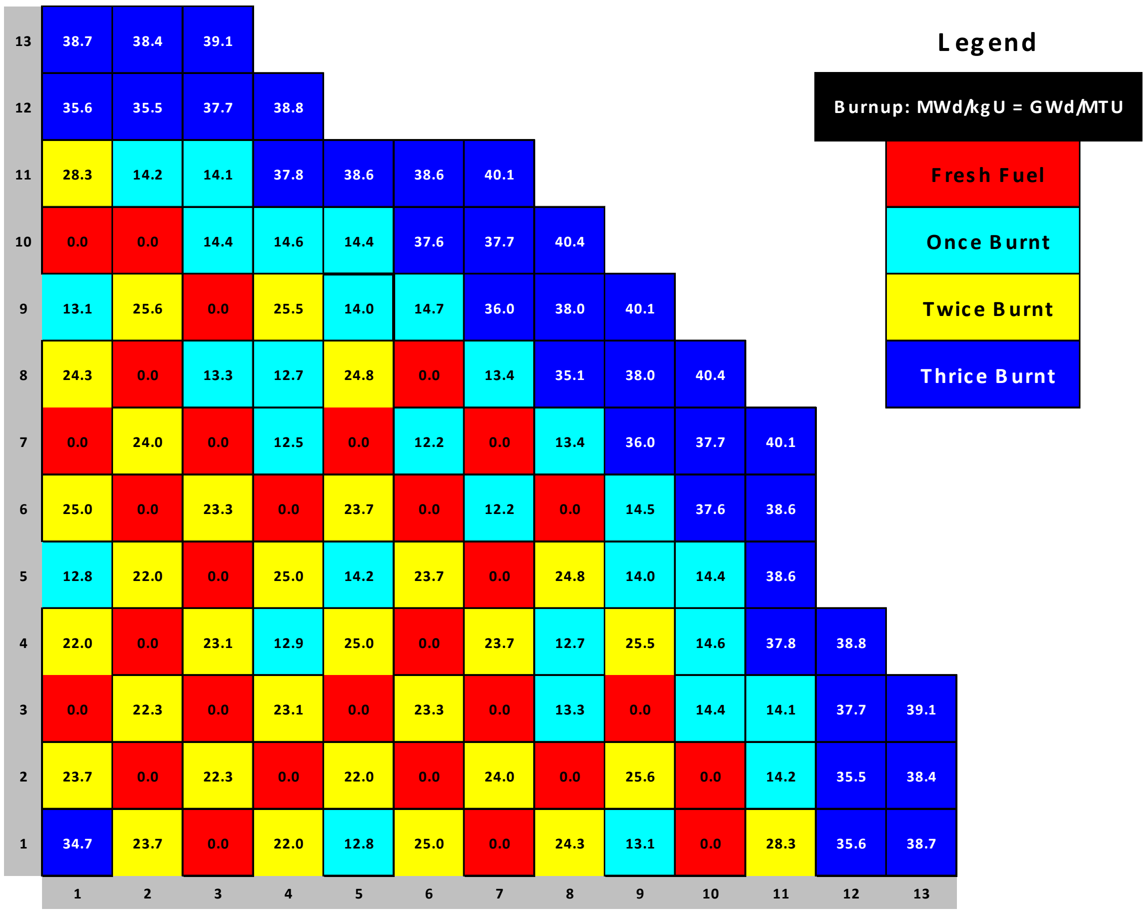

Figure 2.2 Equilibrium Core Loading Pattern

Using the equilibrium analysis and core loading pattern described above, the total amount of ^{241}Am destroyed throughout the cycle is shown in Figure 2.5. Observe also that the expected amount of ^{241}Am build up for a standard bundle is also included for reference where approximately this amount of ^{241}Am is expected to be accumulated throughout the cycle due to the presence of a significant amount of ^{238}U, the main source for ^{241}Am production.

Observed is that 209 g of ^{241}Am was transmuted in one spiked bundle when burned to approximately 50 MWD/kg-U. Compare this to a standard accumulation of 20 g of ^{241}Am due to

Upper Blanket with vanishing zone (6.9")

0.71	0.71	0.71	0.71	0.71	0.71	0.71	0.71	0.71	0.71
0.71	VAN	0.71	VAN	0.71	0.71	VAN	0.71	VAN	0.71
0.71	0.71	0.71	0.71	0.71	0.71	0.71	0.71	0.71	0.71
0.71	VAN	0.71	0.71	0.71	H2O	H2O	0.71	VAN	0.71
0.71	0.71	0.71	0.71	VAN	H2O	H2O	0.71	0.71	0.71
0.71	0.71	0.71	H2O	H2O	VAN	0.71	0.71	0.71	0.71
0.71	VAN	0.71	H2O	H2O	0.71	0.71	0.71	VAN	0.71
0.71	0.71	0.71	0.71	0.71	0.71	0.71	0.71	0.71	0.71
0.71	VAN	0.71	VAN	0.71	0.71	VAN	0.71	VAN	0.71
0.71	0.71	0.71	0.71	0.71	0.71	0.71	0.71	0.71	0.71

Upper Blanket

Upper Vanishing Zone (42")

2.00	2.80	3.60	4.40	4.40	4.40	3.95	3.60	2.80	2.00
2.80	VAN	3.95	VAN	3.95	3.95	VAN	3.95	VAN	2.80
3.60	3.95	4.40/5.00	3.95	4.40/5.00	4.90	4.40	4.40/4.00	3.95	3.95
4.40	VAN	3.95	4.40/2.00	4.90	H2O	H2O	4.40	VAN	4.40
4.40	3.95	4.40/5.00	4.90	VAN	H2O	H2O	4.40/5.00	4.40	4.40
4.40	3.95	4.90	H2O	H2O	VAN	4.40	4.40	4.40/4.00	4.40
3.95	VAN	4.40	H2O	H2O	4.40	4.40	4.40/4.00	VAN	4.40
3.60	3.95	4.40/4.00	4.40	4.40/5.00	4.40	4.40/4.00	4.40	3.95/4.00	3.95
2.80	VAN	3.95	VAN	4.40	4.40/4.00	VAN	3.95/4.00	VAN	3.60
2.00	2.80	3.95	4.40	4.40	4.40	4.40	3.95	3.60	2.00

Vanishing Zone

Lower Dominant Zone (90")

2.00	2.80	3.60	4.40	4.40	4.40	3.95	3.60	2.80	2.00
2.80	4.40	3.95	4.90	3.95	3.95	4.90	3.95	4.40	2.80
3.60	3.95	4.40/5.00	3.95	4.40/5.00	4.90	4.40	4.40/4.00	3.95	3.95
4.40	4.90	3.95	4.40/2.00	4.90	H2O	H2O	4.40	4.90	4.40
4.40	3.95	4.40/5.00	4.90	4.40	H2O	H2O	4.40/5.00	4.40	4.40
4.40	3.95	4.90	H2O	H2O	4.40	4.40	4.40	4.40/4.00	4.40
3.95	4.90	4.40	H2O	H2O	4.40	4.40	4.40/4.00	4.90	4.40
3.60	3.95	4.40/4.00	4.40	4.40/5.00	4.40	4.40/4.00	4.40	3.95/4.00	3.95
2.80	4.40	3.95	4.90	4.40	4.40/4.00	4.90	3.95/4.00	4.40	3.60
2.00	2.80	3.95	4.40	4.40	4.40	4.40	3.95	3.60	2.00

Dominant Zone

Lower Blanket (6")

0.71	0.71	0.71	0.71	0.71	0.71	0.71	0.71	0.71	0.71
0.71	0.71	0.71	0.71	0.71	0.71	0.71	0.71	0.71	0.71
0.71	0.71	0.71	0.71	0.71	0.71	0.71	0.71	0.71	0.71
0.71	0.71	0.71	0.71	0.71	H2O	H2O	0.71	0.71	0.71
0.71	0.71	0.71	0.71	0.71	H2O	H2O	0.71	0.71	0.71
0.71	0.71	0.71	H2O	H2O	0.71	0.71	0.71	0.71	0.71
0.71	0.71	0.71	H2O	H2O	0.71	0.71	0.71	0.71	0.71
0.71	0.71	0.71	0.71	0.71	0.71	0.71	0.71	0.71	0.71
0.71	0.71	0.71	0.71	0.71	0.71	0.71	0.71	0.71	0.71
0.71	0.71	0.71	0.71	0.71	0.71	0.71	0.71	0.71	0.71

Lower Blanket

Figure 2.3 Equilibrium Core Bundle Design

production from ^{238}U, and the percent of original ^{241}Am transmuted is on the order of 91%. Thus, if two bundles were loaded in quarter core symmetry every reload and the batch size was roughly one third, for a full core computation the transmutation that would result would be approximately 1700 g of ^{241}Am destroyed every cycle, with a production of around 2500 g. This results in a net production of 800 g of ^{241}Am every cycle. However if 16 bundles were loaded every cycle (thus four bundles in quarter core symmetry), a total destruction of 3400 g per cycle is observed. This rate of transmutation results in a net destruction of 900 g per cycle which then operates in a realm where the overall americium inventory, and associated heat load contributions, is being reduced.

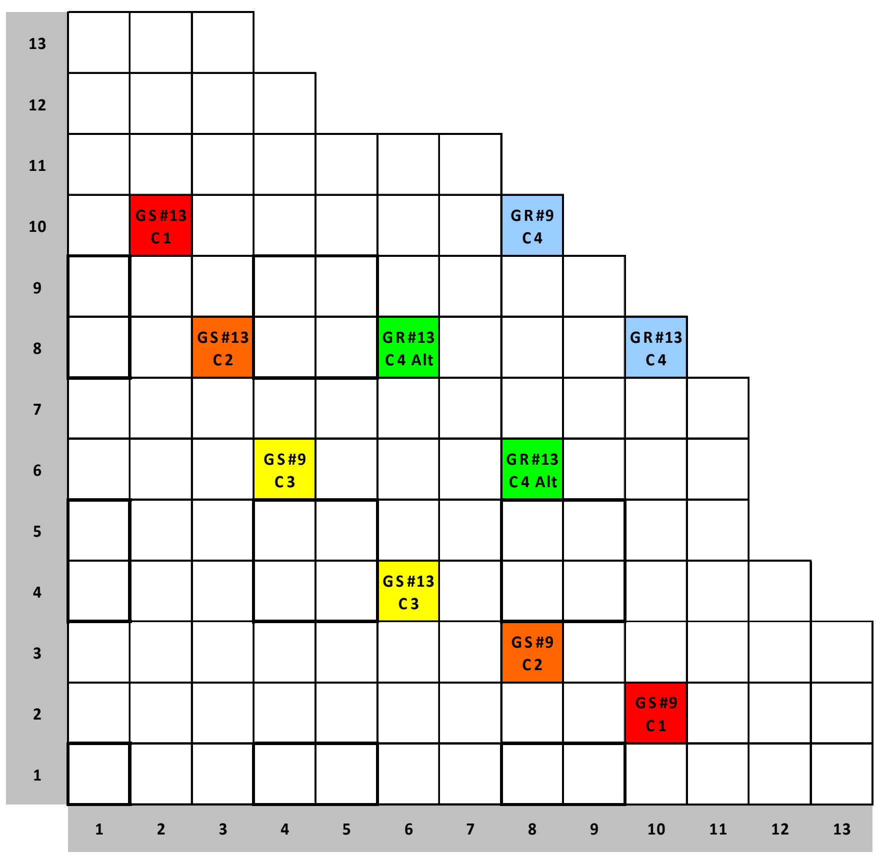

Figure 2.4 Spiked Bundle Locations

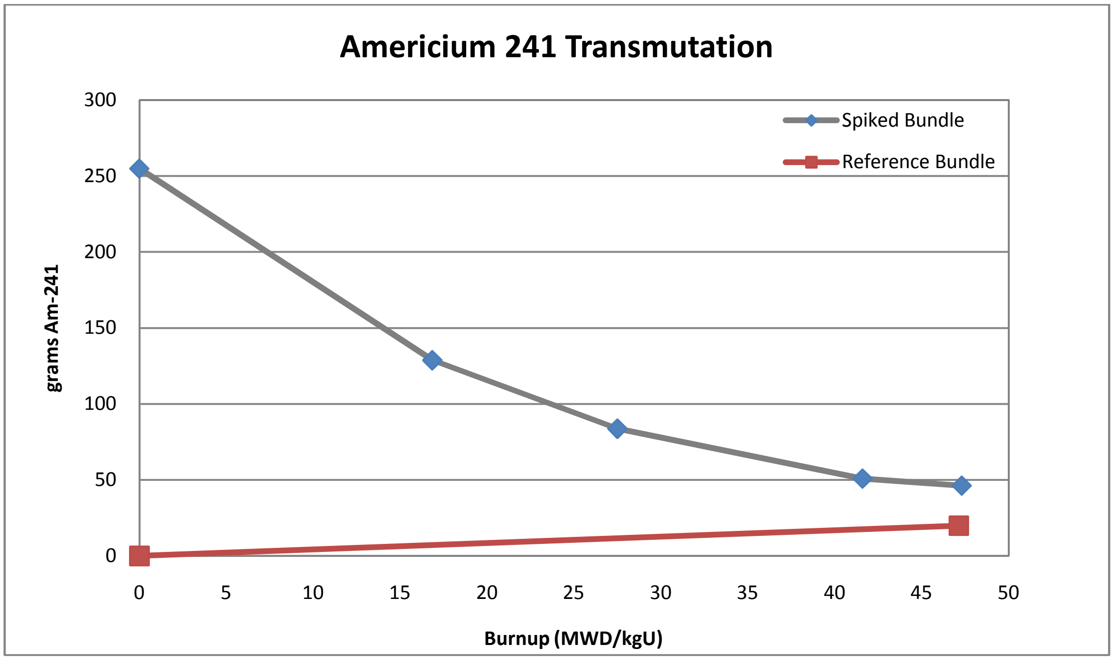

Figure 2.5 Spiked Bundle ^{241}Am Transmutation

One particular characteristic of the loading of the spiked bundles that deviates greatly from standard fuel designs is the lack of gadolinium as a reactivity control mechanism. In the design phase of the spiked bundles, it was decided upon to supplant the gadolinium loaded pins with the spiked pins, with the hopes that the ^{241}Am could potentially act as a burnable absorber. In order to achieve an end-of-life reactivity that is representative of current fuel designs it was necessary to have a higher ^{235}U enrichment than the gadolinium loaded counter-part. This is due to the ^{235}U burning out faster at beginning-of-life due to the absence of gadolinium, or any other reactivity suppression mechanism. As a result, the bundles end up being much hotter at beginning-of-life, which was a possible concern regarding shutdown margin for the cells in the neighborhood of the spiked bundle. A shutdown margin calculation was performed for the whole core, with the results given here in Figure 2.6.

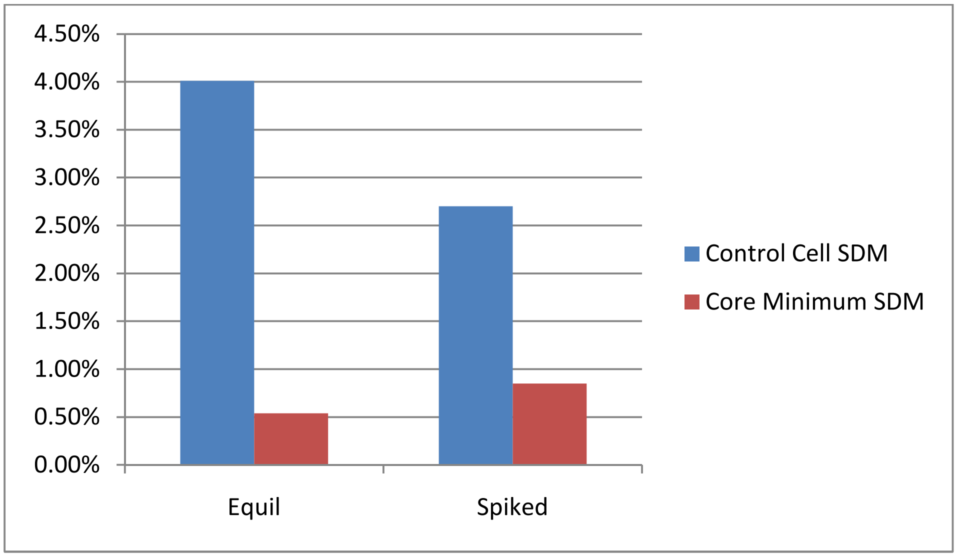

Figure 2.6 Equilibrium Core Shutdown Margin

While the limiting condition for shutdown margin actually increased (yielding more safety margin) for the limiting control cell in the whole core, this is a large function of the loading pattern and control rod pattern used and should not be seen as an inherent feature of a spiked bundle loaded core. Minimum shutdown margin is very sensitive to core designs. That said, what can be seen is the shutdown margin in the cell closest to the spiked bundle dropped by 1.3% from 4% to 2.7%. While still having plenty of margin in this cell, it is well observed that loading these bundles must be performed judiciously since they come in as very active fuel which could pose a safety concern if loaded into a limiting control cell. These bundles tend to behave in a fashion quite similar to traditional once-burned bundles, bundles that had gadolinium initially but which has since burned out and now are more reactive fuel than when initially loaded.

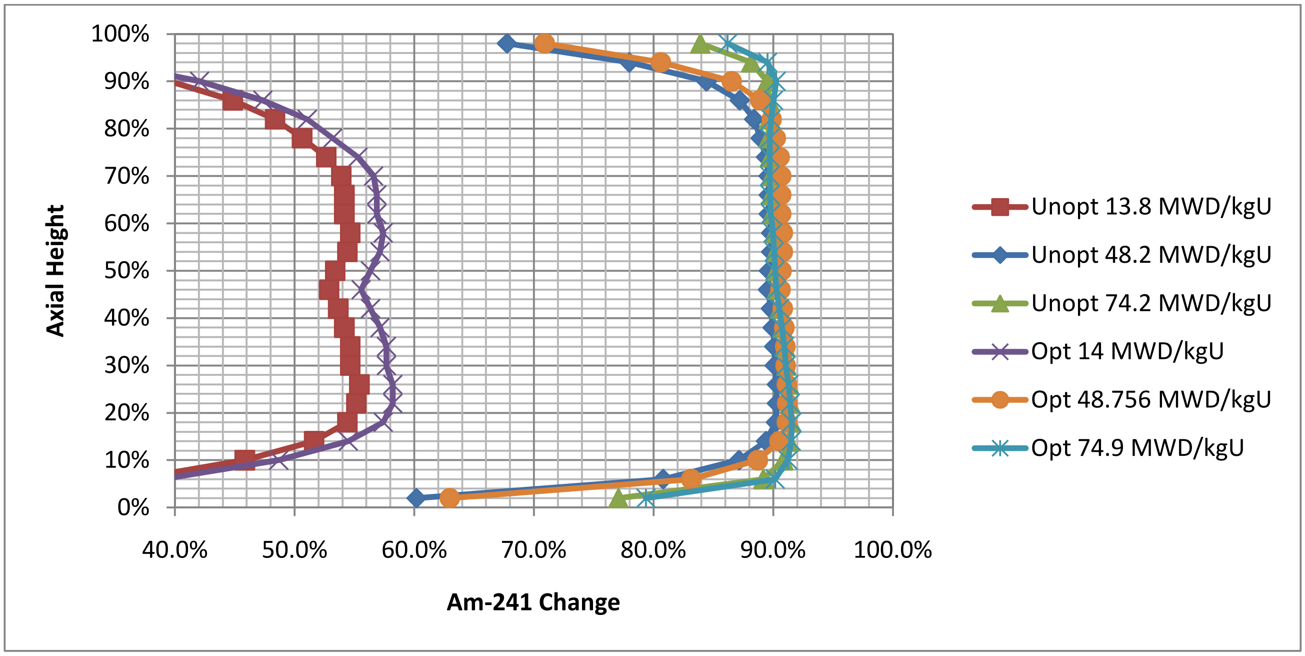

Figure 2.7 Axial ^{241}Am Transmutation

In addition to a simulation utilizing the optimized lattice design, a comparison using a "base" lattice, which included ^{241}Am loading not yet processed through an optimization routine, was also performed to assess the effectiveness of the optimization routine in determining an optimum lattice design. A comparison of the behavior of the optimized lattice in comparison to a non-optimized lattice was thus available where Figure 2.7 shows these results. Two items of particular interest are the variation (or lack thereof) when looking at axial transmutation dependencies and the transmutation results observed as burnup increases, as it pertains to the optimized and un-optimized lattices.

With respect to axial transmutation, the higher axial locations were thought to experience better transmutation rates due to the more advantageous absorption to capture ratios present in harder spectra. The results here show that the transmutation of ^{241}Am can be achieved in either the traditional thermal (axially lower) or harder spectrum (axially higher). One major limitation is that this simulation only tracks overall inventory changes of ^{241}Am (production and losses included), but does not have the ability of tracking where exactly the ^{241}Am went. For example, did the ^{241}Am fission, or was it lost to higher actinides? The code employed, in fact, does not have the ability to track the full suite of actinides needed to address such question. That said, it is clear that ^{241}Am can be transmuted in a thermal spectrum and that there is not an obvious clear benefit of axial location in the BWR environment.

Also of interest are the transmutation results for the optimized and un-optimized bundles, as well as the trend with increasing burnup. At low burnup values, corresponding with once-burned fuel (~14 MWD/kgU), the optimized bundle showed a clear tendency to transmute the ^{241}Am fuel faster than the non-optimized bundle, with approximately 5% greater transmutation than the un-optimized counterpart. This accelerated transmutation rate is not sustained throughout multiple cycles though, evidenced by the similar transmutation rates achieved at high burnups of around 50 to 75 MWD/kgU, where it appears a saturation point for ^{241}Am transmutation exists.

These proof-of-principle studies proved insightful and promising with regard to the potential of the effective transmutation of ^{241}Am in a BWR core. A major deficiency, however, was the inability to track the full suite of actinides, a capability needed to accurately evaluate if there is a clear advantage of the upper axial portions of a BWR core versus the lower, as well as needed to track if the americium isotopes are being incinerated through fission or simply transmuted into higher actinides that may still pose a radiological and storage hazard. The ability to track the full suite of actinides also leads to a much better evaluation of the benefit, or perhaps lack thereof, of the harder spectrum observed at the top of the core.

3 Two-Phase Thermal-Hydraulic Model

3.1 Thermal-Hydraulics Overview

In the conversion of NESTLE from a PWR modeling code to one that can also model a BWR core, the key need is that of a thermal-hydraulic model capable of accurately capturing the boiling that occurs in each channel. Two boiling regimes are of primary interest in BWR channels, the section where sub-cooled boiling occurs and the section where saturated boiling occurs. Each of these two regimes needs to be modeled accurately in order to capture the correct moderator density, which has a strong impact upon core neutronics. Implemented into NESTLE, as part of this project, is a drift-flux scheme which has historically proven to be an accurate solution scheme in the steady-state solution regimes, with relatively efficient code execution time. This scheme includes a model to capture sub-cooled boiling, and subsequently track when bulk boiling occurs. The determined flow conditions, both sub-cooled quality in the sub-cooled boiling regime and equilibrium quality in the saturated regime, are passed to a void-quality correlation to obtain the void fraction in each node, which is then used for the density calculation.

In addition to requiring a two-phase solution scheme, an accurate scheme for determining the correct flow inside each channel across the core is needed. The scheme employed inside NESTLE allows each user to choose to converge to a desired core pressure drop, or to converge to a total core mass flow rate. Once the user selects which option is desired and sets the appropriate target values, the code adjusts the flow inside each channel until the solution converges to within a user-defined tolerance, ensuring that there is an equal pressure drop across each channel, since the upper and lower plenums are common across all channels and each channel must then have the same inlet and outlet pressures.

The initial set of equations used includes the mixture continuity equation, mixture internal energy, and mixture momentum equations. These are illustrated by Equations 3.1-3.5. While the equations shown here include time dependency, since the model is intended to simulate steady-state conditions the time dependent terms disappear in the discretized form of the equations which follow.

Mixture continuity

$$A_x \frac{\partial \rho}{\partial t} + \frac{\partial}{\partial z}(G A_x) = 0$$

Equation 3.1

Mixture internal energy

$$A_x \frac{\partial}{\partial t}(\rho u) + \frac{\partial}{\partial z}(G u A_x)$$
$$= -P \frac{\partial}{\partial z}\left(\frac{G}{\rho} A_x\right) + q''' A_x - P \frac{\partial}{\partial z}\left(\frac{\rho_l - \rho_g}{\rho} j_D^g A_x\right) - \frac{\partial}{\partial z}\left(\frac{\rho_l \rho_g}{\rho}\left(u_g - u_l\right) j_D^g A_x\right)$$

Equation 3.2

Mixture momentum

$$\frac{\partial}{\partial t}(\rho v) + \frac{1}{A_x}\frac{\partial}{\partial z}\left(\frac{G^2 A_x}{\rho}\right) = -\frac{\partial P}{\partial z} - \frac{\tau_w P_w}{A_x} - \frac{1}{A_x}\frac{\partial}{\partial z}\left(\frac{\rho_l \rho_g}{\rho}\left(\frac{1}{\alpha(1-\alpha)}\right) {j_D^g}^2 A_x\right) - \rho g \cos\theta$$

Equation 3.3

with

$$\frac{\tau_w P_w}{A_x} = f\left(\frac{G^2}{2 D_e \rho_l}\right) \emptyset_{fric}^2 + \sum_m \delta(z - z_m)\, K_m \left(\frac{G^2}{2\rho_l}\right) \emptyset_{local}^2$$

Equation 3.4

and

$$\rho = \rho(u, P)$$

Equation 3.5

Lastly, the relationship of the mixture quantities to the separate liquid and vapor phasic quantities are given by Equations 3.6-3.8.

$$v_g = +\frac{\rho_l}{\rho}\frac{j_D^g}{\alpha};\ v_l = v - \frac{\rho_g}{\rho}\frac{j_D^g}{(1-\alpha)}$$

Equation 3.6

$$v \equiv \frac{\rho v}{\rho} = \frac{G}{\rho} = \frac{(1-\alpha)\rho_l v_l + \alpha\rho_g v_g}{(1-\alpha)\rho_l + \alpha\rho_g}$$

Equation 3.7

$$\rho \equiv (1-\alpha)\rho_l + \ \alpha\rho_g$$

Equation 3.8

3.2 Nestle Drift-Flux Solution

The drift-flux solution implemented uses a staggered mesh solution scheme so that thermodynamic properties are evaluated at node edges while the pressure is evaluated at node center, an illustration of the discretization of two nodes is shown in Figure 3.1.

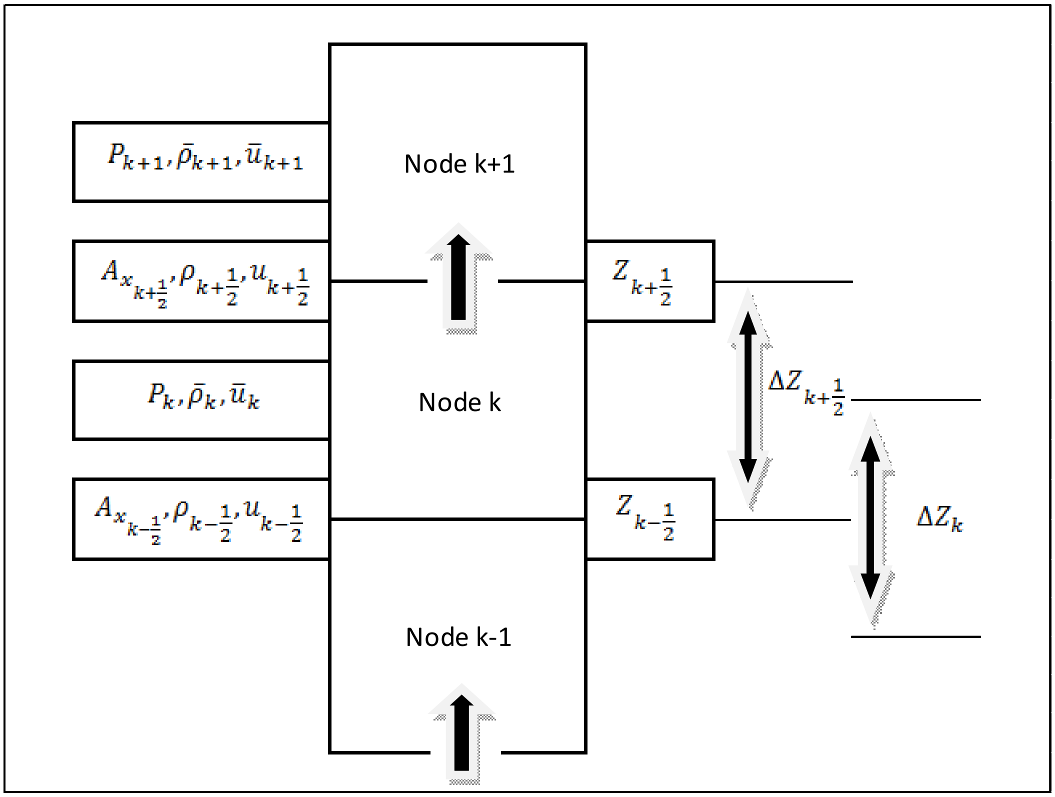

Figure 3.1 Thermal Hydraulic Nodal Discretization

Using the discretized form of the equations, the first step involves solving the mass continuity equation up the channel.

Mixture Continuity

$$(GA_x)_{k+1/2} = (GA_x)_{k-1/2}$$

Equation 3.9

Next the internal energy equation is solved up the channel to allow for the determination of material thermal properties (density, temperature, quality, void fraction etc…).

Mixture Internal Energy

$$u_{k+1/2} = \left[\frac{(GA_x)_{k-1/2}}{(GA_x)_{k+1/2}}\right] u_{k-1/2} + \frac{q'''\overline{A_x}\Delta z_k}{(GA_x)_{k+1/2}} - P_k\left[\frac{1}{\rho_{k+1/2}} - \left[\frac{(GA_x)_{k-1/2}}{(GA_x)_{k+1/2}}\right]\frac{1}{\rho_{k-1/2}}\right]$$
$$- \frac{P_k}{(GA_x)_{k+1/2}}\left[\left[\left(\frac{\rho_l - \rho_g}{\rho}\right) j_D^g A_x\right]_{k+1/2} - \left[\left(\frac{\rho_l - \rho_g}{\rho}\right) j_D^g A_x\right]_{k-1/2}\right]$$
$$- \frac{1}{(GA_x)_{k+1/2}}\left[\left[\frac{\rho_l \rho_g}{\rho}(u_g - u_l) j_D^g A_x\right]_{k+1/2} - \left[\frac{\rho_l \rho_g}{\rho}(u_g - u_l) j_D^g A_x\right]_{k-1/2}\right]$$

Equation 3.10

Once the internal energy distribution is known, it is then used to calculate the enthalpy distribution in order to determine the equilibrium quality up the channel. Subsequently, using the equilibrium quality distribution, the coolant temperature distribution is calculated; if equilibrium quality is less than zero, sub-cooled properties are used for temperature determination, alternatively if equilibrium quality is greater than zero the temperature is set to the saturation temperature at the node pressure. Following the determination of temperature, the true quality distribution up the channel is desired. In order to obtain an accurate estimate of true quality, determining the quality of net vapor generation (x_{nvg}) is necessary to account for sub-cooled boiling contributions. Two correlations are available as determinations of x_{nvg}, the Saha-Zuber model [29] , which relates sub-cooled boiling to the surface heat flux and Peclet number, as well as an EPRI model developed by Lellouche and Zolotar [19] which contains a more complicated solution dependent on several flow parameters, material parameters as well as the heat flux; the EPRI model is the default model.

Saha-Zuber

If Pe < 70,000 then

$$xnvg = \frac{-0.0022 * q'' * D_e * C_p}{k} \times \frac{1}{(h_v - h_l)}$$

Equation 3.11

If Pe >= 70,000 then

$$xnvg = \frac{-154 * q''}{G} \times \frac{1}{(h_v - h_l)}$$

Equation 3.12

Where:

q'' = Heat flux

D_e = Equivalent Diameter (ft)

C_p = Specific Heat Capacity (BTU/lbm*°F)

k = Thermal Conductivity (BTU/hr-ft-°F)

h_v,h_l = vapor enthalpy, liquid enthalpy (BTU/lbm)

G = Mass Flux (lbm/hr-ft^2)

EPRI

$$xnvg = \frac{C_p * Z}{(h_v - h_l)}$$

Equation 3.13

$$Z = \frac{-B + \sqrt{B^2 - 4 * A * C}}{2A}$$

Equation 3.14

$$C = q'' * (4 * HB * q'' + HDB^2)$$

Equation 3.15

$$B = 2 * HDB^2 * \left(HHN + {}^{HDB}/_{2}\right) + 8 * q'' * HB * (HDB + HHN)$$

Equation 3.16

$$A = 4 * HB * (HDB + HHN)^2$$

Equation 3.17

$$HB = \frac{e^{\left({}^{P}/_{630}\right)}}{0.072^2}$$

Equation 3.18

$$HDB = CDB * Re^{0.8} * Pr^{0.4} * {}^{k}/_{D_e}$$

Equation 3.19

$$HHN = CHN * Re^{0.662} * Pr * {}^{k}/_{D_e}$$

Equation 3.20

$$CHN = 0.2 * {}^{D_e}/_{(4 * R_{rod})}$$

Equation 3.21

$$CDB = 0.033 * \varepsilon_{FRAC} + 0.013$$

Equation 3.22

$$\varepsilon_{FRAC} = \frac{A_x}{(A_x + A_{rods})}$$

Equation 3.23

$$A_{rods} = N_{rod} * \pi * \frac{D^2}{4}$$

Equation 3.24

C_p = Specific Heat Capacity (BTU/lbm*°F)

h_v,h_l = vapor enthalpy, liquid enthalpy (BTU/lbm)

q'' = Heat flux (BTU/hr-ft^2)

P = Pressure (psia)

Re = Reynolds Number

Pr = Prandtl Number

k = Thermal Conductivity (BTU/hr-ft-°F)

D_e = Equivalent Diameter (ft)

R_{rod} =Heated Rod Radius (ft)

A_x = Cross-sectional Flow Area (ft^2)

N_{rod} = Number of fuel rods in bundle

D = Rod Diameter (ft)

Now that the qualities of net vapor generation, as well as the equilibrium (which will have negative values in the sub-cooled regime) are known, these two parameters are passed into a quality profile fit to determine true quality. There are several profile fits available, while the one implemented is one developed by Lahey and Moody [17] with a hyperbolic tangential fit:

$$x = \frac{\left(x_{eq} - x_{nvg} * \left(1 - \tanh\left(1 - {}^{x_{eq}}/_{x_{nvg}}\right)\right)\right)}{\left(1 - x_{nvg} * \left(1 - \tanh\left(1 - {}^{x_{eq}}/_{x_{nvg}}\right)\right)\right)}$$

Equation 3.25

Taking the newly determined true quality distribution, this is plugged into a void-quality correlation so that the void distribution can be determined and used to compute mixture density. Again, several options are available for void-quality correlations; available in NESTLE is the Chexal-Lellouche model [3] , the Zuber-Findlay model [39] , and the Lellouche-Zolotar model [19] , which is the default option.

Lellouche-Zolotar

If $L_n >= 0.2$

$$\alpha = \frac{A}{\left(1 + {}^{Y}/_{x}\right) * L_n}$$

Equation 3.26

If $L_n < 0.2$

$$\alpha = \sqrt{\frac{A}{\left(1 + {}^{Y}/_{x}\right) * C_1}}$$

Equation 3.27

$$Y = (1 - x) * \frac{\rho_v}{\rho_l}\left(1 + \frac{\rho_l * A * V_{gj}}{G * L_n(1 - x)}\right)$$

Equation 3.28

$$C_0 = {}^{L_n}/_{A}$$

Equation 3.29

$$V_{gj} = \left(\frac{1.41 * (\rho_l - \rho_v) * \sigma * g^2}{{\rho_l}^2}\right)^{1/4} * (1-\alpha)^{3/2}$$

Equation 3.30

$$A = K_0 + (1 - K_0) * \alpha^r$$

Equation 3.31

$$r = \frac{\left(1 + 1.57 * \frac{\rho_v}{\rho_l}\right)}{(1 - K_1)}$$

Equation 3.32

$$K_0 = K_1 + (1 - K_1) * \left(\frac{\rho_v}{\rho_l}\right)^{1/4}$$

Equation 3.33

$$K_1 = \min\left(0.8, \frac{1}{1 + e^{-\left({}^{Re}/_{1E5}\right)}}\right)$$

Equation 3.34

If α=0

$$L_n = 1.0$$

Else

$$L_n = 1 - e^{-(C_1 * \alpha)}$$

Equation 3.35

$$C_1 = 4 * \frac{{P_{crit}}^2}{P * (P_{crit} - P)}$$

Equation 3.36

x = quality

ρ_v, ρ_l = vapor density, liquid density (lbm/ft^3)

G = mass flux ($lbm/hr\text{-}ft^2$)

σ = surface tension (lb/ft)

g = gravitational constant ($lbm\text{-}ft/lbf\text{-}s^2$)

Re = Reynolds number

Pcrit = Critical Pressure (psia)

P = Pressure (psia)

Upon inspection, it is noticed that this is an iterative solution for void fraction, often symbolized by the Greek letter alpha (α). The code must provide an initial guess for alpha, calculate a new alpha, compare the two and repeat until a user specified convergence criteria is achieved.

Now that the void fraction is known, mixture density can be calculated and provided to the momentum equation solution. In addition, at this point it should be noted that both friction and form losses are needed in the solution of the momentum equation and a discussion of how friction losses and forms losses are calculated for two phase flow is needed. First a single phase friction factor term and similarly a single phase loss coefficient are determined. Subsequently, after the single phase terms are known, a two phase multiplier is included to adjust the loss terms for two phase contributions:

$$\Delta P_{fric} = f\frac{G^2}{2D_e\rho_l}\emptyset_{fric}^2$$

Equation 3.37

Where f is the single phase Darcy-Wiesbach friction factor, and for normal BWR conditions takes the form:

$$f = 0.186 * Re^{-0.2}$$

Equation 3.38

In addition, the two phase multiplier is calculated according to the Columbia correlation [27] .

$$\emptyset_{fric}^2 = 1 + x\left(\frac{\rho_l}{\rho_g} - 1\right) * C$$

Equation 3.39

If P > 600 psia

$$C = 1.02 * x^{-0.175} * G^{-0.45}$$

Equation 3.40

Else

$$C = 0.357\left(1 + 10\frac{P}{P_c}\right)x^{-0.175}G *^{-0.45}$$

Equation 3.41

x = quality

ρ_v, ρ_l = vapor density, liquid density (lbm/ft^3)

G = mass flux (Mlbm/hr-ft^2)

Pcrit = Critical Pressure (psia)

P = Pressure (psia)

Similarly, local losses are a combination of a single phase loss term multiplied by a two phase loss coefficient:

$$\Delta P_{local} = K \frac{G^2}{2\rho_l} \emptyset_{local}^2$$

Equation 3.42

Where K is a user defined single phase local pressure loss coefficient for any component that may be an obstruction (spacer grids, lower orifice etc…). The two phase multiplier used is as computed as follows:

$$\emptyset_{local}^2 = 1 + E * x \left(\frac{\rho_l}{\rho_g} - 1 \right)$$

Equation 3.43

Where E is a constant again provided by the user to account for any non-homogenous two phase momentum loss. If E is set to 1.0 the equation reduces to the homogenous form of the two-phase loss multiplier and is the current default setting.

Finally the momentum equation is solved up the channel, using the properties determined from the internal energy equation and subsequent correlations, to obtain the pressure distribution. The new pressure distribution is then fed back into the internal energy equation to repeat the sequence. Again following the process described above, the new thermal properties are plugged into the momentum equation and the pressure distribution is again calculated. This process is iterated until a user defined convergence is achieved, where the pressure distribution and appropriate physical properties are then known. It should be noted that the internal energy equation and momentum equation are both solved in the drift-flux derived forms, given here in the momentum equation, and seen in the internal energy equation above.

Mixture Momentum

$$P_{k+1} = P_k - \frac{1}{(A_x)_{k+1/2}}\left[\frac{(GA_x)^2_{k+1/2}}{(A_x\bar{\rho})_k} - \frac{(GA_x)^2_{k-1/2}}{(A_x\bar{\rho})_{k-1}}\right] - \Delta z_{k+1/2}\left[\frac{f_{k+1/2}(GA_x)^2_{k+1/2}}{2(D_e\rho_l)_{k+1/2}(A_x)^2_{k+1/2}}\right] - \left[\frac{K_{k+1/2}(GA_x)^2_{k+1/2}}{2(\rho_l)_{k+1/2}(A_x)^2_{k+1/2}}\right] - \Delta z_{k+1/2}(\rho)_{k+1/2}g - \frac{1}{(A_x)_{k+1/2}}\left[\left[\frac{\rho_l\rho_g}{\rho}\frac{\alpha V_{gj}^2}{(1-\alpha)}A_x\right]_{k+1/2} - \left[\frac{\rho_l\rho_g}{\rho}\frac{\alpha V_{gj}^2}{(1-\alpha)}A_x\right]_{k-1/2}\right]$$

Equation 3.44

3.3 Flow Distribution

Another requirement for a robust thermal-hydraulics scheme for the accurate solution of a Boiling Water Reactor during steady-state operation is determining the correct flow rate to each of the fuel channels in the core. Since there is a common pressure shared by the upper plenum, across all channels, as well as a common pressure shared across all channels in the lower plenum, there is a prescribed core ΔP, where each bundle is subject to have this same ΔP. Two options for solving for total core flow rate are often implemented in flow distribution models: solving for a user prescribed core ΔP, or solving for a user defined core mass flow rate. It should be noted that it is generally a more common objective to solve for a total core mass flow rate. In NESTLE, solving for a core ΔP is just a subset of solving for a user defined core mass flow rate, such that creating a robust solver able to match a core ΔP by adjusting flow rates is a necessary first step for either of the solutions.

The method used for solving for a core ΔP, as well as solving for a total core flow rate, is taken directly from the FIBWR (Flow In A BWR) code manual [1] This code was developed in the early 1980s by EPRI and has a proven method for determining correct flow split details.

The solution process for solving for a core ΔP is as follows, on a channel by channel basis:

(1) Guess flow rate for channel

(2) Solve the drift flux set of equations to obtain a channel (and thus core) ΔP

  a. If channel ΔP is within convergence criteria, the code is finished

  b. Otherwise,

    i. If ΔP is too low, increase flow rate in the channel

    ii. If ΔP is too high, decrease flow rate in the channel

(3) Go back to step (2) with new flow rates

Once each channel has achieved the necessary ΔP, the correct flow to each channel and all other necessary thermal-hydraulic parameters (void fraction, density, internal energy, pressure etc…) are known, and the total core flow rate is computed by adding up the individual flow rates. Numerous schemes could be developed for determining the adjustment to the channel flow rate in the attempt to match ΔP; the one chosen is derived from the FIBWR model and is given below:

After the 1st guess, projecting to the 2nd mass flow rate:

$$G_2 = G_1\left(\frac{\Delta P_{req'd}}{\Delta P_1}\right)$$

Equation 3.45

After the 2nd calculation, projection to the 3rd mass flow rate:

$$G_3 = G_1 - (G_1 - G_2)\left(\frac{\Delta P_1 - \Delta P_{req'd}}{\Delta P_1 - \Delta P_2}\right)$$

Equation 3.46

Following the 3rd calculation, from henceforth a polynomial extrapolation of the three most recent sets of G and ΔP values is used to project to the nth mass flow rate:

$$G_n = A + B\Delta P_{req'd} + C\left(\Delta P_{req'd}\right)^2$$

Equation 3.47

$$C = \left[\frac{(G_{n-2} - G_{n-1})}{(\Delta P_{n-2} - \Delta P_{n-1})} - \frac{(G_{n-2} - G_n)}{(\Delta P_{n-2} - \Delta P_n)}\right] \Big/ (\Delta P_{n-2} - \Delta P_n)$$

Equation 3.48

$$B = \frac{(G_{n-2} - G_{n-1})}{(\Delta P_{n-2} - \Delta P_{n-1})} - C(\Delta P_{n-2} + \Delta P_{n-1})$$

Equation 3.49

$$A = G_{n-2} - B\Delta P_{n-2} - C(\Delta P_{n-2})^2$$

Equation 3.50

Typically, convergence on the order of 1E-5 is met in less than 10 iterations, and much of the time convergence is achieved in three to four iterations. Occasionally, when there are several flow and pressure drop combinations that are very close to the solution, the polynomial extrapolation will provide an anomalous projection. To protect against this, a maximum and minimum flow rate/ΔP combination is kept track of and if a solution is provided that is outside of this maximum or minimum, a linear interpolation is used to project the new flow rate and the code continues as usual. In addition, occasionally two subsequent solutions will yield a ΔP identical to the previous, or two previous, solutions which causes a divide by 0 and the code crashes due to a segmentation fault. Several checks have been instituted in the code that catch these errors as well as similar errors, and subsequently coax the code back into a convergent solution.

In the case of converging to a total core flow rate, the code uses the ΔP solver as a subset of the solution process, which goes as follows:

(1) Guess an initial core ΔP
(2) Solve each channel to match the guessed ΔP
(3) Once each channel is solved to the core ΔP, add up the individual channel flow rates
    a. If core flow rate is within convergence criteria, the code is finished
    b. Otherwise,
        i. If core flow rate is too low, increase the ΔP guess
        ii. If core flow rate is too high, decrease the ΔP guess
(4) Go back to step (2) with updated core ΔP guess

In a scenario very similar to predicting what the next guess for channel flow rate should be, the same type of a solution process for predicting the core ΔP has been implemented.

After the 1st guess, projecting to the 2nd ΔP:

$$\Delta \mathrm{P}_2 = \Delta \mathrm{P}_1 \left(\frac{G_{core}}{G_1}\right)$$

Equation 3.51

After the 2nd calculation, projection to the 3rd ΔP:

$$\Delta\mathrm{P}_3 = \Delta\mathrm{P}_1 - (\Delta\mathrm{P}_1 - \Delta\mathrm{P}_2)\left(\frac{G_1 - G_{core}}{G_1 - G_2}\right)$$

Equation 3.52

Following the 3rd calculation, from henceforth a polynomial extrapolation of the three most recent sets of G and ΔP values is used to project to the nth ΔP:

$$\Delta\mathrm{P}_\mathrm{n} = A + BG_{core} + C(G_{core})^2$$

Equation 3.53

$$C = \left[\frac{(\Delta\mathrm{P}_{n-2} - \Delta\mathrm{P}_{n-1})}{(G_{n-2} - G_{n-1})} - \frac{(\Delta\mathrm{P}_{n-2} - \Delta\mathrm{P}_{n})}{(G_{n-2} - G_{n})}\right] \Big/ (G_{n-2} - G_n)$$

Equation 3.54

$$B = \frac{(\Delta\mathrm{P}_{n-2} - \Delta\mathrm{P}_{n-1})}{(G_{n-2} - G_{n-1})} - C(G_{n-2} + G_{n-1})$$

Equation 3.55

$$A = \Delta\mathrm{P}_{n-2} - BG_{n-2} - C(G_{n-2})^2$$

Equation 3.56

The sample size for this is much smaller in a core simulation than the solution for pressure drop, since the ΔP solver may solve hundreds of channels for every single iteration on core flow rate. That said, it has been seen that usually no more than five to six iterations on core ΔP is required to achieve total mass flow rates within a convergence on the order of 1E-5.

3.4 Thermal Limits

Part of the ongoing work with NESTLE will ultimately connect the simulator results of relative power distributions and two-phase flow conditions to a reasonable assessment of core thermal limits. Typical assessments that will be sought will be the evaluation of the critical power ratio (CPR) and assessments related to linear power density (kw/ft) generation in each bundle. Currently, these assessments can be indirectly inferred via reasonable expectations in radial and axial relative power distributions. The solution of the various desired thermal limits can be directly implemented with the current information available. Since the evaluation of theses thermal limits is not a primary focus of the research the capability was not implemented, but the code is readily capable of calculating the various parameters of interest for verification of operation within accepted safety constraints.

4 Code Validation

4.1 Water Property Validation

When the drift-flux subroutine was programmed it was observed that a critical component needed for this evaluation was the water properties, both as a function of temperature and pressure. As a result, a library of water information was retrieved from the NIST website [24] , initially simply using the approximation of sub-cooled properties being approximated by the saturated liquid properties at the water temperature. In time it was observed that this approximation is fine for coarse calculations, but to evaluate to the desired fidelity a more accurate water property library was required.

The first approach was to purchase the FORTRAN library, including the source code, provided by NIST [24] and use this in the nodal call for property evaluation. While this approach gives excellent fidelity, the time constraint in property evaluation was prohibitive. Using this mechanism, as opposed to tabulated tables used for interpolation, the time requirements for calculation were on the order of 100 times longer; thus in a calculation over a whole core of 764 bundles (which originally may require 10 minutes) the calculation would require 1,000 minutes, which is simply not acceptable. To verify that this was as expected, the responsible scientist at the NIST organization was contacted about these computational results, who verified that other researchers who needed water properties in CFD applications have typically generated their own interpolation libraries in the spirit of speeding up these calculations. As a result, tables of all water properties at saturated conditions were tabulated in one degree Fahrenheit increments, as well as one psi increments in pressure so that saturated conditions were available for either temperature or pressure constrained problems. The saturated properties available are given in Table 4.1, where the prefix “l” denotes liquid properties and “v” denotes vapor properties.

Table 4.1 Water Properties Available

Water Properties	
Property	Units
Temperature	F
Pressure	Psia
Density	l, lbm/ft^3
Specific Volume	l, ft^3/lbm
Internal Energy	l, BTU/lbm
Enthalpy	l, BTU/lbm
Entropy	l, BTU/lbm*R
Cv	l, BTU/lbm*R
Cp	l, BTU/lbm*R
Sound Spd.	l, ft/s
Joule-Thomson	l, F/psia
Viscosity	l, lbm/ft*s
Therm. Cond.	l, W/m*K
Surf. Tension	l, lb/ft
Density	v, lbm/ft^3
Specific Volume	v, ft^3/lbm
Internal Energy	v, BTU/lbm
Enthalpy	v, BTU/lbm
Entropy	v, BTU/lbm*R
Cv	v, BTU/lbm*R
Cp	v, BTU/lbm*R
Sound Spd.	v, ft/s
Joule-Thomson	v, F/psia
Viscosity	v, lbm/ft*s
Therm. Cond.	v, W/m*K

In addition, the capability of back calculating temperature from a given enthalpy was also added as this function is needed within the drift-flux solver. Sub-cooled properties were evaluated and tabulated, but it should be noted that the sub-cooled property units available are analogous to the saturated properties available, but obviously not vapor conditions since sub-cooled conditions only exist in the liquid state.

The tabulation of sub-cooled properties created another difficulty which required determining what an appropriate interplay between fidelity and quantity of data was. After several scoping calculations it was decided that sub-cooled properties evaluated at 100 psia increments provides a good balance between accuracy and memory requirements, thus libraries were tabulated at 100 psia increments up to 2800 psia. Sub-cooled properties vary extremely linearly as a function of pressure; thus with the tabulated libraries of 100 psia increments, and one degree Fahrenheit increments at each pressure (100, 200, 300 psia … at 40, 41, 42 F... for each pressure state-point) a double interpolation between pressure libraries and temperatures is performed to evaluate the correct sub-cooled properties.

The main benefit to this tabulation is the speed up observed. Since the libraries were tabulated in a systematic and structured manner, it allowed for a programming scheme where the exact locations needed to interpolate for a data point are known based upon the temperature or pressure itself, such that the correct data points in the array of information could be directly pointed to eliminating the need for a binary search (or any other type of search implemented) for any property desired as a function of pressure or temperature. For the one data point extraction that is not a function of temperature or pressure, temperature as a function of enthalpy, a binary search algorithm was implemented.

Once the programming was completed a benchmark of the newly created steam tables was performed to ensure accuracy. For saturation conditions from 10.5 to 2800.5 psia in one psia increments, the error was nearly steady at 0.0001% for the vast majority properties, falling below 0.1% relative error at every state point. In addition, the same test was performed for saturation conditions in one degree Fahrenheit increments from 40.5 to 700.5. The results observed in this case were similar with over 99% of the evaluated properties registering 0.0000% error, reaching a maximum of less than 0.1% error up to the 691.5 degree Fahrenheit state point. Above 691.5 degrees Fahrenheit the error started to slowly grow up to a maximum of ~1.6% error for the specific heat capacity (Cp), while the majority of the other properties still remained at or below 0.05% error. This non-linear behavior for Cp was only observed at extremely high temperatures which approach the critical point of water, temperatures which are not encountered during standard LWR operation, and for which the errors are still small enough not to have a significant influence.

Finally, the same benchmark was performed for all sub-cooled conditions of which the library will be most frequently used (limited to operating conditions that represent a BWR up to operating conditions that represent a PWR, 950 to 2350 psia in 100 psia increments). Thus, all sub-cooled conditions from 40.5 up to saturation temperature, in one degree Fahrenheit increments, at the pressures aforementioned. Much analogous to the trend observed in benchmark of saturated conditions, it was observed that the vast majority of data points sampled (greater than 99%) resulted in errors less than 0.01% relative error, with the last two to three data points prior to saturation being reached resulting in the largest errors as the linear trend for data points (especially Cp) starts to become non-linear. The errors observed in these cases were believed to be so minuscule and infrequent that the library was accepted as appropriate for the representation of water properties. In addition, as will be discussed in the next section, the thermal-hydraulic benchmark against experimental data showed very good agreement, which serves as a supplementary validation of the water properties over both sub-cooled and saturated conditions

4.2 Thermal-Hydraulic Validation

4.2.1 Benchmark Overview

Upon completion of the thermal-hydraulic drift-flux solution scheme, of which a detailed description is provided in Chapter 3, a benchmark to serve as a check for the validity of the programming as well as the accuracy of the solution was performed. The benchmark used for this is the “OECD/NRC Benchmark Based on NUPEC BWR Full-Size Fine-Mesh Bundle Tests (BFBT)” [23] . The benchmark was conducted in two parts. First a benchmark of the hydraulics is performed, where single phase flow is passed through an 8x8 bundle without power. With a detailed description of the bundle design provided, the various required hydraulic parameters were able to be retrieved (equivalent diameter, heated diameter etc…), in addition locations of spacer grids as well as corresponding loss coefficients were provided. This allowed for an assessment of the accuracy in predicting pressure loss across a channel as water flows, prior to assessing the validity of the calculated void fraction. The second part of the benchmark consists of benchmarking the void fraction calculation against the measured values provided in the experiment, where the channel was supplied various power profiles. Thus this allows for an understanding of the accuracy when using the sub-cooled quality correlation (EPRI model or Saha-Zuber) as well as the void-quality correlation (Lellouche-Zolotar).

4.2.2 Experiment Description

Table 4.2 Benchmark Bundle Specifications

Bundle Specifications	
C2A	C2A
Array -x,y	8 x 8
Nrods	60
Pitch (in)	0.64
Heated length (in)	145.98
Channel Inside dimensions -x,y (in)	5.22
Inside Corner Radius (in)	0.31
Fuel Rod Radius (in)	0.24
Water rod Radius (in)	0.67
Fuel Rod Area (in**2)	12.46
Bundle Total Area (in**2)	27.13
Ax (in**2)	14.67
P-Wet (in)	115.81
P-heated (in)	91.28
De (4*Ax/PW) (in)	0.51
Dheat (in)	0.64

The entire length of heated fuel was the same lattice, an 8x8 bundle with the four center rods being replaced by one large water rod. In the bundle seven spacers were present, centered at axial locations 15.4, 3.22, 4.90, 6.58, 8.26, 9.94, and 11.62 feet. Each spacer was identical and was reported to each have a loss coefficient of 1.2, although there is a discrepancy regarding this which will be discussed in further detail later in the chapter. For the single phase experiments five different test cases were performed for the hydraulic test, P70027, P70028, P70034, P70035, and P70036. The fuel bundle used for experimental analysis was composed of the data provided in Table 4.2. Each of the five cases had different initial conditions and flow rates, which are given in Table 4.3.

4.2.3 Single Phase Results

The first benchmark consists of testing the hydraulic part of the drift-flux solution. While this does not help to assess the accuracy of the sub-cooled boiling and void quality correlations, this does serve to assess the accuracy of the staggered mesh scheme, going from the continuity equation, through the internal energy equation and through the momentum equation. In addition this can provide an assessment of the validity of the quoted spacer loss coefficients, which are also important for an accurate two-phase solution.

Table 4.3 Single Phase Experiment Initial Conditions

	Outlet Pressure		Inlet Temp		Flow Rate		Bundle DeltaP		Inlet Pressure
	MPA	psia	C	F	TON/HR	LB/HR	(kPA)	PSIA	psia
P70027	7.15	1037.02	284.9	544.82	20.3	4.475E+04	3.12	0.453	1037.47
P70028	7.16	1038.47	285.1	545.18	24.9	5.490E+04	4.59	0.666	1039.14
P70034	7.15	1037.02	284.8	544.64	59.7	1.316E+05	23.87	3.462	1040.48
P70035	7.16	1038.47	284.6	544.28	64.8	1.429E+05	27.77	4.028	1042.50
P70036	7.15	1037.02	284.8	544.64	69.9	1.541E+05	32.03	4.646	1041.67

From the five experiments listed in Table 4.3, the data associated with "Bundle Delta P" correlates with the total bundle pressure drop over the active test length and is one metric for the assessment of the accuracy of the drift-flux solver. This "Bundle Delta P" is represented by pressure tap "dp309" in the experimental data. In addition, several additional pressure tap locations were also recorded and used as benchmark experiments. One item that is important to note is that the total pressure drop over the ~146 inches is reported with the static pressure head subtracted out, so as to give a more detailed result of pressure loss mechanisms due to friction and forms losses. The first two results (Figure 4.1 and Figure 4.2) given below show the relative error generated with the use of two different spacer loss coefficient values for the two lower flow experiments.

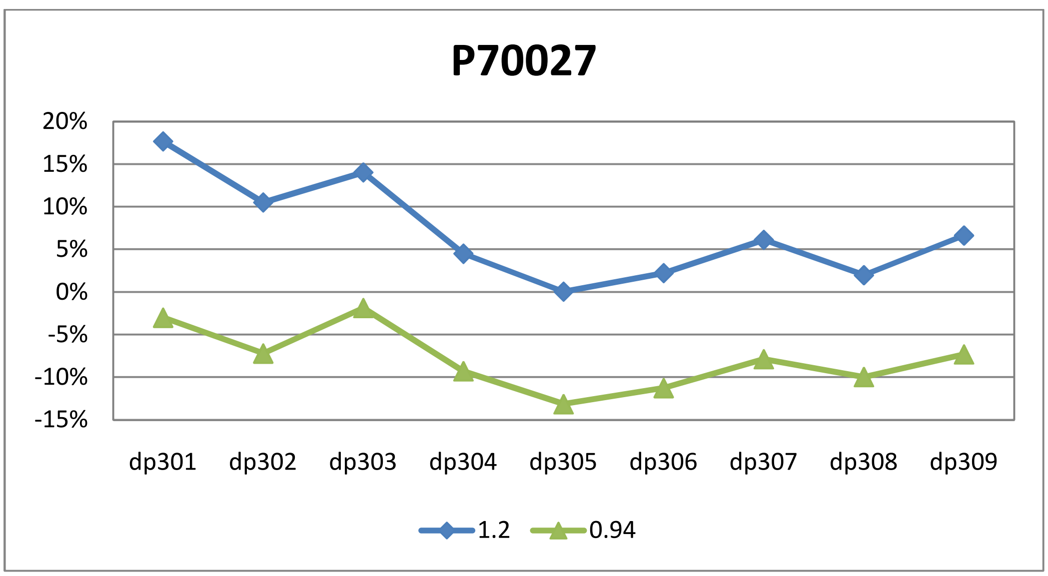

Figure 4.1 Single Phase Pressure Drop P70027 (psi)

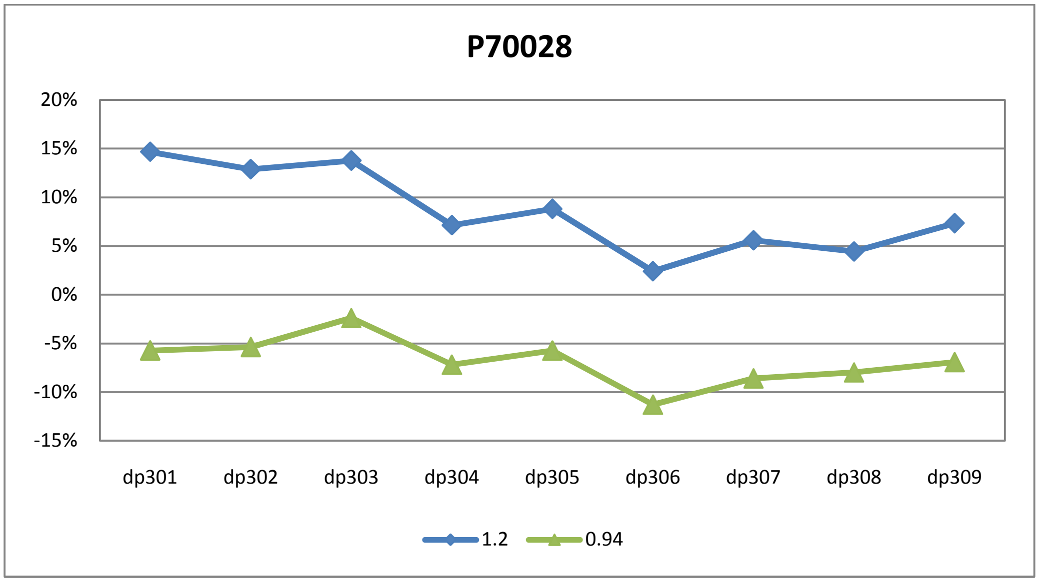

Figure 4.2 Single Phase Pressure Drop P70028 (psi)

The following charts (Figure 4.3, Figure 4.4 and Figure 4.5) show the relative error using the various loss coefficients for the three high flow cases. A discussion of the derivation and applicability of the loss coefficients will follow, as the accuracy of the solution depends strongly on the spacer loss coefficient. Observed is the trend of the error according to the recommended 1.2 loss coefficient growing as the flow rate increases, as well as the clear observation that a loss coefficient of 1.2 leads to an overestimate of the pressure drop. Since the primary mechanism for pressure drop for these two measurements is heavily weighted towards the local losses, the spacer loss coefficient will be the primary driver for pressure loss over the course of the experiment, and this spacer dependency will again be seen below in the Star-CCM+ simulation of one of the higher flow experiments.

Furthermore, a discussion of the loss coefficient was treated in detail by Gluck in [13] Here, a mechanism for calculating sub-channel loss coefficient is introduced, based on the method by Shiralkar and Radcliffe [31] First, individual sub-channel loss coefficients are estimated by hand from design drawings of the spacer grid, according to the Shiralkar and Radcliffe method [31] . These sub-channel loss coefficients are then weighted by the cross-sectional area occupied by each sub-channel to obtain an estimated average bundle loss coefficient via the parallel resistance method. Concurrently, experimentally derived results for the estimated bundle loss coefficient are used to compute a scaling factor that is then used to scale the computationally derived loss coefficient according to the scaling factor. Using this method, an average loss coefficient of 0.94 was determined and thus used as the alternate benchmark loss coefficient seen in the results.

It should be mentioned that in this report there were some doubts about the fidelity of the quoted 1.2 loss coefficient in the original experiment, noting that the results obtained using 1.2 were all overshooting the pressure drop estimates, which is similar to what was seen using the drift-flux model with a loss coefficient of 1.2. In addition, it is pointed out that the same loss coefficient was used for a geometrically different space grid. According to Gluck [13]

> "In the BFBT benchmark specification (Neykov et al., 2006) a constant bundle loss coefficient of 1.2 is given (remarkably the same value as for the geometrically quite different lantern type spacer grid). However, calculations based on this value lead to strong over estimations in pressure loss; whereas calculations with the above derived loss coefficients [0.94 bundle average] yield very good results."

Given the uncertainty in the space loss coefficient, with quoted values ranging from 1.2 to 0.94, the calculated results show good agreement with experimental results. The worst agreement occurred at a loss coefficient of 1.2, and high flow conditions, resulting in errors on the order of 11% and a low error of 6% on the low flow conditions, with reference to the total bundle pressure drop. On the flip side, when using a loss coefficient of 0.94, the high error occurred at low flow conditions and corresponded to an error of ~8% while the low error occurred at the high flow conditions and pertained to an error of ~4%. In addition, the computed pressure drop

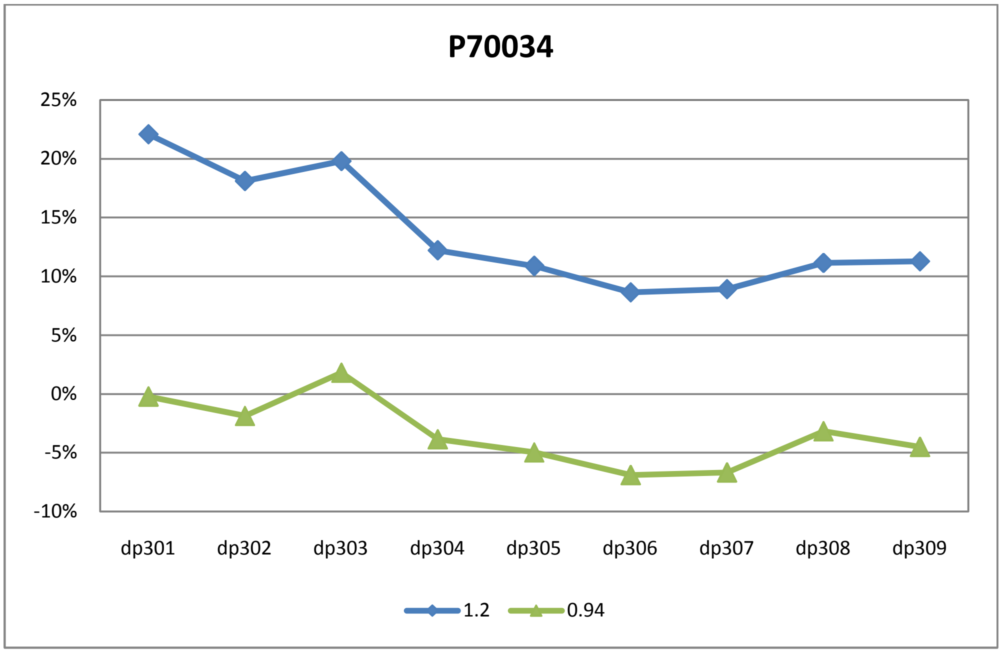

Figure 4.3 Single Phase Pressure Drop P70034 (psi)

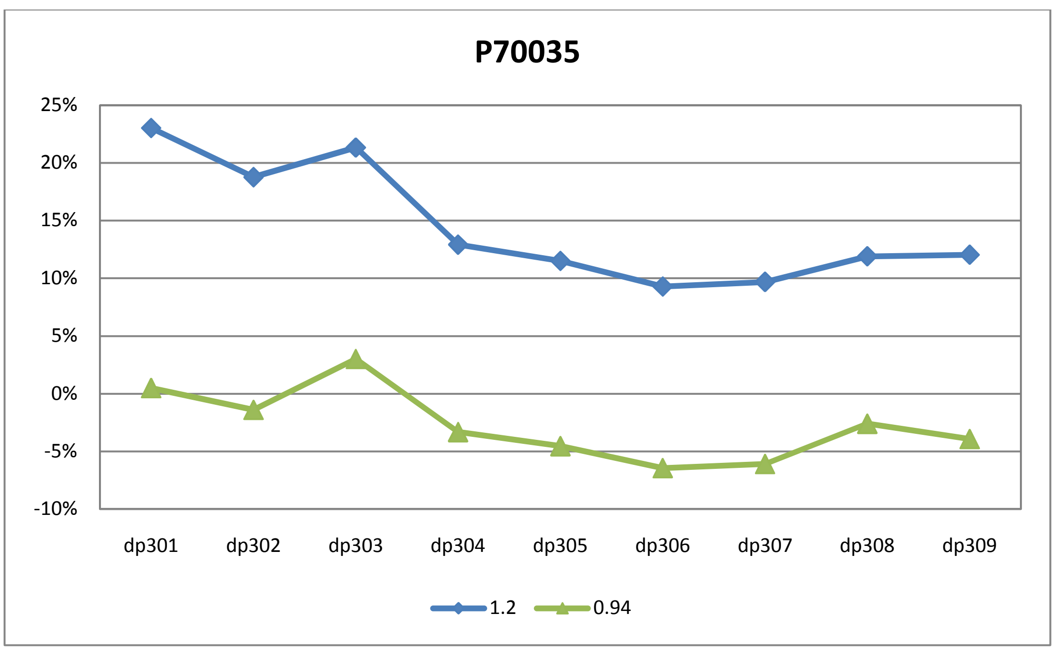

Figure 4.4 Single Phase Pressure Drop P70035 (psi)

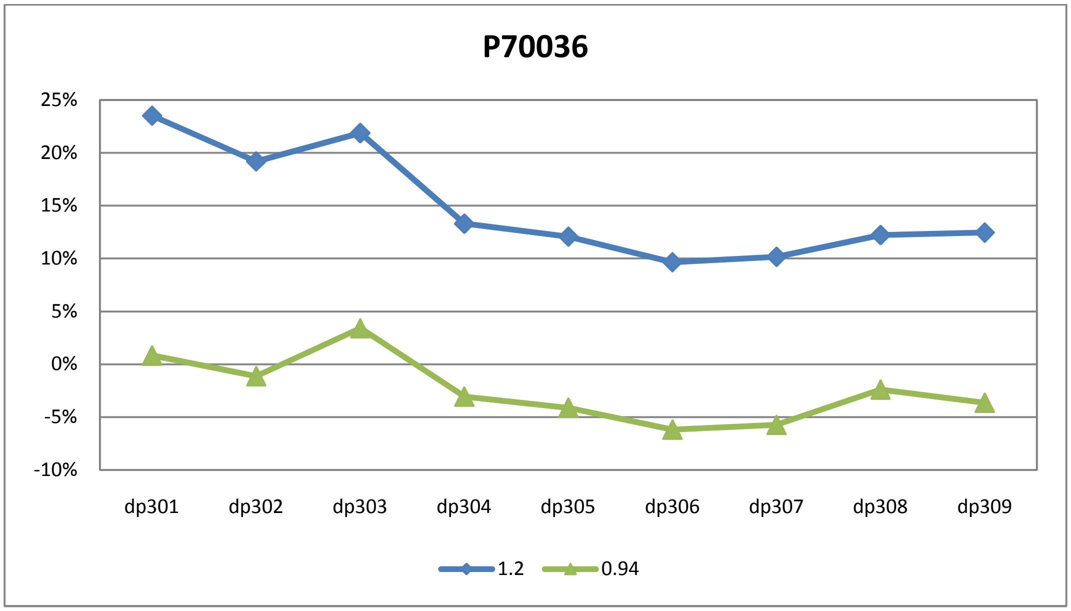

Figure 4.5 Single Phase Pressure Drop P70036 (psi)

profile up the channel was also observed to follow the same trend of the experimental results at both low flow conditions (experiment P70027) and high flow conditions (experiment P70036), as seen in the relative error pertaining to the intermediate pressure taps. In any event, the flow conditions typical of a BWR core are much closer to the high flow condition, represented by test case P70036, which when using a recommended loss coefficient of 0.94 gives a relative bundle pressure drop error of 4.5%.

One final test performed using the high flow single phase pressure drop experiment was a comparison of the pressure drop computed using the 0.94 spacer loss coefficient along with the drift-flux model against a Star-CCM+ model of the same bundle. The results are given in terms of a pressure differential, with each data point being the pressure solved at that location less the outlet pressure; such that the outlet result will be zero. Figure 4.6 shows the results of the simulation comparison, which shows excellent agreement between the two models. The main point of emphasis is that this experiment validates the 0.94 spacer loss coefficient. The total

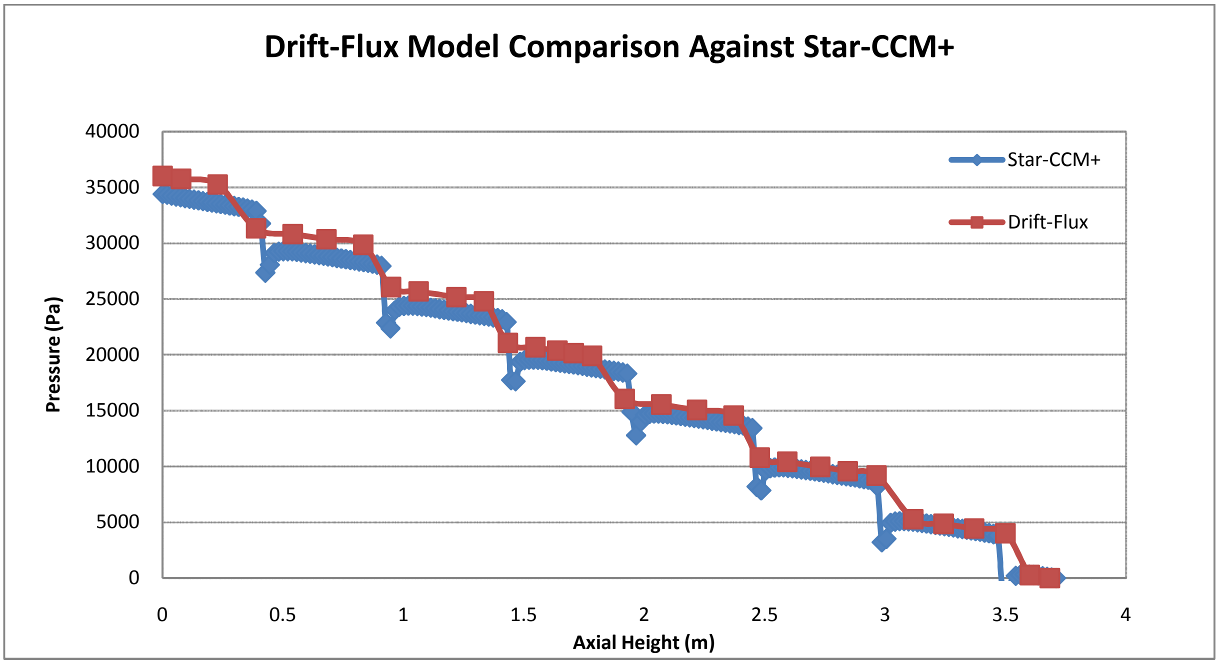

Figure 4.6 Drift-Flux Star-CCM+ Comparison

pressure drop across each of the spacer grids is nearly identical when comparing the results of the drift-flux model using a loss coefficient of 0.94, to the CFD model which includes a complete specification of the bundle and all geometrical intricacies and does not utilize a loss coefficient estimate.

4.2.4 Two-Phase Results

While benchmarking the drift-flux solver against single-phase pressure drop measurements serves beneficial to ensure correct programming and confirm the spacer loss coefficient, the intention of the code is to accurately model two-phase flow primarily to calculate the void fraction in each node, in order to then calculate the moderator density to finally obtain the correct homogenized nodal cross-sections. The benchmark experiment had a large matrix of available data with numerous degrees of freedom including outlet qualities varying from 2% to

25%, various flow rates, various operating pressures, as well as multiple axial power profiles. Due to this, two axial power profiles were chosen: one case with uniform heating as well as a bottom peaked power profile, which is representative of the power profile for BWRs at operating conditions. For each of these two power profiles, five test cases were used for a comparison of void fraction, yielding 10 test cases where the bottom peaked profile is shown in Figure 4.7. The uniform profile is not included since it would simply be a vertical line centered at one. In addition the bundle and experimental physical specifications are the same as given above in Table 4.2.

The experimental mechanism for determining the outlet void fraction is composed of taking high resolution pictures, in these cases using a CT scanner, and using software to compute the volume occupied by the vapor phase as well as the liquid phase in each axial slice [23] . Using this method and the initial conditions given above, the measured outlet void fraction is provided below along with the calculated void fraction by using the drift-flux model for the five

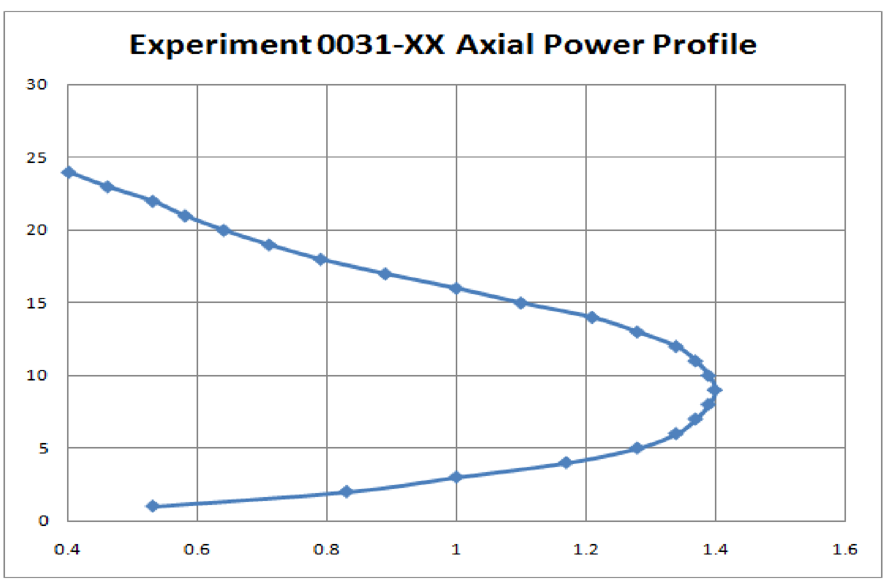

Figure 4.7 Bottom Peaked Power Profile

experiments with each of the two power profiles is given in Figure 4.8. Those five experiments that begin with the 0011-XX are those which utilized a uniform power profile, while those experiments that begin with the 0033-XX numbering scheme are those which were simulated with the bottom-peaked power profile. The initial conditions for both experiments are given in Table 4.4, where the power is the total power in the bundle which is then scaled by the relative power in each node. Equal power distribution is present in each node for the uniform case and split nodally according to the previously shown bottom peak profile for the bottom power peaked cases.

As can be inferred by the increasing void fraction, the power across each experiment increases with increasing within experiment number, meaning that 0011-61 is higher power than 0011-59, and so forth. Of particular interest is the decrease in error as the void fraction increases, hence relative errors on the order of 30% are present at low void fractions of 20%, yet the error when increasing above 70% shrinks to be on the order of 1 to 2%.

Table 4.4 Two-Phase Experiment Initial Conditions

	Inlet Pressure		***Inlet Temp***		***Flow Rate***		***Power***	
	MPA	**psia**	**C**	**F**	**TON/HR**	**LB/HR**	**MW**	**BTU/hr**
0011-53	7.21	1046	278.6	533.5	54.47	1.20E+05	1.24	4.23E+06
0011-55	7.21	1046	278.5	533.3	54.03	1.19E+05	1.9	6.48E+06
0011-57	7.19	1043	278.6	533.5	54.84	1.21E+05	2.59	8.84E+06
0011-59	7.24	1050	277.9	532.2	54.96	1.21E+05	4.87	1.66E+07
0011-61	7.28	1056	277.9	532.2	54.79	1.21E+05	6.44	2.20E+07
0031-15	7.21	1046	278.4	533.1	54.97	1.21E+05	1.23	4.20E+06
0031-16	7.22	1047	278.4	533.1	55	1.21E+05	1.92	6.55E+06
0031-18	7.23	1049	278.4	533.1	54.79	1.21E+05	3.52	1.20E+07
0031-20	7.22	1047	278.1	532.6	54.83	1.21E+05	4.86	1.66E+07
0031-21	7.25	1052	275.5	527.9	54.9	1.21E+05	6.45	2.20E+07

Practically, this result is beneficial as the most reactive fuel bundles in the core will experience void fraction values greater than 70%, rather closer to 80%, where the drift-flux model produces the most accurate results. In addition, the quoted uncertainty for the void fraction measurement test was 2%, thus the two very high void cases nearing 80% are both within the uncertainty of the experimental results. Figure 4.9 shows a graphical representation of the uncertainty that would be induced into a density calculation as a result of the uncertainty in void fraction, as well as the accuracy potential when taking the 2% uncertainty into account and propagating this through to the density calculation, using data at 1045 psia and 550 °F which is very representative of BWR operating conditions. This is an important assessment since the void fraction calculation is performed for the primary purpose of determining the correct moderator (water) density in order to obtain the correct macroscopic cross-sections.

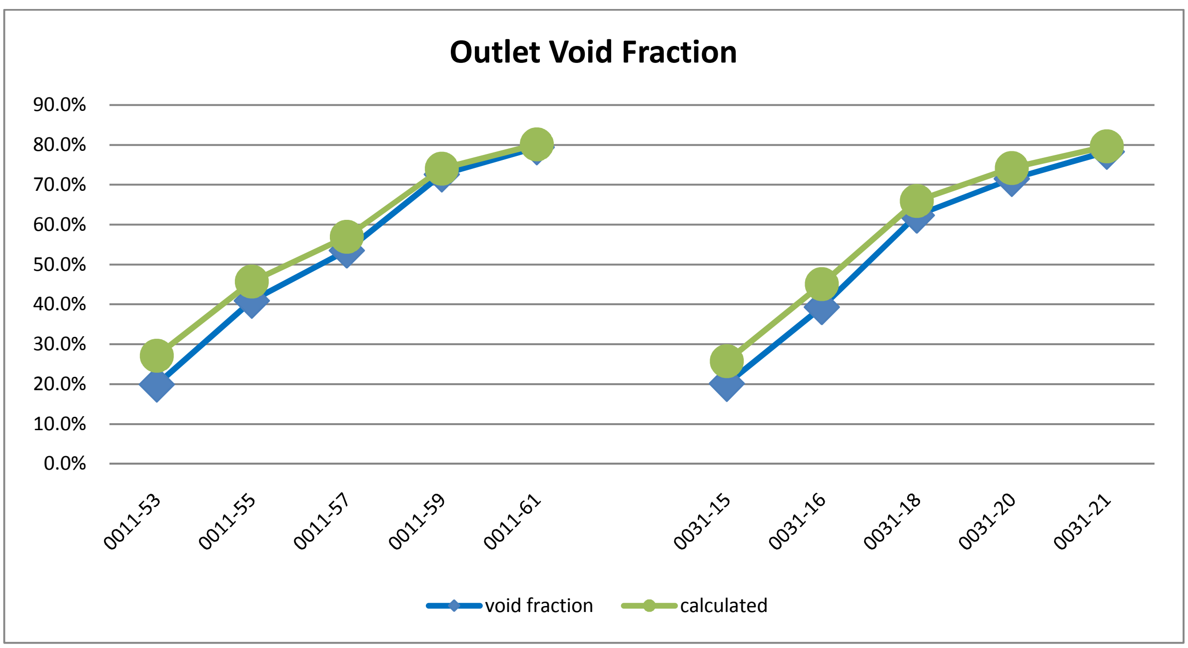

Figure 4.8 Outlet Void Fraction

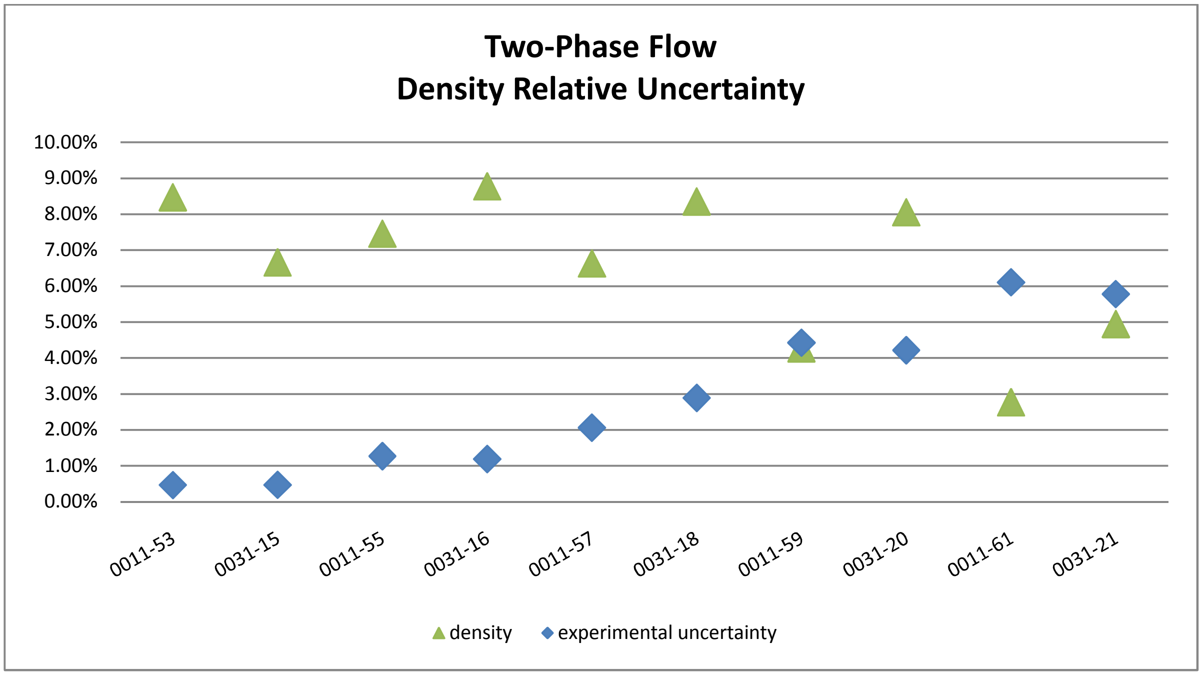

Figure 4.9 Two Phase Benchmark Density Results

Notice the change in the magnitude of the uncertainty for the low void fraction experiments, 0011-53 and 0031-15. Uncertainties that were on the order of 30% in void fraction decreased to less than 10% in moderator density. To further quantify the effect that the uncertainty in void fraction will ultimately have on core neutronics, which is the primary purpose in calculating void fraction, lattice physics simulations were performed at void fractions representative of three of the experiments. In these simulations, k_∞ was calculated at the experimental void fraction as well as at the calculated void fractions. These data were then used to assess the uncertainty introduced in the core neutronics since k_∞ serves as "catch all" for important neutronics parameters affected by void fraction. Experimental and calculated results for experiments 0011-53, 0011-55 and 0031-20 were used, where the simulations were performed with burnup extending out to 45,000 MWD/MTU to investigate any possible propagated uncertainty, with the results given below in Figure 4.10.

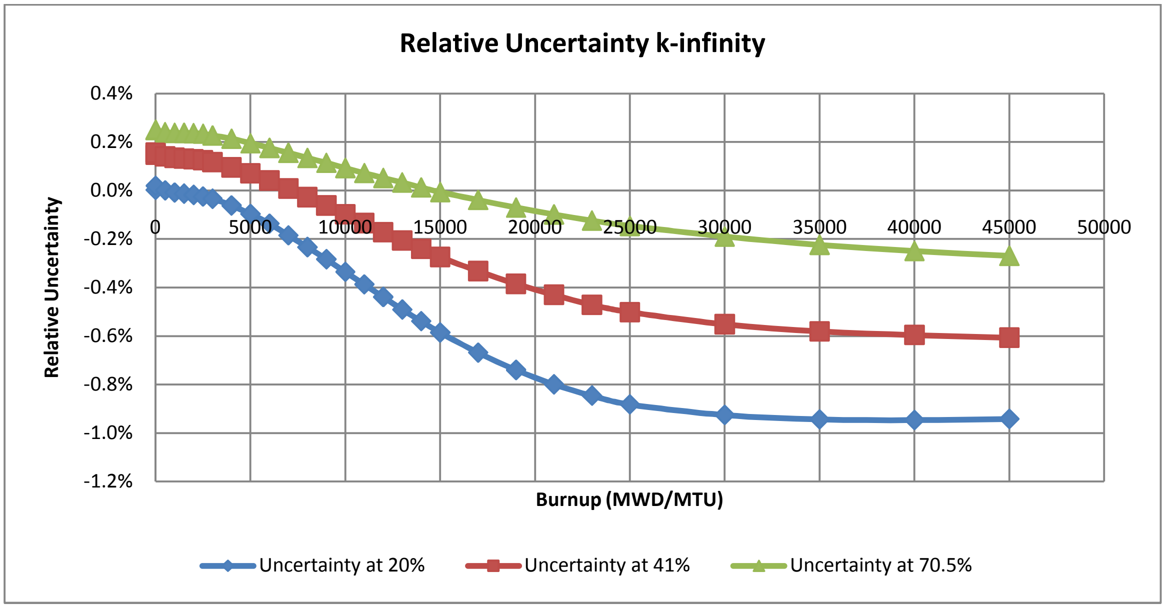

Figure 4.10 Two Phase Benchmark Void Fraction Propagated Error

At low burnup, typical of bundles in once-burned state, the uncertainty for all three bundles is low, and actually decreases for two of the cases during the early burnup. Following this early behavior, all three tend to increase slowly and move towards an under-estimate of reactivity due to the overestimate of void fraction. All appear to approach an asymptotic uncertainty.

In addition to the outlet void fraction being measured using a CT scanner 50mm above the end of active fuel height, three axial locations also had densitometer readings to assess the accuracy of the void fraction profile up the heated length of fuel. For the comparison of the axial void fraction variation, only three of the five experiments referenced prior for each of the power profiles (bottom peaked and uniform) are used. The lowest power, middle power and highest power experiments were used for the comparison. This allows for an accurate assessment of the drift-flux model over a wide range of power, while limiting to some degree the amount of data required to be reported. Figure 4.11 and Figure 4.12 show the results for the uniform power profile and bottom peaked power profile, respectively.

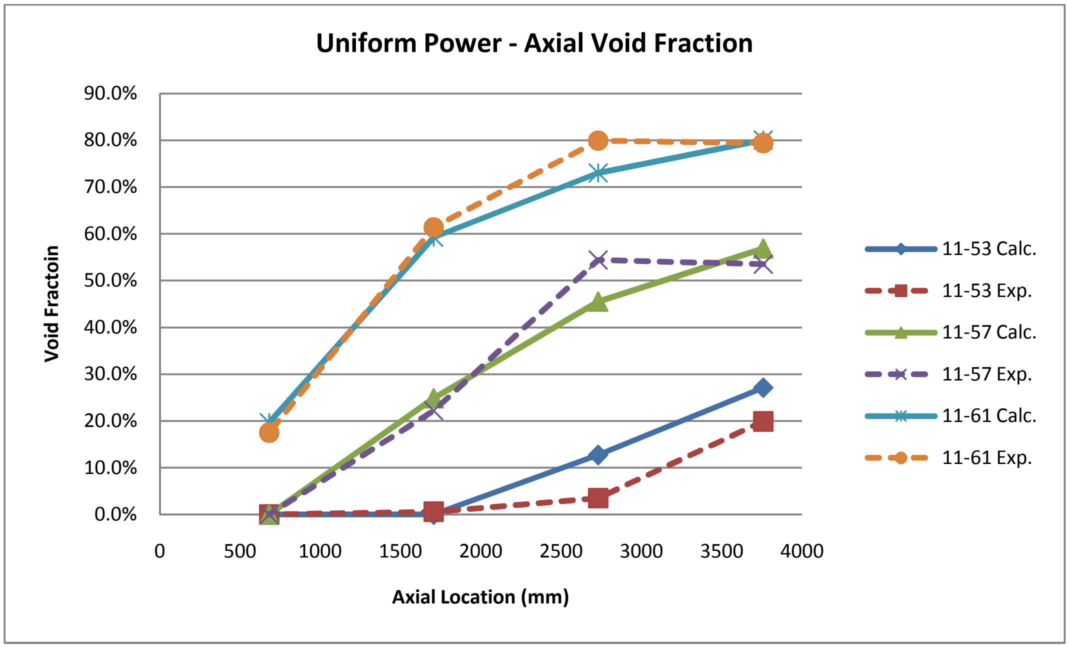

Figure 4.11 Axial Void Fraction Variation - Uniform Power

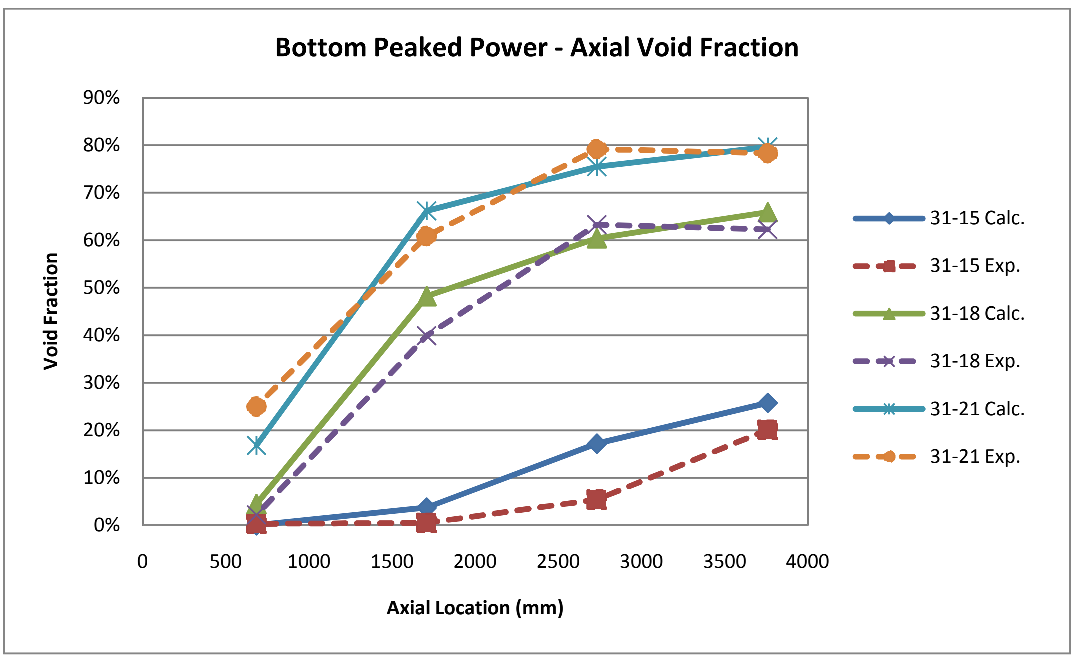

Figure 4.12 Axial Void Fraction Variation - Bottom Peaked Power

Practically, when coupling the thermal-hydraulic solver to the full 3-D core simulator and benchmarking against known core configurations and core loading patterns, an implicit benchmark will be performed; albeit a benchmark that has multitudes of sources of uncertainty beyond the thermal-hydraulic solution.

4.3 Coupled Neutronics and Thermal Hydraulics Validation

4.3.1 NESTLE Input

In the process of adding BWR modeling capabilities to NESTLE, as well as the adding of an ORIGEN microscopic depletion model, numerous new inputs were required. One of the enhancements that accompanied this work was the conversion of the input style into SCALE style input, using the same types of block structure seen in other SCALE codes such as TRITON, NEWT, KENO and others. Following this same convention all NESTLE BWR models must use the new SCALE style input. Legacy input decks are still compatible with NESTLE, but any new features are only accessible with new SCALE style input. Attached in Appendix A – Peach Bottom II Cycle 1 Input Deck is the input deck used for the BWR Peach Bottom II Cycle 1 model which illustrates this new input style.

4.3.2 Peach Bottom Benchmark Description

Upon the completion of the drift-flux model, as well as the flow redistribution model the key question is whether these developments are accurate. The benchmark chosen for the coupled neutronics and thermal-hydraulics test was an EPRI report regarding the Peach Bottom Unit 2 Cycle 1 core [18] . This cycle is somewhat of an anomaly of a core with respect to the control blade movements and power changes, when compared against modern core designs, but with the vast publicly available operating data, as well as TIP (traveling in-core probe) data, it serves as an excellent reference. In addition, there are various power changes and flow changes which allows for benchmarking over a wider range of thermal-hydraulic conditions.

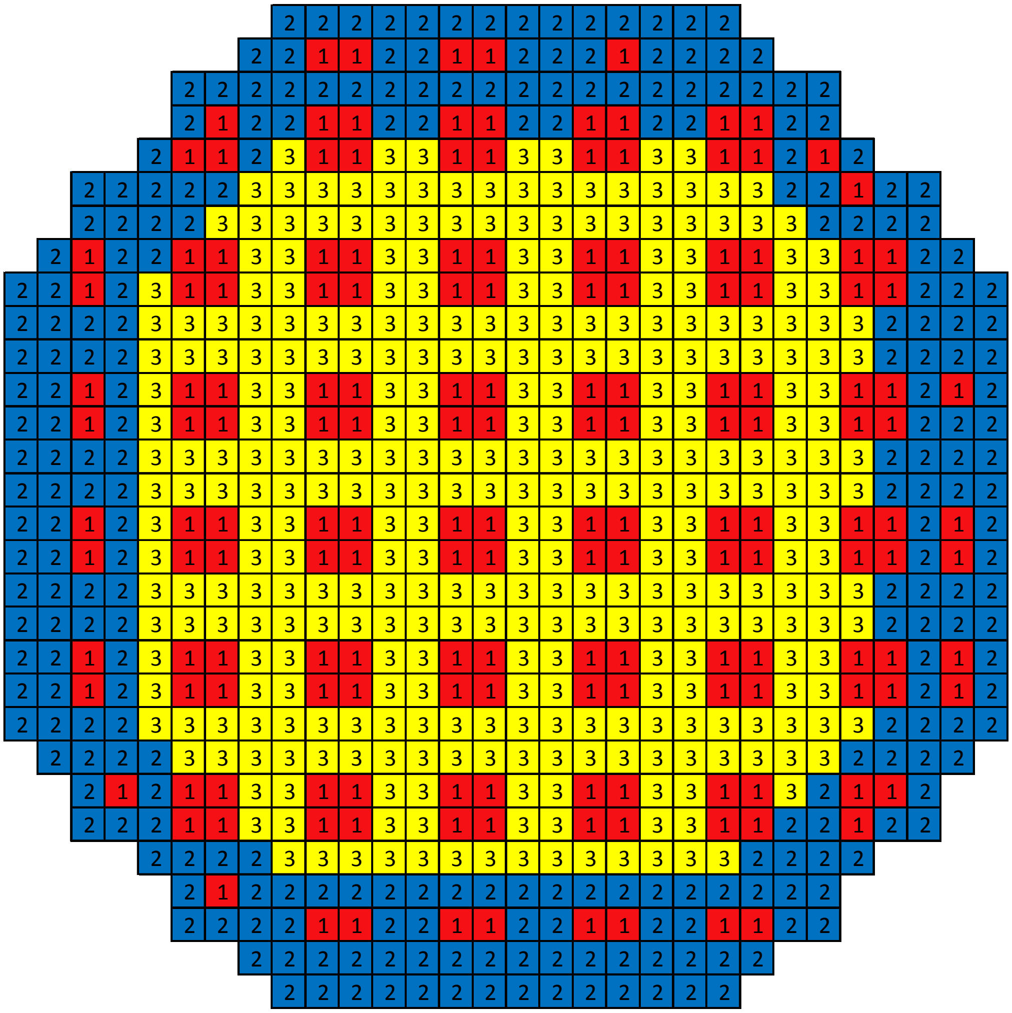

Figure 4.13 Peach Bottom Cycle 1 Core Loading Pattern

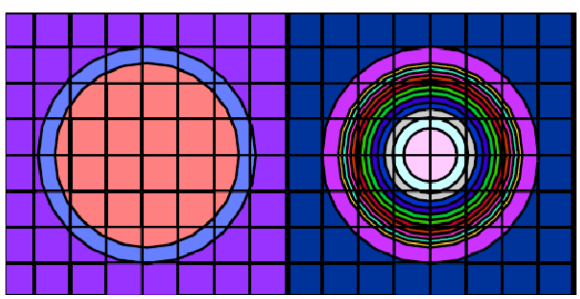

Figure 4.14 Gadolinium Pin Design

Peach Bottom II Cycle 1 is a large 764 bundle core, with a rated power of 3293 MW, a rated flow of 102.5 Mlbm/hr and 185 control rods. Inlet pressure is estimated to be 1050 psia, with the inlet enthalpy being 521.3 BTU/lbm. The core loading pattern, contrary to modern loading patterns, is not symmetric in any dimension, half-core, quarter-core, neither mirrored nor rotational. Three different bundle types are present in the core. Bundle type 1 is enriched to 1.10% in ^{235}U and has no gadolinium rods present, bundle type 2 is enriched to 2.50% with four gadolinium loaded rods, and lastly bundle type 3 is also enriched to 2.50% with five gadolinium loaded rods. The cycle 1 core loading pattern, illustrating the various bundle types, is given here as Figure 4.13.

The lattice physics code used to generate cross-sections for this cycle 1 simulation is TRITON, one of the codes in the SCALE suite. While there are three bundle types used in the loading pattern, these bundles do not all have uniform loading axially. Bundle type 1 is composed of only one lattice over the entire length, bundle type 2 is composed of two different lattice types and bundle type 3 is composed of three different lattice types. The lattice loading, geometrical, mesh and material definitions used for bundle type 1 is shown here in Figure 4.15, as an example. It should be noted that bundle type 1 did not have any gadolinium loading, while bundle types 2 and 3 do have gadolinium present. Due to the extremely high absorption cross section of gadolinium, numerous unique material definitions for one single gadolinium pin is needed to accurately model the neutron absorption and depletion of gadolinium. Due to the older nature of the bundles, being 7 x 7 designs, the fuel pins have a larger radius than more modern designs, requiring more gadolinium rings. Given that the radius is approximately 50% larger than current designs, which can be modeled with eight unique material rings of equal volume, these older and larger pins were modeled using 12 unique material rings of equal volume. Using this multi-ring approach, illustrated in Figure 4.14 and including a standard non-gadolinium loaded pin adjacent for reference, the gadolinium is allowed to burn out in an “onion ring” fashion which simulates reality much better than a homogenized depletion for the pin. The state point dependent parameters required for input throughout the cycle (excluding rod patterns) are given in Figure 4.16.

Cycle 1 rod patterns at each state-point are included in the report, but only the initial rod pattern will be listed below in Figure 4.17; if further rod patterns are needed the aforementioned EPRI report contains the full listing. The numbers given indicate the number of notches inserted (from the bottom), where each notch is three inches. Also in BWR cores the control blade occupies four fuel bundle locations, thus for each control rod location four fuel bundles are within the control cell, with the nomenclature referencing the top left bundle. In addition, listed in Figure 4.18 is a data sheet that shows the active nature of cycle 1, with power and flow changing almost daily while the rod-patterns hold much more constant.

In reference to core flow rate specification, bypass flow rate is an important parameter in BWR cores and needs some clarification. Since BWR bundles are canned, meaning there is a box wall that encloses the fuel rods within the lattice, there are two flow rates of importance: the flow in-bundle and the flow outside of the bundles, and it is this outside flow that is called the bypass flow. In modern core designs there are also water rods designed in the bundle to increase moderation, and there appears to be no general consensus if bypass flow does or does not include water rod flow. In NESTLE, the bypass flow represents the total flow outside the bundles, as well as the flow inside the water rods and should be computed and input as such. For Peach Bottom Cycle 1, none of the bundles were designed with water rods present so it is a moot point, but since NESTLE is capable of modeling modern reactor designs as well this should be mentioned to avoid confusion.

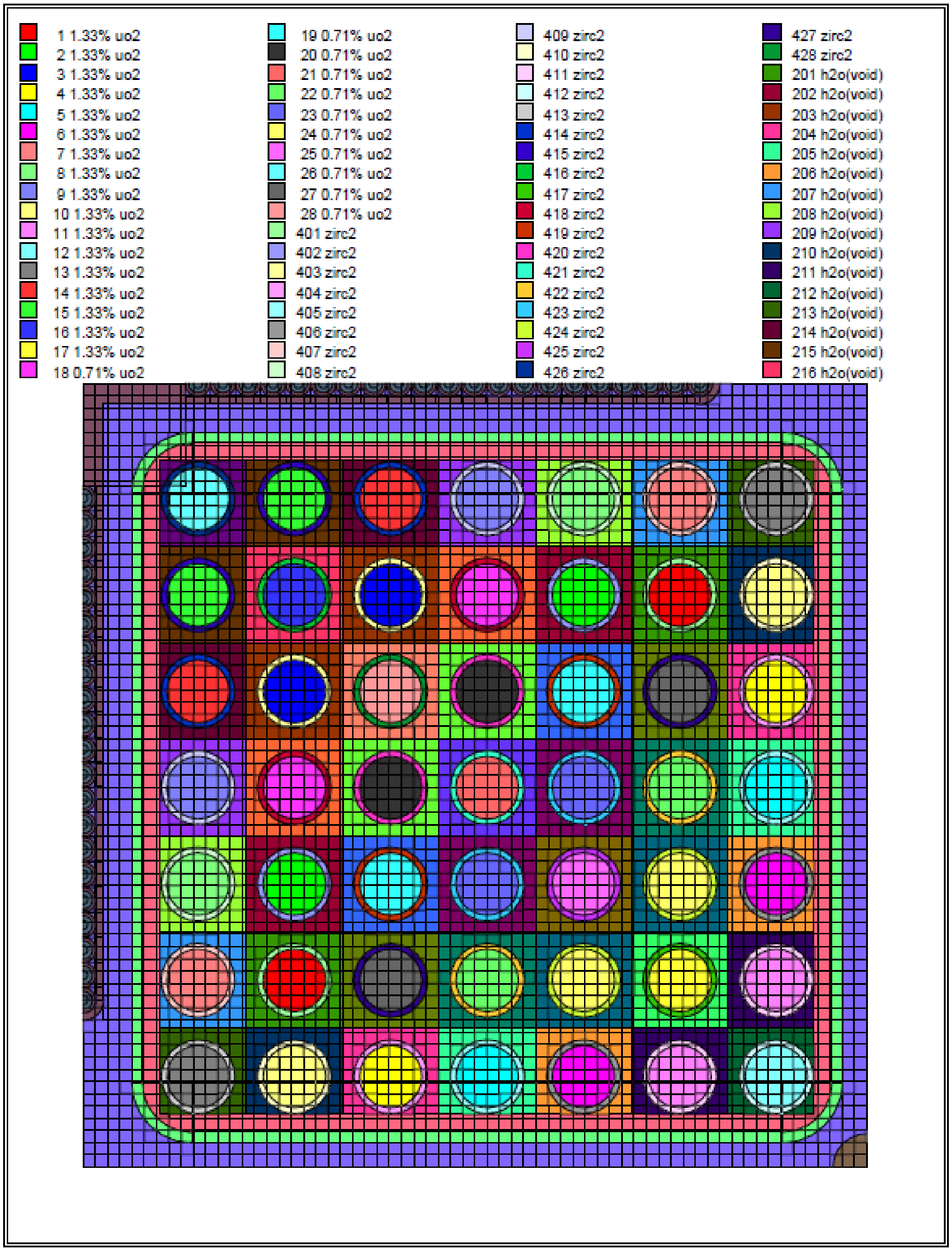

Figure 4.15 Lattice Type 1

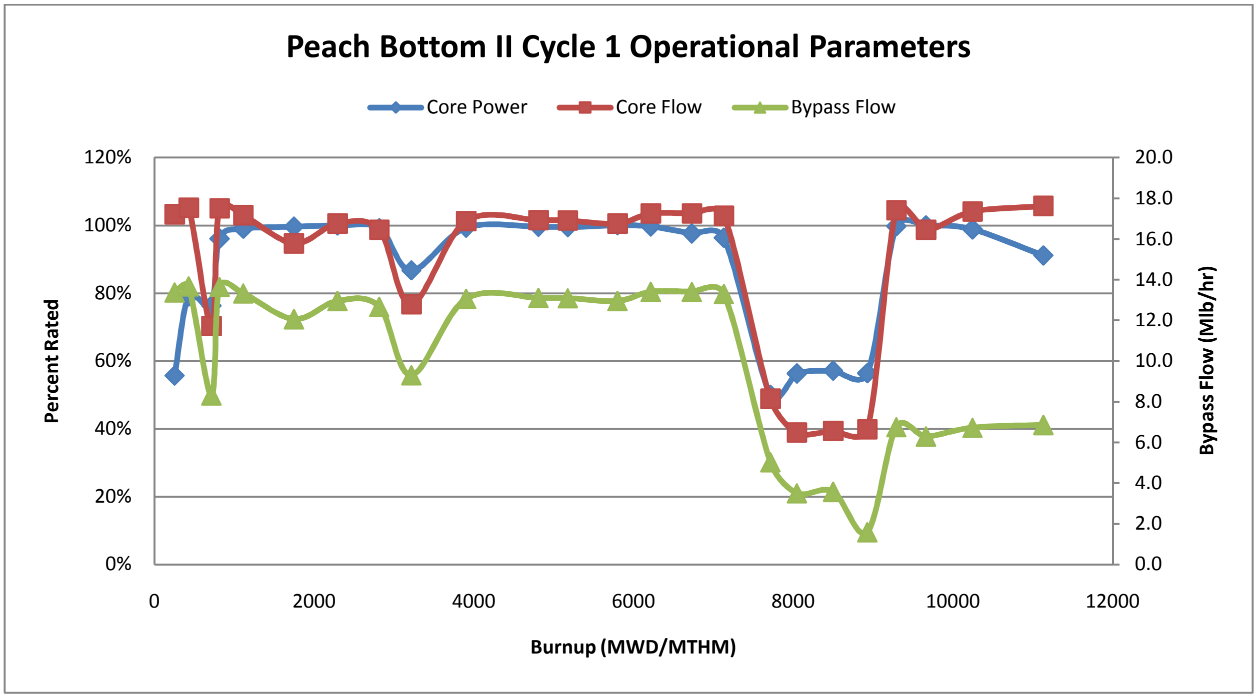

Figure 4.16 Peach Bottom II Cycle 1 Operational Parameters

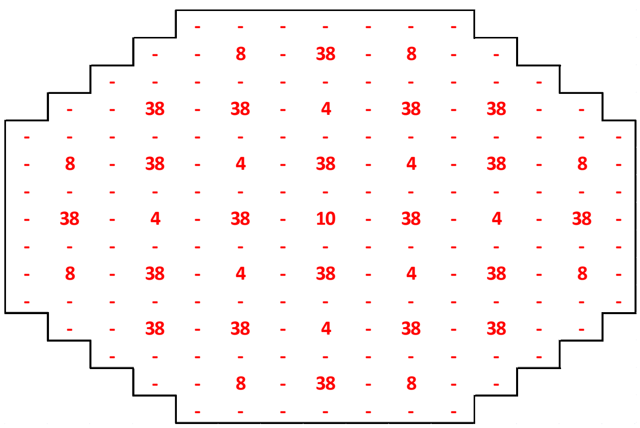

Figure 4.17 BOC Control Rod Pattern

In a BWR, flow profiling is accomplished via designing inlets and tie plates to control the pressure drop across each channel via local losses at these components. Since two-phase pressure losses are greater than single phase pressure losses, the natural inclination is for the flow to divert away from the hot channels to the lower power channels which are typically located on the periphery. To help redistribute this flow to the center of the core, the orifice loss coefficients used on the peripheral bundles is typically designed to be much greater than the orifices for the internal bundles. In addition, different lower tie plate designs may be used to divert flow to, or away from, certain bundles. Figure 4.19 shows the orifice and lower tie plate specifications for Peach Bottom II Cycle 1.

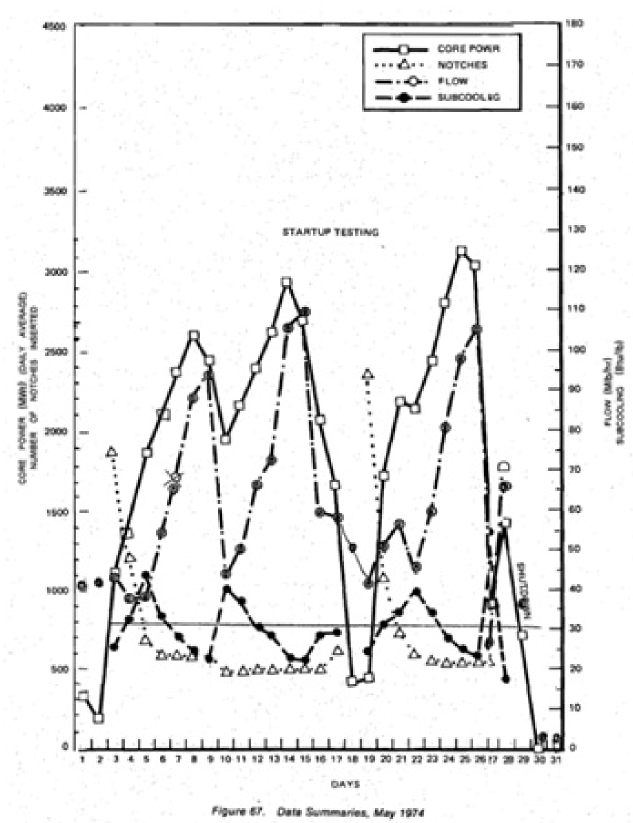

Figure 4.18 Peach Bottom II Cycle 1 Data Summary

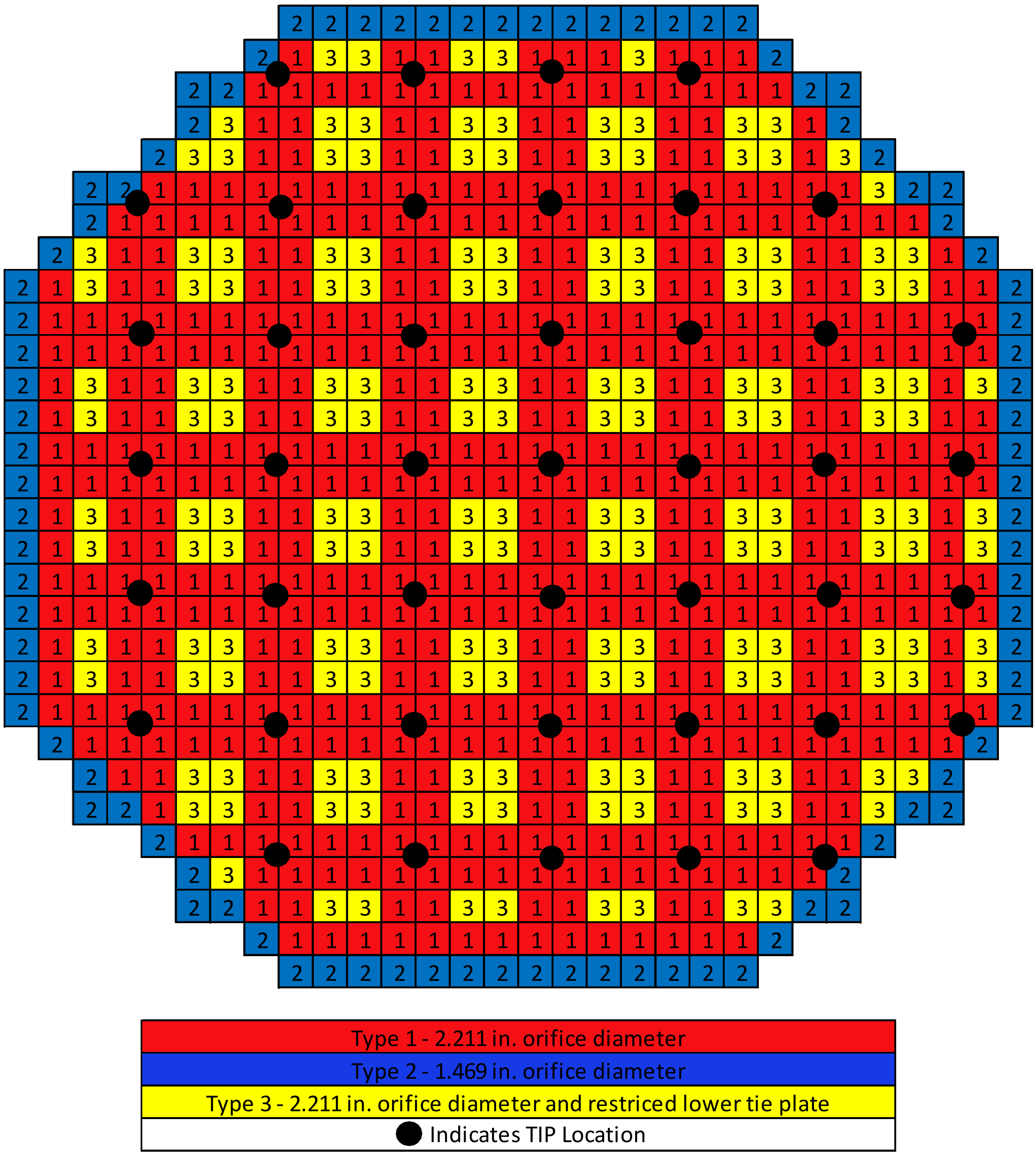

Figure 4.19 Peach Bottom Cycle 1 Orifice and TIP Locations

Lastly, to correctly capture the effects of neutron reflection, cross sections for water with conditions at the inlet (thus slightly sub-cooled conditions) was placed as an axial reflector nine inches below the active fuel and ~12 inches (two extra radial nodes) on the periphery. In the case of the top axial reflector, homogenized cross-sections calculated at 80% void were used nine inches above the fuel, since this is a valid representative void fraction for a BWR at hot operating conditions.

4.3.3 Peach Bottom Benchmark Results

The first benchmark performed of the Peach Bottom core was a test of initial conditions at start-up, without tracking the core through the entire first cycle. Using the given rod pattern at beginning of cycle (BOC), shown above, and the appropriate conditions of 55.7% rated power, 103.3% rated flow, with a bypass flow rate of 13.64 Mlbm/hr the first state point simulation was performed, which showed excellent initial agreement. The radial power distribution, shown below as Figure 4.20, gave very promising results. The peak radial power was ~1.33, where the rest of the radial power distribution demonstrated expected behavior. In the control cells where control blades were inserted, the center bundles of the core for example, the power was suppressed. In addition the power on the peripheral ring is low as well, and as expected, due to neutron leakage.

To ensure that the drift-flux model and flow redistribution model are working correctly, the channel by channel bundle flow matrix was checked to ensure several things. First, since the peripheral bundles have much smaller orifice diameters, the loss coefficient associated with them should serve to distribute less flow to the peripheral bundles, while diverting more flow to the central bundles. Secondly, since two-phase pressure losses are greater than single-phase pressure losses there should be more flow diverted to bundles in the presence of a control blade, and less flow to the bundles producing high power. In this sense, the flow map should be somewhat of an inverse mirror of the radial power map. Where there is high power, there

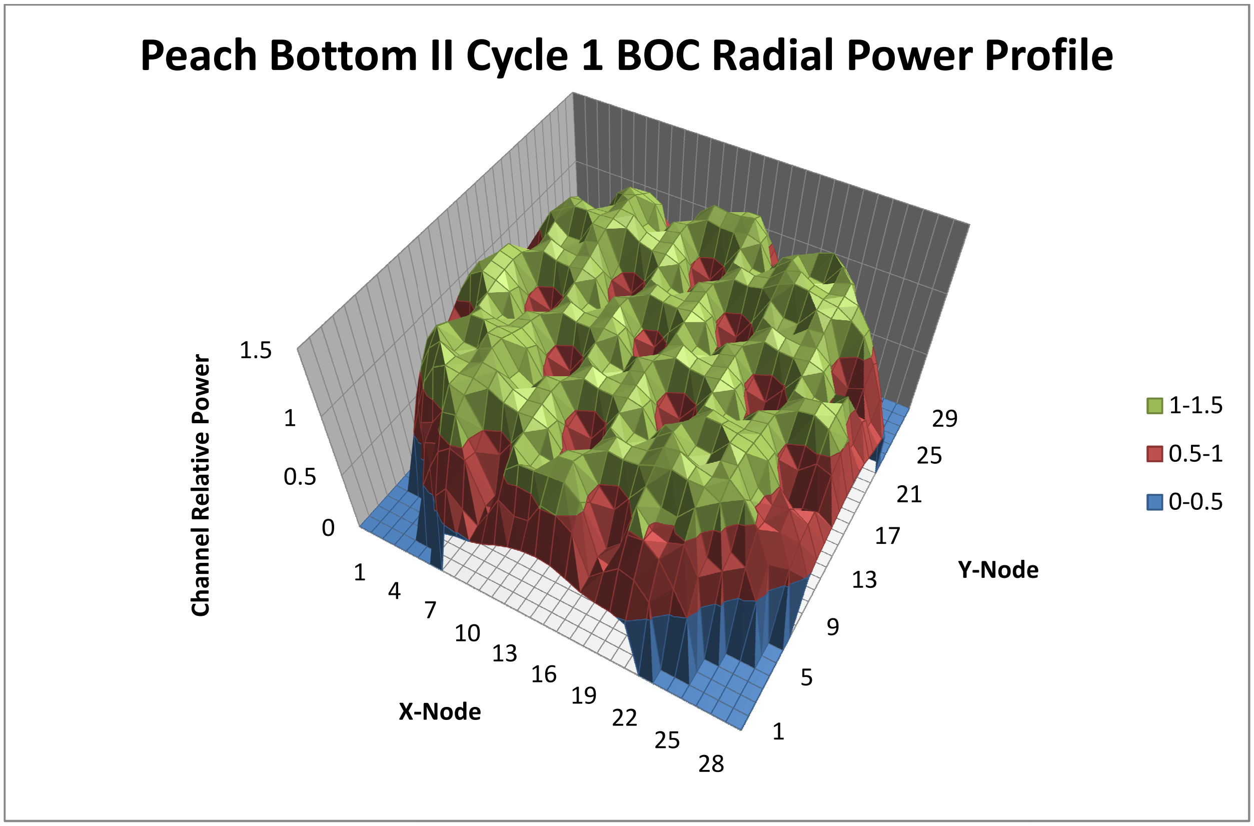

Figure 4.20 Peach Bottom Cycle 1 Radial Power Distribution

should be lower flows and vice-versa. The attached Figure 4.21 shows the flow distribution throughout the core. Right away it noticed that the periphery does have lower flow rates on the order of 70% of core average flow while the bundles in the very center of the core, in the presence of a deep control blade, demonstrate some of the highest flows. Thus the flow distribution implementation appears to be working correctly.

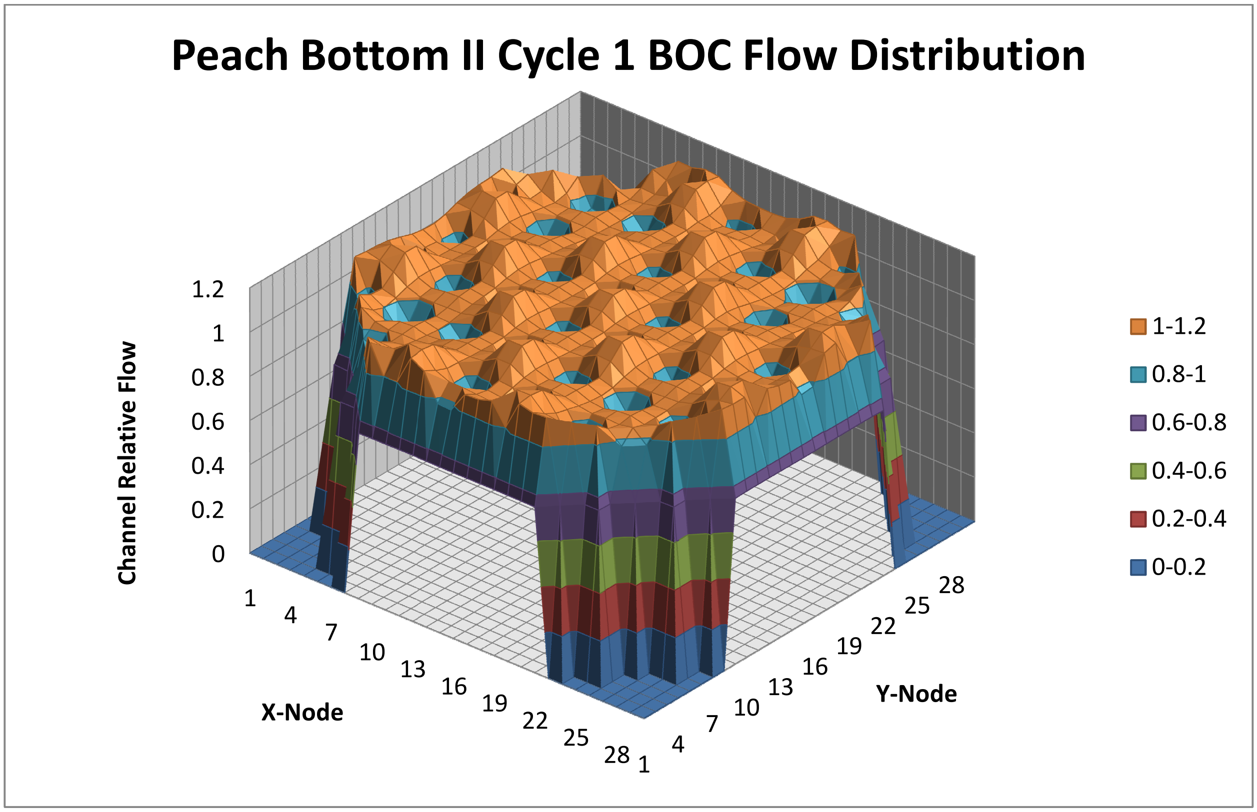

Figure 4.21 Peach Bottom Cycle 1 Core Flow Distribution

In addition to the radial features behaving as expected, axial variations also exhibited expected behaviors. Due to boiling in the core, typically BWR channels will see axial power profiles shifted to the bottom of the core, where neutron moderation is greater. This behavior is exhibited here in Figure 4.22, albeit with a double humped shape. While the neutron moderation is one factor affecting axial power profile, it is not the only factor. Hence the bottom peaked power shape is illustrated, but there is also a distinct peak towards the top of the bundle. While this would seem counterintuitive given the discussion about void fraction and the affect on power, another factor coming in to play here is the axial fuel loading. The fuel bundle this occurs in has an axial loading pattern with a higher gadolinium fraction from 48

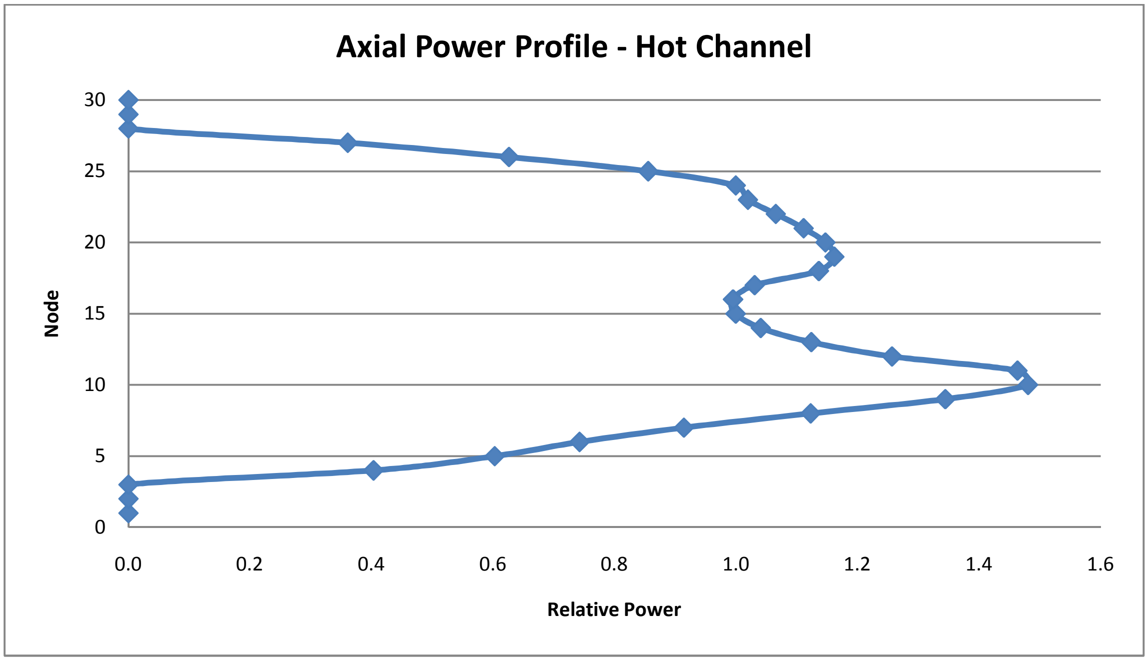

Figure 4.22 Axial Power Profile – Hot Channel

inches through to 84 inches. This gadolinium loading profile mirrors the power suppression in the axial power profile as expected, with the power increasing again at the end of the fuel height loaded with higher gadolinium inventories.

The axial void fraction for the most reactive channel is given below in Figure 4.23 for the channel corresponding to the axial power profile previously given. The first of several pertinent items, the three lowest nodes correspond to the lower axial reflector, thus no power is generated and no heating experienced. Following this, nodes four through nine represent the first 36 inches of active fuel, whereupon the onset of boiling occurs after node 10. Also worth noting is that the peak void fraction does not reach 60% void, which appears low for the hot channel since void fractions of up to 80% and higher are expected. The main reason for the suppression is the lower power state of the core, 55% rated power coupled with operating at rated flow conditions. During scoping calculations at full power and full flow, void fractions at

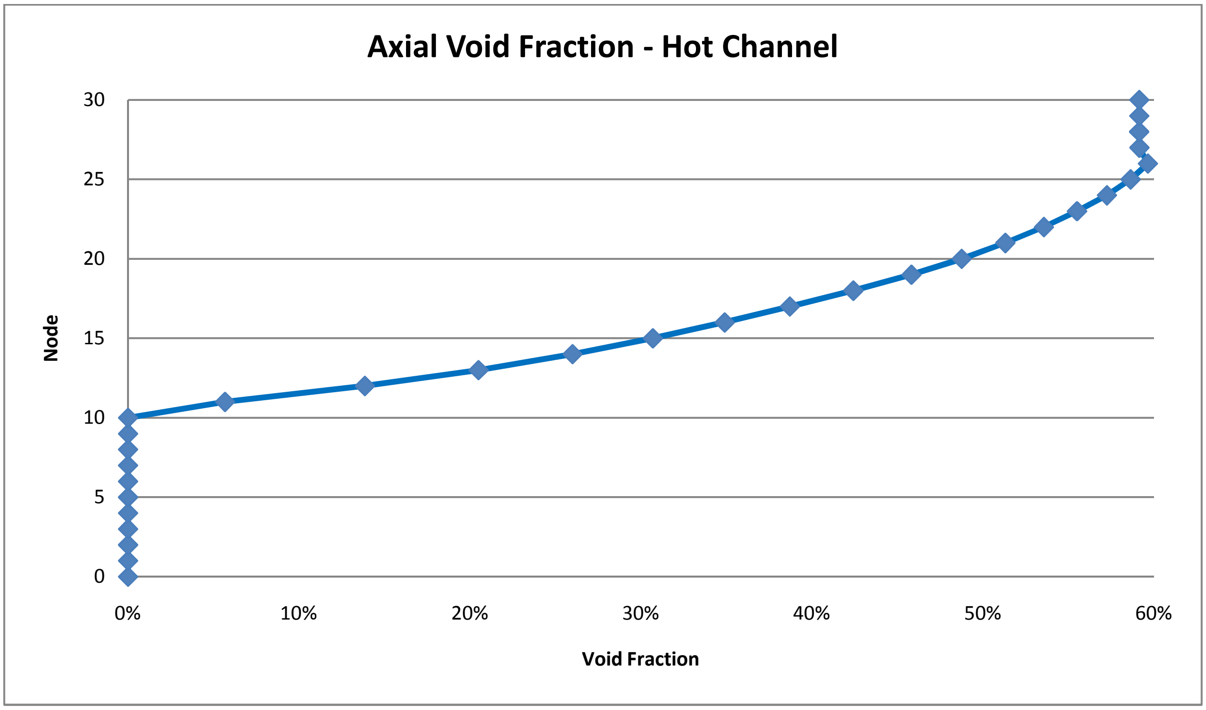

Figure 4.23 Axial Void Distribution – Hot Channel

or above 80% were observed in the hottest channel. When checking other major core parameters the benchmark shows favorable results. The nodal power peak, defined as the ratio of the power in the most reactive node to the power in the average node, is calculated to be 2.053, a very reasonable number for BWR operating conditions. Finally, since this is operating core data that is being compared against, the k_{eff} value throughout the cycle will be compared to 1.000. The accuracy to which the code predicts k_{eff} is one of the most important "catch all" parameters to benchmark against. The BOC calculation performed, once equilibrium xenon and samarium conditions are achieved, gave a value of 1.005934 for k_{eff}, indicating very good BOC agreement. Initially the core was modeled with historically available TRITON input decks for the lattice physics computation, where previous work and simulations had been performed on this Peach Bottom II Cycle 1 core. The initial depletion results from NESTLE when utilizing cross-sections obtained from these input decks were not as close to unity as hoped. Upon further inspection it was determined that two items stood out in the input decks that needed to be corrected. First, and most importantly, the gadolinium loading was incorrect. ^{157}Gd has an enormous neutron capture cross-section, the highest of all stable isotopes, and second only to ^{135}Xe in all known isotopes. With a thermal fission capture cross-section on the order of 61,000 barns for ^{155}Gd and 255,000 barns for ^{157}Gd, any inaccuracy in the loading can greatly affect the calculation. As it turns out, the original gadolinium loading input was based while assuming the weight percent prescribed, 5% for example, was solely the weight percent of Gadolinium in the fuel, whereas it is actually the weight percent of the gadolinium oxide (Gd_2O_3). As a result, the amount of gadolinium in the fuel was being slightly overestimated, which is extremely important due to the enormous capture cross-section. The second item that was discovered was that the fuel pin loadings had a homogeneity approximation, which assumed that all fuel pins of the same enrichment could be depleted as a uniform mixture or an average depletion for all. This was refined such that each fuel pin along the symmetric diagonal would be a unique fuel mixture and depleted as thus. These two items were corrected and cross-sections were regenerated and the Peach Bottom II Cycle 1 core follow performed. The first predictable change was that the BOC value for k_{eff} slightly increased due to the removal of a small fraction of gadolinium. While the change in k_{eff} at BOC was small, the burnup dependent effects are much greater due to the changing control rod patterns. If the gadolinium is present in the wrong quantity, the burnout rate will be different from reality which will in turn throw the k_{eff} estimation off significantly as control rod patterns are adjusted for reactivity control. Figure 4.24 shows both the k_{eff} behavior obtained initially and subsequently following the lattice refinement. It is clear that the corrections and upgrades to the lattice inputs greatly improved the solution in the desired direction. At virtually every exposure point, the solution moved closer to the desired outcome of unity. The lowest reactivity point rose from 0.975 to 0.985, occurring at the middle of the cycle; similarly, the highest reactivity point dropped from 1.11 to 1.007, where this reduced the reactivity swing from an original value of 0.135 down to 0.022. While the lattice refinement had the desired outcome of flattening out the k-effective prediction throughout cycle, the bias from unity is still further off than would be desired. The reasons for this are still not clear, with several potential reasons for the drift observed. First and foremost, this cycle is by far not traditional in operational characteristics, with power and flow maneuvers extremely frequent between state points, as evidenced by data sheet seen in Figure 4.18 with the power and flow changing daily. The downstream effects of not capturing this accurately could result in incorrect nodal burnup distributions occurring. While the average burnup will still be captured by the core, higher or lower flow and power combinations will result in a shift of the power being produced lower or higher up in the active fuel; deviating from the true burnup distribution.

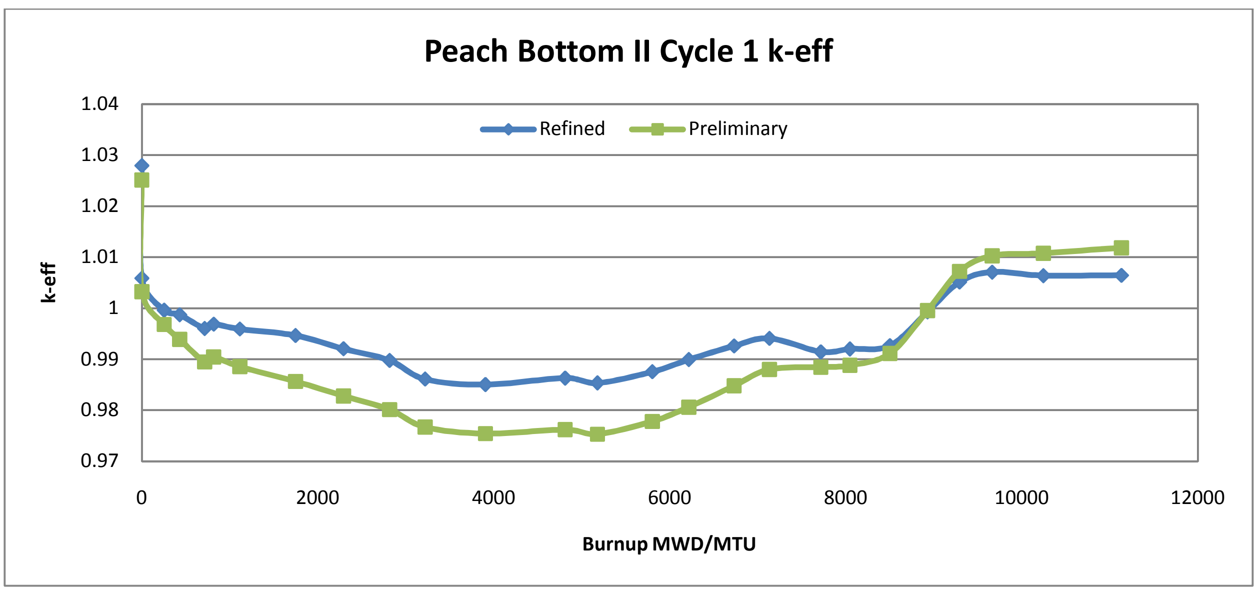

Figure 4.24 Peach Bottom II Cycle 1 k-eff

In summary, it should be highlighted that this "bathtub shape" drift from unity is not, in fact, an unusual occurrence in industrial BWR designs. The profile and magnitude of this bias are both within a range encountered with vintage codes used in industry.

5 Implementation of Generalized Isotopic Tracking

5.1 Description of SCALE Lattice Physics Coupling to NESTLE

One of several major input requirements for NESTLE are energy-collapsed and lattice-homogenized macroscopic cross-section data. Historically, 3-D core simulators have followed a two-step sequence in which a series of lattice physics calculations are performed at various state points, in order to obtain cross-sections on a sufficiently narrow mesh to allow interpolation to be performed. Thus, for many BWR codes this implies running up to thousands of lattice physics state points. Performing lattice physics calculations at 0%, 20%, 40%, 60% and 80% void is generally required, at numerous burnup steps (with even smaller time steps due to the presence of gadolinium), including restart conditions at each state point; where controlled and uncontrolled conditions also need to be considered. In addition, various fuel temperature conditions, as well as soluble poison state points (for PWRs) also need to be added to the response matrix, resulting in a very large number of calculations and corresponding cross-section sets. NESTLE is somewhat unique in that the code stores cross-sections in the form of polynomial fits, instead of tabulated sets of data. Lattice physics runs are performed at any combination of the conditions described above, but instead of bringing in the actual cross-section data points for use in interpolation schemes, polynomial fits are applied to the data with a given cross-section used as the “base” cross-section and perturbations from the base case being accounted for through the polynomial coefficient adjustments. Thus the amount of data required to be stored in memory is much smaller and the cross-section files are not nearly as large.

In the SCALE version of NESTLE, the lattice physics code used to generate collapsed and homogenized cross-section calculations is TRITON [30] a SCALE depletion sequence which uses the NEWT discrete ordinates transport solver and the ORIGEN code for isotopic tracking.

TRITON input decks are created for the various fuel lattices required for a given fuel bundle design, allowing the user many degrees of freedom regarding how refined the spatial mesh is, as is the energy group structure and many other options. Once the lattice runs are completed, collapsed and homogenized cross-sections at each state point are available, then a coupling code called “T2N”, an acronym for “TRITON to NESTLE”, is executed which performs polynomial fitting calculations and generates a cross-section file compatible with NESTLE for each lattice type required. Once each lattice has a unique NESTLE compatible cross-section file, these files are then compiled into one larger cross-section file which is used in the NESTLE calculations.

5.1.1 TRITON Computational Enhancement

Over the course of developing NESTLE enhancements, numerous lattice physics runs were required, some of which were discussed under the Peach Bottom Benchmark, in Section 4. After the aforementioned lattice refinements were performed on the Peach Bottom II Cycle 1 TRITON lattice physics input files, the computational time requirement greatly increased; due heavily in part to the addition of numerous new material definitions which required greater computational runtime and disk space requirements.

One major development, concurrent to this project, was the construction of a modern computer cluster at the University of Tennessee Nuclear Engineering department with a fundamentally different architecture than many traditional clusters, a different architecture which in time was tuned to allow for the fastest TRITON computations possible. The architecture platform used to manage the Linux based cluster is called “DRBL”, standing for “Diskless Remote Boot Linux”. In this paradigm, the auxiliary nodes do not necessarily need to host physical hard-drives as the boot process occurs over the network. The head node contains a stripped down image file of the Ubuntu operating system, the OS chosen to host the head node, which is then sent over the network to each of the computational nodes which then boot off of this image file which sits in RAM on the system, occupying ~0.5 GB. In addition, the RAM is mounted as an accessible file system, residing in the "/tmp" directory, a feature that is invaluable for speeding up TRITON computational time.

In the TRITON depletion sequence, the first major sets of calculations are a series of stacked codes which work together to perform cross-section processing. This calculation utilizes a significant size of data transfer, which occurs in whichever directory the user specifies as their temporary directory (TMPDIR in the various SCALE scripts). At this point is where the feature of having the RAM mounted as file system can be clearly seen as advantageous. We are then able to point to the base directory "/tmp" as the TMPDIR, which then allows all cross-section processing to be performed in RAM, as opposed to on hard-disks, which has been the traditional way of performing cross-section processing.

One major hurdle that occurred along the way was the realization that even eight GB of storage space was not sufficient space for performing cross-section processing, especially on the lattices that contained gadolinium fuel pins, due to the memory requirements needed. When doing four simultaneous calculations on one of the quad core central processing units (CPU's), the memory requirement approached 40-50 GB of required space. What was also observed was that only a tiny fraction (less than 1%) was actually used once the computation reached the NEWT discrete ordinates calculation, where much of the time is spent computationally. Hard-drives were then added to each of the computational nodes, but mounted only as swap space, effectively acting as spill over memory, which is only accessed and utilized if the RAM capacity is exceeded. It should be noted that we chose to purchase Western Digital Velociraptor hard-drives, which spin at 10,000 rpm and have sequential read and write speeds on the order of 100 Mb/s, with much lower random read and write speeds. These hard-drives were chosen since they had the best price per gigabyte storage capacity and, in fact, the sequential speeds were comparable to the solid state hard drives available at the time. Nevertheless, it is highly likely that solid state hard drive prices will drop rapidly in time, which coupled with anticipated speed up times suggest that solid state hard drives should be the better option as the technology matures.

Despite the new storage capacity with the addition of swap space, problems still occurred when running four or more TRITON runs simultaneously, as four separate runs were attempting to read or write to the hard-drive simultaneously, and the operating system tried to move data into and out of the swap space to perform all calculations in RAM as opposed to using the hard-drive which is significantly slower. CPU wait time increased dramatically and the losses were much greater than linear. If one run took 20 minutes in cross-section processing, four runs simultaneously would require several hours (or more) of calculations as much of the computational effort was spent moving data in and out of swap space and all four calculations attempted to be simultaneously managed, as opposed to 80 minutes if it was truly a linear relationship.

Further refinements were made to the system to help linearize the cross-section processing using up to the maximum amount of RAM on the system. If one run requiring six GB was executing, then a second run requiring six GB started up, the system would pause one of the runs, allowing the other run to finish through all cross-section processing prior to then restarting the second case. If the first run only require three GB of RAM, and the second required four GB, the system would determine that there was enough available RAM for both and allow them to occur simultaneously. This fix was implemented through the usage of a shell script which managed programmatic control. The shell script is attached as Appendix B – TRITON Memory Management Script for reference. Once the first run begins the NEWT calculation, which uses very little memory, the second cross-section processing run would restart while the NEWT calculation continued uninterrupted.

Once all of these architecture-specific improvements were instituted, combined with the latest Core i7 processors from Intel, the computational speed up over traditional architectures was in the neighborhood of three to seven times faster depending on the problem definition, size requirements, and number of parallel calculations. This script runs real time on all nodes, but takes up virtually no resources as it has a wait time of 29 seconds, thus execution is a fraction of a second (in the 1/10,000 of a second range or less) then waits for 29 seconds before performing the check again. Initially this wait time was reduced to a very few seconds as it was thought that it was important to not waste the 29 seconds of computational time if the memory is exceeded, but this resulted in much longer calculations. The script would catch the TRITON sequence as it was changing from one code used for cross-section processing to another, and decide it was time to promote a paused job, but then the initial run would jump back into cross-section processing which then would overwhelm the hard-drive with wait time while data was swapped into and out of the swap space until the script again caught that two runs were occurring with memory requirements exceeded and would again pause a run. This would happen quite frequently with what could be called a frequent “script refresh rate”, which correlates to the wait time instituted in the script. When using longer wait times or less frequent script refresh rates (such as the 29 seconds currently implemented), this problem is much less infrequent, although occasional, and overall computational time reduced.

5.2 ORIGEN Validation

The “Oak Ridge Isotope Generation” code ORIGEN, “computes time-dependent concentrations and radiation source terms of a large number of isotopes, which are simultaneously generated or depleted through neutronic transmutation, fission, and radioactive decay” [12] . There are numerous options within ORIGEN for various isotopic tracking scenarios including fuel irradiation within a nuclear reactor, radioactive decay in storage, and chemical processing of spent fuel elements to name several [12] . Any number of these capabilities could be implemented in NESTLE, whereas fuel irradiation is currently the only option for an ORIGEN solution where the capability to include fuel cooling times (radioactive decay) could be implemented in order to simulate transmutation scenarios which include cooling times between periods of irradiation. The usage of ORIGEN as the primary isotopic depletion method has been used in several well-known codes, including MCNP/MONTEBURNS [25] as well as TRITON [30] . ORIGEN was originally designed, and still primarily used as a standalone code [12] , however a recent project included the creation of an ORIGEN subroutine which is able to correctly setup and solve ORIGEN problem definitions via a subroutine call [30] . The use of subroutine calls as opposed to the creation of text file input decks allows for a more efficient usage of computational resources, reducing computational time constraints. This reduction is not insignificant when performing isotopic calculations in every node of a full core simulation, which would represent 18,336 independent solutions per burnup step for a whole core evaluation of the Peach Bottom core described in this manuscript.

When the subroutine version of ORIGEN was first implemented the results were not as expected and required significant effort in learning and understanding of the ORIGEN subroutine and code. After several iterations of discovering coding bugs and implementing subsequent fixes, a benchmark of the ORIGEN subroutine was performed against the standalone version of ORIGEN. The lattice physics code TRITON uses the standalone ORIGEN as the means for depletion calculations, providing an excellent opportunity for benchmarking the ORIGEN subroutine against the widely used and accepted results of the stand-alone version. Thus, the input mass of initial nuclide weight in the problem definition was obtained, along with burnup dependent power, as well as the time in days for each burnup step, all of which is needed for setting up the problem definition and comparing to the TRITON generated results. The base libraries used by TRITON are written to the file “ft33f001”, adding a base library after each depletion calculation. Ensuring that the correct burnup step pointed to the correct base library on file, the same calculation was performed using the ORIGEN subroutine as was performed using standalone ORIGEN within the TRITON sequence, as a benchmark between the two versions of ORIGEN. Figure 5.1 shows the results of this benchmark.

Four isotopes were selected as appropriate representations of the accuracy of the ORIGEN benchmark. ^{235}U and ^{239}Pu are the two most reactive fissionable isotopes in reactor fuel, thus serve as excellent checks. As can be seen on Figure 5.1, there is essentially no difference in solution between the two versions of ORIGEN for the two most important nuclides with respect to reactivity. In addition, ^{241}Am was benchmarked to ensure that the higher actinide chain solution was occurring correctly and is shown to have excellent agreement, with the right side axis being the number density due to the significantly smaller scale. The last isotope that was used for comparison was ^{137}Cs, one of the most prevalent fission products, to ensure that the correct fission distribution was being calculated, and again it is seen that the agreement is excellent. When performing a check on the relative error with respect to all four isotopes at every state point, the maximum uncertainty observed was less than 0.05%, where the vast majority of the data points had uncertainties less than 0.01%.

5.3 Coupling ORIGEN to NESTLE

In order to correctly implement the ORIGEN solution within NESTLE, several input parameters are required. While there are numerous degrees of freedom with variable inputs into ORIGEN, most of these are currently hardwired in the internals of the code, with a small subset that the user can actually control. If needed, additional inputs can be included but due to their large number and the infrequent need for this level of flexibility, only a few are currently coded as user inputs. Three of the most important inputs into ORIGEN are the length of burn - including the number of smaller time steps each burnup step is divided into, the power (or flux, thermal for a thermal system, or total for a fast system), and the reaction type dependent microscopic cross-sections for each isotope being tracked. Most of these inputs can be calculated internally

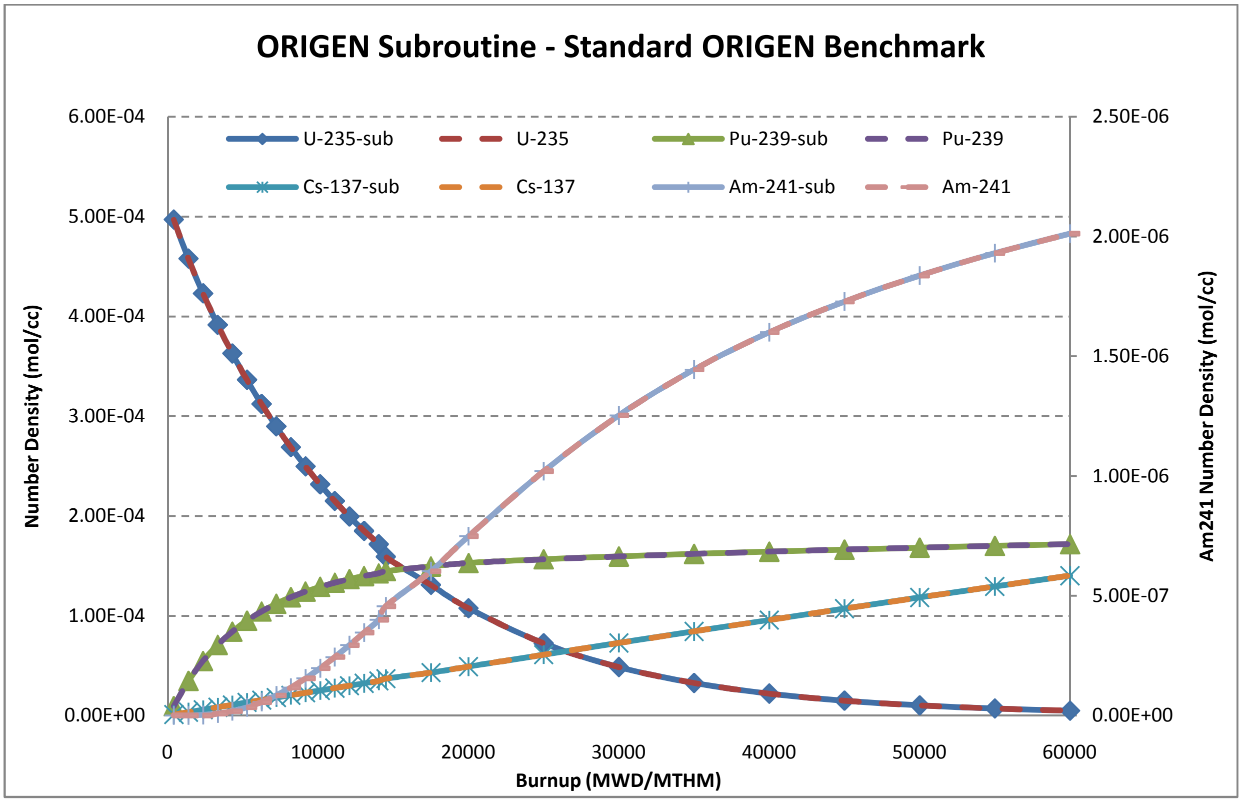

Figure 5.1 Origen Subroutine Benchmark

within NESTLE, such as the number of days corresponding to each burnup step or the total power in each node, as examples. However, the reaction dependent microscopic cross-sections are obtained as an input from the TRITON lattice physics run, and computed using a linear burnup interpolation scheme, as well as a linear interpolation scheme for any other spectral conditions such as moderator density, fuel temperature and controlled or uncontrolled conditions. The cross-sections brought in from TRITON are brought in n-group form, corresponding to the n-group solution performed in NESTLE, but must be collapsed to one-group form for calculation within ORIGEN, computed via a flux-weighted collapse. Due to the difference between the n-group nodal flux, versus the n-group fuel flux, disadvantage factors are calculated which are then interpolated to obtain the correct cross-section. This complication arises due to the fact that TRITON calculates both a nodal flux as well as a fuel flux, whereas NESTLE only calculates a nodal flux. Since only fuel depletion is desired, a fuel flux must be used and the lack of a fuel flux solution in NESTLE is accounted for by computing the disadvantage factors which are then used for flux-weighted microscopic cross-section collapsing for the ORIGEN solution. Lastly, the default input for the ORIGEN calculation requires the nodal power in units of MW, which is internally calculated within NESTLE and passed into the ORIGEN subroutine.

In the absence of a suitable mechanism for passing the reaction dependent microscopic cross-sections from TRITON into NESTLE, a new file format was implemented for use in TRITON by staff researchers at the Oak Ridge National Laboratory which creates a binary file in a format called “silo”. The silo format is a DOE-sponsored open-source binary format originally developed at Lawrence Livermore National Laboratory for the flexible storage and viewing (via the open-source code “visit”) of large amounts of scientific data. The TRITON silo file contains the reaction dependent microscopic cross-sections, initial lattice number densities, as well as numerous other parameters. Reading the contents of this file into an array of data for each lattice type provides a streamlined process for storage and retrieval of several parameters of interest, primarily the reaction dependent microscopic cross-sections required in ORIGEN. The group structure of the data on the silo file is congruent with the group structure defined on the “read collapse” block defined in the TRITON input file. The microscopic cross-section data available on the silo file is user dependent via the materials defined in the various “hmog” blocks on the input file; however two particular “hmog” blocks are required for accurate fuel depletion and calculation of disadvantage factors. The first block is required to be numbered as the 500 block within the “hmog” block which includes all materials in the fuel lattice - fuel, clad, moderator, control material and any other materials present. The second required block is required to be numbered as the 501 block within the “hmog” block which includes only the fuel materials present in the lattice and gives collapsed data (cross-sections, fluxes, etc.) for the fuel only. While the fuel collapsed data contains the vast majority of the data required, the nodal collapsed data are also needed to retrieve nodal fluxes used in the calculation of the flux disadvantage factors discussed above.

While ORIGEN has the capability of tracking greater than 14,000 isotopic reactions and approximately 2,000 isotopes, NESTLE is limited to updating the cross-sections only for those isotopes and reactions that are present on the silo file. The user has much flexibility for increasing or decreasing these through several TRITON options. First, the “addnux” input parameter provides the first layer of options where the addnux=3 option resulted in the tracking of 229 isotopes, and 741 different reactions. The options addnux=2 result in fewer isotopes and reactions, and likewise with addnux=1 resulting in less tracking than addnux=2. If addnux=0 is specified, no isotopes other than those present on the input file itself will be tracked. In addition to the predefined isotopes on each addnux option the user may track additional isotopes provided the isotope is defined in one of the materials on the input file, thus adding an isotope in a trace quantity would cause the inclusion of these cross-sections on the silo file to be used within NESTLE without adversely affecting the neutronics solution.

When calling ORIGEN during the TRITON depletion sequence, the one-group reaction dependent microscopic cross-sections are computed via a program called COUPLE, which sets all appropriate cross-sections within the ORIGEN library. In the NESTLE implementation, in lieu of using COUPLE, the cross-sections are collapsed and evaluated in three subroutines. This is done to maintain consistency and preserve the speed up of using the ORIGEN subroutine instead of utilizing text input files; which is required by couple. Inside the first subroutine, origen_sub.f90, each unique reaction type other than fission, determined by each respective reaction type (“mt” number), is defined by the specification of a parent, daughter and respective cross-section. For example, the radiative capture reaction for ^{238}U would be defined with parent=922380, daughter=922390, cross-section=1 barn, with radiative capture being defined by mt=102. With respect to fission cross-sections, mt=18, only a parent and cross-section are needed since the fission yields are pre-determined and included in the base ORIGEN library. While most isotopes have only one natural ground state, there are some that have additional metastable states where the parent isotope may have two or more potential daughter products, the ground state or possible additional metastable states. In order to correctly handle these cross-sections it was required that the branching ratio for each reaction type also be determined, such that if a parent isotope has multiple daughter products for a given reaction type, this dependency would be captured since there are certain metastable states with very large cross-sections and occasionally metastable states with half-lives much longer than the ground state. These branching ratios are computed using the data on the base ORIGEN library by first computing the total cross-section for a given reaction type by summing all potential parent/daughter cross-sections for a given isotope and reaction type. Subsequently, once the total cross-section is known, the appropriate branching ratio for each of the parent/daughter reactions is determined by dividing the incremental cross-section for one specific pair by the total cross-section previously determined. This is illustrated by Equations 5.1 and 5.2.

$$Xsec\_Total_{mt}^{isotope} = \sum_{i=1}^{\#\,Daughters} Xsec_i$$

Equation 5.1

$$Branching\_Ratio_{mt}^{Parent/Daughter_i} = \frac{Xsec_i}{Xsec\_Total_{mt}^{isotope}}$$

Equation 5.2

To ensure that this calculation is performed correctly, a comparison of the cross-sections computed by COUPLE and those calculated in NESTLE was performed, where the results for a select number of isotopic reactions is shown here in Table 5.1 for BOC cross-sections and Table

5.2 for end of cycle (EOC) cross-sections, where the full comparison is provided in Appendix C – BOC Microscopic Cross-Sections and Appendix D – EOC Microscopic Cross-Sections. The six reactions were all chosen due to their importance for BWR calculations: ^{135}Xe capture cross-section, due to fission product buildup and the associated extremely large cross-section, similarly ^{157}Gd often used as a burnable absorber and associated large cross-section, two plutonium (^{241}Pu and ^{239}Pu) fission cross-sections, ^{235}U fission cross-section and the ^{238}U capture cross-section which is extremely important for actinide accumulation.

In order to expect a true one-to-one correlation between COUPLE and NESTLE cross-sections, a NESTLE input case was created that modeled a lattice physics scenario. In other words, a NESTLE core model is subject to reflective boundary conditions on all sides, cross-sections brought in from an identical problem definition in TRITON, identical power assignments and so forth. This model would allow the cross-sections to be compared, and subsequently the isotopic solution to validate that the ORIGEN subroutine was being implemented correctly, as a nearly identical isotopic distribution was to be expected.

Table 5.1 BOC Microscopic Cross-Section Comparison

Parent	Daughter	mt	NESTLE XS	COUPLE XS	% Difference
541350	541360	102	421290.8	421303	-0.0029%
641570	641580	102	20347.72	20348.3	-0.0029%
942410	fission	18	208.3514	208.357	-0.0027%
942390	fission	18	189.4151	189.42	-0.0026%
922350	fission	18	79.46591	79.4679	-0.0025%
922380	922390	102	0.9160061	0.916012	-0.0006%

Table 5.2 EOC Microscopic Cross-Section Comparison

Parent	Daughter	mt	NESTLE XS	COUPLE XS	% Difference
541350	541360	102	254980.8	255506	-0.2056%
641570	641580	102	12430.9	12456.5	-0.2055%
942410	fission	18	126.6093	126.839	-0.1811%
942390	fission	18	111.2493	111.461	-0.1899%
922350	fission	18	50.67509	50.7629	-0.1730%
922380	922390	102	0.8393278	0.839572	-0.0291%

Once it was demonstrated that the cross-sections were in close agreement from BOC to EOC, the isotopic distribution throughout the cycle, from 0 – 60,000 MWD/MTHM, was calculated and the results compared to the ORIGEN solution performed within TRITON which served as an excellent validation study for the newly implemented ORIGEN solution scheme within NESTLE. With identical problem definitions the agreement proved excellent, as illustrated with the number density agreement in ^{235}U, ^{239}Pu on the left axis, and ^{241}Am on the right axis, shown in Figure 5.2.

5.4 End to End Demonstration of Actinide Recycling Illustrations

After ORIGEN was fully integrated into the NESTLE code and validated to ensure a correct implementation, a demonstration of the capabilities of the new code suite was performed. Using bundles spiked with americium loaded in the lattice, the tracking of the full suite of actinides tracked by TRITON is shown and compared against those of a standard bundle in the same locations. A much greater understanding of the path of ^{241}Am transmutation or any other desired isotope can be obtained from this simulation, as the net accumulation of all the various actinides can be compared against a reference bundle. This simulation was particularly important since the ^{241}Am path leads directly to ^{242gs}Am as well as ^{242m}Am, neither of which are included when specifying the addnux=3 option in TRITON. As a result, both the ground state

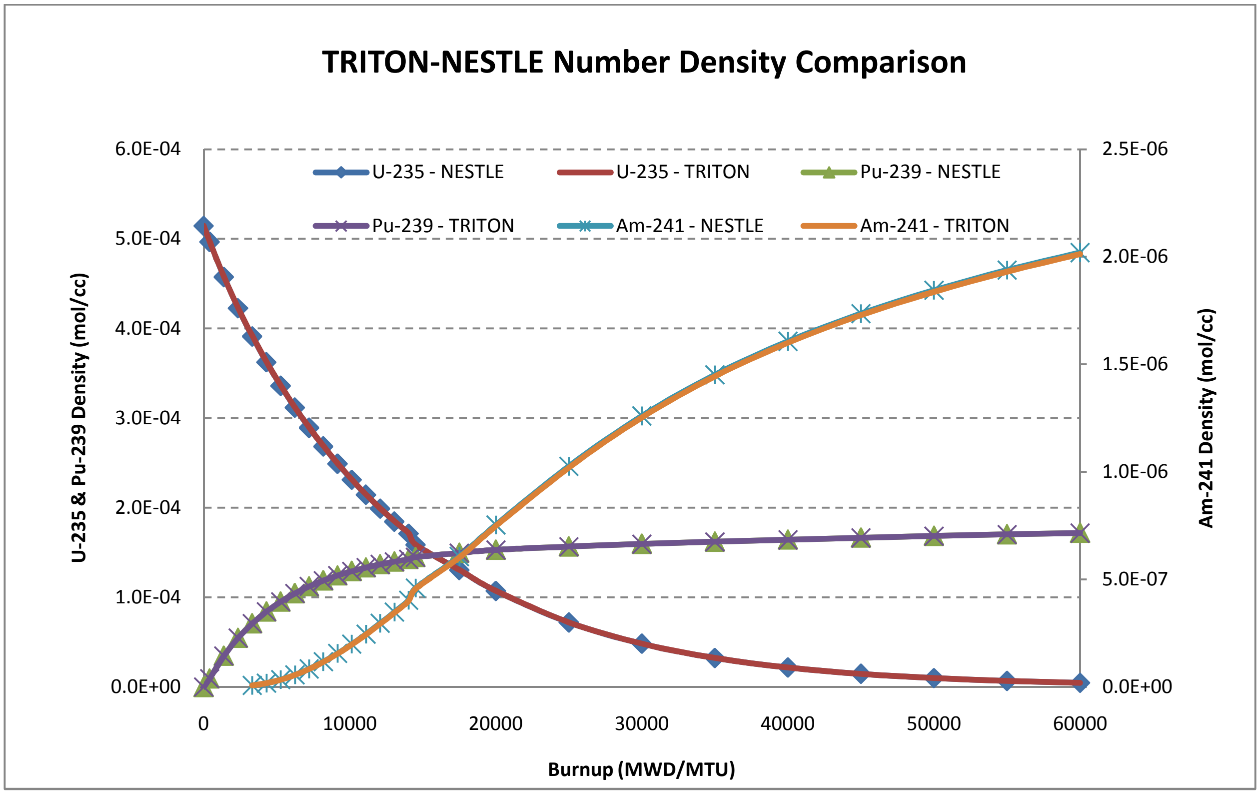

Figure 5.2 TRITON-NESTLE Comparison

and metastable isotopes of ^{242}Am were added in trace quantities on the input file demonstrating the flexibility that is available with respect to isotopic tracking. In addition, the branching ratio between the production of the ground state or metastable state was investigated to assess the importance of tracking one or both of the isotopes of ^{242}Am. Typically these two isotopes are not tracked in a standard 3-D reactor simulator thus the ability to track this high level of isotopic detail is a key contribution of the work herein presented. In particular, the potential for recycling scenarios in which the fuel may be enriched in ^{241}Am, or contain other families of minor or major actinide isotopes. Moreover, noting the large fission cross-sections for either ^{242gs}Am or ^{242m}Am, with fission cross-sections of 1,000 and 3,000 barns respectively, the importance of tracking these isotopes correctly for transmutation scenarios is readily apparent. It was observed that the branching ratio was on the order of 90% ^{242gs}Am and 10% ^{242m}Am, which points to the ground-state, counter-intuitively with the much shorter half-life, as being more important as it pertains to the likelihood of accumulation. Due to the fact that the metastable state has a cross-section roughly three times higher, the importance level of the metastable state is thus increased as the likelihood for incineration through fission is of higher likelihood when the metastable state is produced with a lower likelihood of leading to higher actinides up the chain as a result of radiative capture reactions.

In the Peach Bottom II Cycle 1 simulation utilizing bundles spiked with ^{241}Am, as well as trace amounts of both ^{242gs}Am and ^{242m}Am, it was determined that loading the bundles in two preferential axial locations would serve as a suitable simulation that would allow the evaluation of the different minor actinide transmutation and fission rates resulting from the different spectra in the lower and upper axial regions of a BWR. Thus, four radial locations in the core were chosen with axial locations for evaluation at 18 inches and 132 inches from the bottom of the active fuel. In other words, low enough and high enough respectively to help illustrate spectral differences, especially pertaining to moderator density, but also still in locations that tend to be more reactive. Using the addnux=3 option and adding the trace amounts of the two ^{242}Am isotopes, six isotopes from ^{241}Am and higher were able to be tracked which included: ^{241}Am, ^{242gs}Am, ^{242m}Am, ^{243}Am, ^{242}Cm, ^{243}Cm, and ^{244}Cm. Keeping in mind that traditionally only ^{241}Am is able to be tracked as well as the fact that further curium isotopes, californium isotopes or any other number of actinides could be tracked depending upon the input file definition it should be readily evident that the fidelity in tracking actinides is vastly superior to the previously available options.

In the simulation herein illustrated, approximately 230 unique isotopes were tracked by ORIGEN, which included microscopic cross section updates and interpolation for the spectral effects in fuel temperature, moderator density as well as controlled or uncontrolled conditions.

It should be stated here that as currently programmed a user must have a fully populated matrix of branch data in the TRITON simulation to be able to correctly track isotopes within the NESTLE core simulator. For example, if the user chooses three branches in fuel temperature as well as three branches in moderator density, this must result in a total of nine cases. Table 5.3 shows a tabular illustration of this requirement.

In this example there must be a branch defined for all potential combinations. As illustrated in Table 5.3 this requirement means a branch must exist for all "x" locations. Keep in mind that this requirement holds true for both controlled and uncontrolled conditions, however both the controlled and uncontrolled branch cases need not be the exact same set of branches, such that the controlled matrix may only result in a two by three matrix, but with the requirement that it be fully populated. This flexibility allows for the user to choose to save computational time by not spending resources calculating conditions that may not exist (such as 80% void conditions for controlled locations).

In Figure 5.3 a comparison of the behavior of ^{241}Am, ^{242gs}Am, and ^{242m}Am is shown for both the lower axial location as well as the higher. These isotopes are of particular interest since the transmutation of ^{241}Am was the originating topic of inquiry for this research. In addition the demonstration of the ability to track both isotopes of ^{242}Am illustrates the fidelity and flexibility

Table 5.3 TRITON Branch Conditions

		Fuel Temperature (K)		
		600	900	1200
Moderator Density (g/cc)	0.15	**x**	**x**	**x**
	0.5	**x**	**x**	**x**
	0.75	**x**	**x**	**x**

that this newly developed tool contains. Of particular interest are the different transmutation results that are observed as a result of the differing neutron spectra present due to the significant boiling in the upper region of the core. While the differences are not largely pronounced, this is partially due to the fact that these bundles have only been in the core for one cycle. The burnup values referenced for this transmutation comparison are the nodal values for each axial location, where the lower portion of the core experienced higher exposure as a result of the lower void fraction throughout the cycle thus creating a more reactive environment. As these lattices accumulate higher burnup values the difference in ^{241}Am transmutation results will become more pronounced. Also, when analyzing the results for ^{242gs}Am it is seen that an equilibrium quantity is achieved quite rapidly, due to the short half-life which is on the order of ~17 hours coupled with the large thermal fission cross section. It should be noted that this particular lattice design was not optimized to be employed as a spiked lattice design of choice should a thermal transmutation approach be taken, but instead this lattice was generated to illustrate the computational capabilities that have been developed. In Figure 5.3 also note that the left vertical axis applies to ^{241}Am, while the right side vertical axis is for both isotopes of ^{242}Am. The simulation of spiked bundles in the Peach Bottom core covered both controlled and uncontrolled conditions, such that NESTLE coupled with ORIGEN depletion was tested over the full suite of branch conditions, which included perturbations in moderator density and fuel temperature for both controlled and uncontrolled conditions.

In addition to the transmutation of ^{241}Am via radiative capture to either ^{242gs}Am or ^{242m}Am, which both exhibit significant fission cross-sections, additional higher actinides are created since not all ^{242}Am reactions end in fission. While the fission cross sections for these isotopes are very large, the capture cross sections are not insignificant and lead to additional curium production. Figure 5.4 shows a cumulative sum of the six isotopes of americium and curium

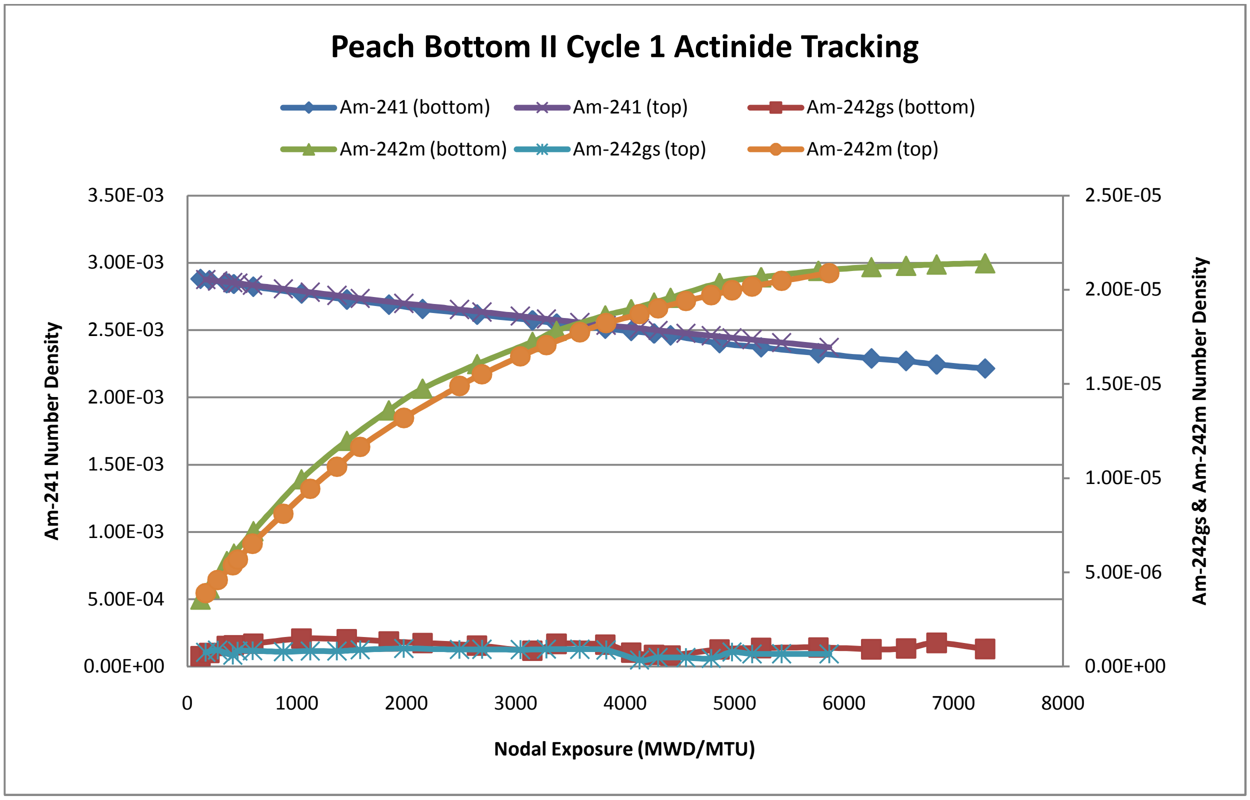

Figure 5.3 Peach Bottom II americium Results

detailed above. Somewhat contrary to the result seen when observing the ^{241}Am transmutation in the Figure 5.3, the cumulative results do not show a dependency upon spectral differences and the transmutation rates occurring between the low void and high void neutron spectra are not noticeably different. This result, coupled with the results seen for ^{241}Am alone provide intriguing details which illustrate the benefit of being able to track depletion results with such fidelity. The potential benefit of the thermal spectrum seen when investigating ^{241}Am alone is possibly mitigated since the buildup of curium isotopes occurs at a higher rate when in the presence of an increasingly thermal environment. Of course, if recycling scenarios were to be performed, these bundles would need to be burnt to a much higher exposure, on the order of 45 to 50 GWD/MTU, before being removed from the core environment, per the discussion in section two. It should be noted that these six isotopes are not the only transuranic isotopes available via the addnux=3 option. Clearly the user could track virtually any isotope desired with the control afforded by adding trace amounts on the input, but even as such, significant transuranic isotopes are still tracked by default when using the addnux=3 option. The transuranic isotopes available when choosing this option are as follows: ^{237}Np, ^{238}Pu, ^{239}Pu, ^{240}Pu, ^{241}Pu, ^{242}Pu, ^{241}Am, ^{242gs}Am (problem dependent), ^{243}Am, ^{242}Cm, ^{243}Cm, and ^{244}Cm, all of which were reported as a result of the aforementioned simulation.

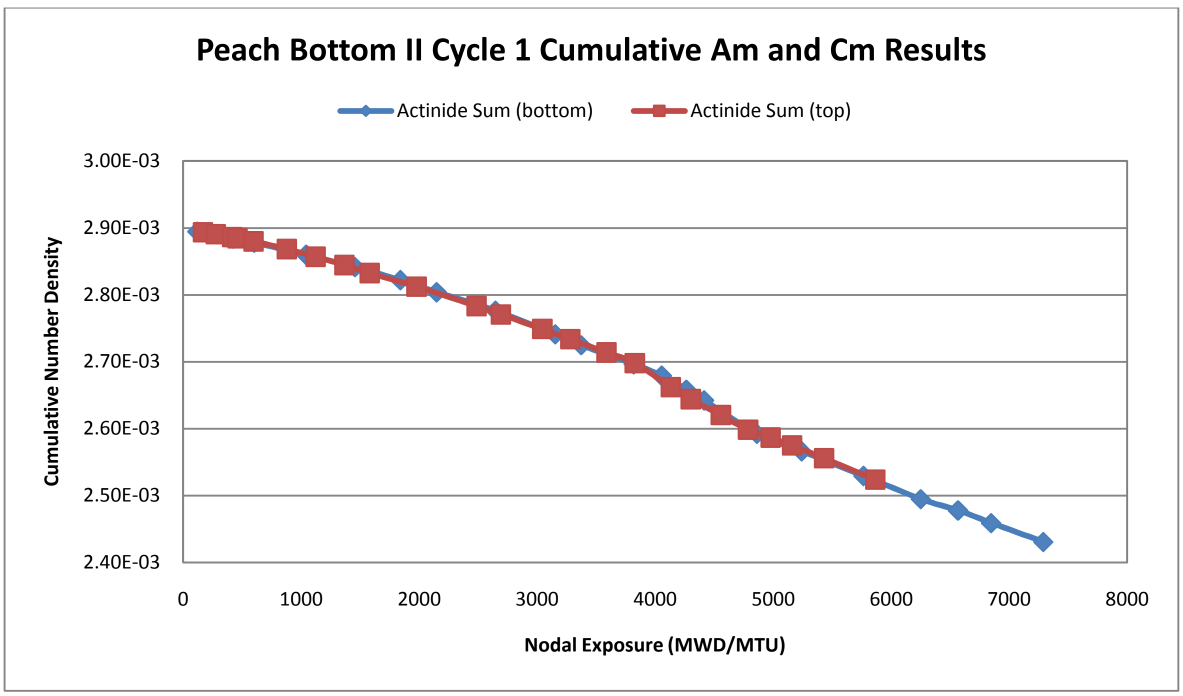

Figure 5.4 Peach Bottom II Am and Cm Results

The discussion of which scenario provides a better transmutation environment requires a multitude of decisions including, but not limited to identifying which isotopes are worse than others. For example, is ^{241}Am clearly worse to have than various isotopes of curium or vice versa? Furthermore, what is happening to the rest of the actinides, are Np and Pu isotopes building up at significantly different rates? Undoubtedly the decision of which scenario is optimum incorporates knowledge from a breadth of disciplines within nuclear engineering, but this also is not the intention of this study. This study developed the needed tools required to evaluate such scenarios and ultimately make informed decisions. In particular, to be able to track in exceptional geometrical (3-D) detail the various components of spent nuclear fuel in a LWR.

6 Conclusions

Over the course of the project a major deficiency was encountered which was the lack of a computational tool that could perform accurate assessments of transmutation scenarios, such as capturing the details of spectral differences coupled with a complete tracking of actinides. This deficiency was remedied through the enhancement of the nodal 3-D core simulator NESTLE.

First the needed capability of modeling BWR cores was added through the development of a robust drift-flux solver capable of simulating the non-homogenous nature of boiling water in BWR cores. Included in this model is a sub-cooled boiling model which captures the sub-cooled nucleate boiling that occurs in the bottom regions of a core before the transition to bulk boiling, as well as a robust model for capturing the correct boiling phenomena once bulk boiling is reached. In addition the development and implementation of an accurate flow split and redistribution model to correctly determine the flow to each bundle in the core was developed which is imperative in order to determine the correct moderator density conditions within each node. This thermal-hydraulic solve was robustly tested over a wide range of flow and power conditions and exhibited excellent agreement when benchmarked against experimental data.

Subsequently, a first of a kind implementation of a microscopic depletion model utilizing the world renowned ORIGEN code was developed and implemented which allows for high fidelity evaluation of transmutation scenarios, intended for the assessment of actinide transmutation but fully capable of tracking literally hundreds of isotopes, transuranics, light elements or fission products. This capability also allows extraordinary flexibility in the geometrical fidelity to which the user desires to evaluate transmutation scenarios while tracking nearly any isotope desired. This implementation also allows for the evaluation of various reactor types, any reactor type able to be modeled by NESTLE, and has the capability to account for spectral differences in moderator density, moderator temperature, soluble poison concentration and fuel temperature. In addition, the four aforementioned spectral differences can be accounted for in both controlled and uncontrolled conditions. This added capability for microscopic depletion was also rigorously tested and benchmarked against the proven lattice depletion code TRITON to ensure correct implementation and accurate answers, where the agreement between TRITON and NESTLE proved to be exceptional. Given that there are essentially no publicly available 3-D simulators, and those simulators that do exist within the proprietary control of private companies do not have the capability of tracking microscopic depletion scenarios beyond a very limited selection important to core neutronics, this computational development is truly unique.

While the code has been greatly enhanced, there are still several improvements for the future that could be implemented to increase accuracy, usefulness and computational efficiency. The first major enhancement for a more accurate simulation of BWR cores would be the addition of a void history element to the macroscopic neutronic solution. Currently a core average void history is used for all nodes, typically chosen to be 40%. This means that all nodes in the core are assumed to be depleted according to a 40% void spectrum, and isotopic accumulation in all nodes is performed at a 40% void spectrum (or whatever other spectrum the user desires). Branch conditions for various conditions are then performed at burnup steps from 0 to the maximum burnup assuming isotopic accumulation at the chosen void (typically 40%). For lower burnup fuels, those from approximately 0 – 15,000 MWD/MTU this does not cause a significant deviation, but as nodal exposures exceed these values the errors propagated can become meaningful. Thus, fresh core designs can be accurately modeled through the first cycle but greater errors will be introduced as higher burnup values are accumulated. A void history interpolation scheme which accounts for the average void each node has been exposed to, averaged over time, and calculates macroscopic cross sections based on this void history would be a useful improvement. Additionally the calculation of the various thermal limits used by the

NRC to ensure safe and stable core designs would be a relatively easy addition which would certainly add capabilities to the code.

With respect to isotopic improvements, currently the microscopic depletion algorithm is performed after a converged neutronic solution is reached, where the information calculated in the neutronic solver is passed into the microscopic depletion scheme to perform analyses. A potential enhancement would be to tie the microscopic depletion algorithm utilizing ORIGEN into the neutronics solver. While this would be a great enhancement, much work would need to be performed to enhance memory management and code speed up as currently there is a noticeable delay when importing in the microscopic information for less than 1% of the core, thus projecting out to a full core importing of data would require judicious assessments to enhance computational efficiency.

Finally, at the current state of the code the full core simulation for Peach Bottom II Cycle 1, including transmutation for select lattices at 32 nodal locations took approximately an hour and fifteen minutes to simulate. While this is not a terribly significant amount of time, potentially simulating every node in the core (as mentioned previously) may become a significant constraint. The two major components added as a result of this research, namely the thermal-hydraulics solver and the microscopic ORIGEN depletion, both are perfectly suited to be solved using modern parallel programming techniques, specifically an MPI (message passing interface) implementation. Each channel in the thermal-hydraulics solver is independent, thus providing a completely de-coupled problem ideal for solving across numerous CPUs. Similarly, each ORIGEN solution is independent and is also generally ideal for parallel programming under the MPI paradigm. While an OpenMP implementation for multi-threading also seems potentially viable, this was attempted and two conclusions reached. First, due to the constraints given on OpenMP implementations the thermal-hydraulic solver was not appropriately conditioned to an OpenMP application. The ORIGEN microscopic depletion is however appropriately conditioned and thus an OpenMP parallel implementation was instituted, which ended up not being useful. While CPU usage increased greater than 100%, a sign that multi-threading is occurring, due to the speed of the ORIGEN solution, CPU usage greater than 150% was never achieved when having resources up to 800% available. More importantly the time consumed for the calculation was essentially the same, where the increased CPU usage was spent on communication between the various threads as opposed to any measurable speed increase. Furthermore, while some cases would execute without error, other cases would encounter ill-conditioned problem definitions which caused the code to crash. Practically, the stability and controlled nature of MPI implementations appears to be advantageous.

References

References

[1] A. Ansari, *et al.* “FIBWR: A Steady-State Core Flow Distribution Code for Boiling Water Reactors – Computer Code Manual”, EPRI NP-1924-CCM, Electric Power Research Institute (1981).

[2] S. M. Bowman, and D.F. Gill, “Validation of SCALE/TRITON 2-D and 3-D Models for LWR Fuel,” *Proc. Physor-2006*, Vancouver, British Columbia, Canada, Sept. 10-14 (2006).

[3] B. Chexal, G. Lellouche, “A Full Range Drift-Flux Correlation for Vertical Flows”, EPRI NP-3989-SR (1986).

[4] E. D. Collins, G. D. DelCul, J. P. Renier, B. B. Spencer, “Preliminary Multicycle Transuranic Actinide Partitioning-Transmutation Studies”, ORNL/TM-2007/24, February 2007.

[5] E.D. Collins, J.P. Renier, “Comparative Evaluation of TRU Actinide Transmutation in Fast and Thermal Burner Reactors”, *Trans. Am. Nucl. Soc*., **95**, 224-226, (2006).

[6] M. D. Dehart and A. P. Ulses, “Lattice Physics Capabilities of the SCALE Code System Using TRITON,” *Proc. Of PHYSOR-2006*, Vancouver, British Columbia, Canada, Sept. 10-14 (2006).

[7] M. Erighin, C. Yin, J. Galloway, G. I. Maldonado, “Analysis of BWR Lattices to Recycle americium,” *PHYSOR-2006, ANS Topical Meeting on Reactor Physics Organized and hosted by the CNS*, Vancouver, BC, Canada, D063, 1-10/10, Sept. 10-14, 2006.

[8] Fioni G., Cribier M., Marie F., Aubert M., Ayrault S., Bolognese T., Cavedon J.-M., Chartier F., Deruelle O., Doneddu F., Faust H., Gaudry A., Gunsing F., Leconte P., Lelievre F., Martino J., Oliver R., Pluquet A., Rottger S., Spiro M., Veyssiere C., “Incineratin of ^{241}Am Induced by Thermal Neutrons”, *Nuclear Physics A*, **Volume 693**, Number 3, 22 October 2001 , pp. 546-564(19).

[9] Francois, J.L., Guzman, R. “BWR Fuel Design Using Minor Actinides as Burnable Absorber”, *Trans. Am. Nucl. Soc*., **96**, 748-749, (2007).

[10] J. Galloway and G.I. Maldonado, "Three-dimensional Core Simulations of BWR Bundles with americium Target Pins", Trans. Am. Nucl. Soc., 97, 400-401 (2007)

[11] J. Galloway, H. Hernandez, and G.I. Maldonado, "Optimization of americium-Loaded Lattices Tested in 3D BWR Core-Wide Simulations", Proceedings of the International Conference on the Physics of Reactors, September 14-19, 2008, Interlaken, Switzerland (CD-ROM, Log #617)

[12] I. Gauld, O.W. Hermann, R.M. Westfall, "ORIGEN-S Scale System Module to Calculate Fuel Depletion, Actinide Transmutation, Fission Product Buildup and Decay, and Associated Radiation Terms", ORNL/TM-2005/39, Version 6, Vol. II, Sect. F7, (2009).

[13] Gluck, M. (2008). "Validation of the sub-channel code F-COBRA-TF Part I. Recalculation of single-phase and two-phase pressure loss measurements" *Nuclear Engineering and Design*. **238**, 2308.

[14] H. Hernandez, and G.I. Maldonado, "Application of Simulated Annealing Optimization to Recycle Minor Actinides in a BWR Lattice," *Trans. Am. Nucl. Soc*., **96**, 771-773 (2007)

[15] H. Hernandez and G. I. Maldonado, "Added Features and MPI-based Parallelization of the FORMOSA-L Lattice Loading Optimization Code," Proceedings of ANS Advances in Nuclear Fuel Management IV, Hilton Head Island, SC, 2009.

[16] V.N. Koscheev, G.N. Manturov, M.N. Nikolaev, A.M. Tsiboulia, S.M. Bedniakov, V.A. Dulin, Yu. S. Khomiakov, "Nuclear Data for Plutonium and Minor Actinides", Proc. 3d Conf. on Accelerator Driven Transmutation Technology, Report We-I-15, Prague, (1999).

[17] R. Lahey and F. Moody, *The Thermal Hydraulics of a Boiling Water Nuclear Reactor*, American Nuclear Society, La Grange Park, IL (1977).

[18] N.H. Larson, "Core Design and Operating Data for Cycles 1 and 2 of Peach Bottom 2", Electric Power Research Institute (EPRI), (1978).

[19] G. Lellouche and B. Zolotar, "Mechanistic Model for Predicting Two-Phase Void Fraction in Vertical Tubes, Channels, and Rod Bundles", EPRI NP-2246-SR (1982).

[20] G. I. Maldonado, J. Galloway, H. Hernandez, "Recycling Heterogeneous americium Targets in a Boiling Water Reactor", Annals of Nuclear Energy, 37(2), 256-264, February 2010.

[21] G. I. Maldonado, J. Galloway, H. Hernandez, K. T. Clarno, E. L. Popov, M. A. Jessee, "Integration of the NESTLE Core Simulator with SCALE", *Trans. Am. Nucl. Soc.*, **100**, 619-620, (2009).

[22] B.R. Moore, "Higher Order Generalized Perturbation Theory for In-Core Nuclear Fuel Management Optimization", Ph D. Dissertation North Carolina State University, 1996.

[23] B. Neykov, F. Aydogan, L. Hochreiter, K. Ivanov (PSU), H. Utsuno, K. Fumio (JNES), E.Sartori (OECD/NEA) "NUPEC BWR Full-Size Fine-Mesh Bundle Test (BFBT) Benchmark, Volume I: Specifications", OECD 2006, NEA No. 6212, NEA/NSC/DOC(2005)5, ISBN 92-64-01088-2 (2006).

[24] <u>NIST Scientific and Technical Databases</u>. National Institute of Standards and Technology. Feb. 2010. < http://www.nist.gov/srd/nist10.htm>

[25] D. Poston, H. Trellue, "User's Manual, Version 2.0 for MONTEBURNS" Version 1.0. LA-UR-99-4999.

[26] G. Raitses, M. Todosow, A. Aronson, A. Galperin (Ben-Gurion University of the Negev), "Initial Studies of Transmutation Options for Boiling-Water Reactors", BNL-AFCI-2005-002, Brookhaven National Laboratory, September 30, 2005.

[27] D. Reddy, S. Sreepada, and A. Nahavandi, "Two-Phase Friction Multiplier Correction for High-Pressure Steam-Water Flow", EPRI NP-2522, Electric Power Research Institute (1982).

[28] The RELAP5-3D Code Development Team, "RELAP5-3D Code Manual Volume 1: Code Structure, System Models and Solution Methods", INEEL-EXT-98-00834, Revision 1.3a, February (2001).

[29] P. Saha and N. Zuber, "Point of Net Vapor Generation and Vapor Void Fraction in Subcooled Boiling", in *Proc. 5th. International Heat Transfer Conference*, Tokyo, Japan, p. B4.7 (1975).

[30] SCALE: A Modular Code System for Performing Standardized Computer Analyses for Licensing Evaluations, ORNL/TM-2005/39, Version 6, Vols. I–III, January 2009. Available from Radiation Safety Information Computational Center at Oak Ridge National Laboratory as CCC-750.

[31] B.S. Shiralkar, D.W. Radcliffe, 1971. “An Experimental and Analytical Study of the Synthesis of Grid Spacer Loss Coefficients”, General Electric Technical Report NEDE-13181.

[32] M. Stalek, C. Demaziere, “Development and Validation of a cross-section interface for PARCS”, *Annals of Nuclear Energy*, **35**, 2397-2409, (2008).

[33] Taiwo, T.R. and Hill, R.N, “Comprehensive Summary of AAA and AFCI Transmutation Analysis Studies,” ANL-AFCI-198, September 30, 2007.

[34] P. J. Turinsky, R. M. Al-Chalabi, P. Engrand, H. N. Sarsour, F. X. Faure and W. Guo, "Code Abstract - NESTLE: A Few-Group Neutron Diffusion Equation Solver Utilizing the Nodal Expansion Method for Eigenvalue, Adjoint, Fixed-Source Steady-State and Transient Problems," *Nucl. Sci. & Engr*., **120**, 72, 1995.

[35] Varaine, Frederic, Zaetta, Alain. “Transmutation in Nuclear Reactors: Scientific and Technical Feasibilities Aspect”, *Trans. Am. Nucl. Soc*., **96**, 736-738, (2007).

[36] Y. Xu, T. Downar, R. Walls, K. Ivanov, J. Staudenmeier, J. March-Lueba, “Application of TRACE/PARCS to BWR Stability Analysis”, *Annals of Nuclear Energy*, **36 Issue 3**, 317-323, (2009).

[37] C. Yin, J. Galloway, G. I. Maldonado, E. Fuentes, J. Casal, “University of Cincinnati and Westinghouse Collaboration: PHOENIX-4 Lattice Physics Studies”, Trans. Am. Nucl. Soc., 94, 483-485 (2006)

[38] A. Zaetta, “Prospective of LWRs to Reduce Minor Actinide Inventories”, Nuclear Science Committe Meeting, Paris, June 9-11 (2004).

[39] N. Zuber and J. Findlay, “Average Volumetric Concentration in Two-Phase Flow Systems”, *J. Heat Transfer*, **87**, 453 (1965).

Appendices

Appendix

Appendix A – Peach Bottom II Cycle 1 Input Deck

```
Peach Bottom Cycle 1
read parameter
  usexsecfile=yes xsecfile=XSEC.TOTAL.MACRO
  thfeedback=yes
  thsolver=twophase
  quality=epri
  void=l-z
  powerden=50.7379
  t2n=yes
  eps_pres=5E-5
  longedit=yes
  depl_update=3
  accel=cheby
  chebymax=5
  diffusionmethod=nem
  outers=250
  demand_conv=yes
  specshiftcorr=no
  therms=1
  printscreen=yes
  deplete=yes
  scalefact=no
  thupdate=5
  eps_void=1e-7
  microdeplete=no
  ratiohmfuel=0.881481
'  epsinner=5e-4
'  epsouter=1e-5
end parameter

read edit
  kinf
  power
end edit

read heattransfer
  mcore=102.5
  bypass=6.779
  flow=yes
  mode=m
  rhovsat=2.3299
  tinlet=527.485
  tinletmin=500
  tinletmax=550
  tsat=548.84
  uvsat=1109.8

' DUMMY VALUES FOR THESE - SHOULD TEST DRIFT-FLUX COMPLETENESS
  rho_vs_ufit .1  end rho_vs_ufit
  t_vs_ufit .1 end t_vs_ufit
  u_vs_Tfit .1 end u_vs_Tfit

end heattransfer

read fuelmech
  wc=1.0 wp=0 fiss_frac=0.975 fuelden=643.994

  heff_vs_t 0.78363116E-01 -0.19203380E-04 0.73696720E-08 end heff_vs_t
```

```
  tavg_vs_lpd  530.2 99.429 0.0075 end tavg_vs_lpd
'  heff_vs_t 2.0 end heff_vs_t
  tsurf_vs_lpd  530.2 99.429 0.0075 end tsurf_vs_lpd
  cp_vs_tfit 0.8110000193E-01 end cp_vs_tfit

  fuelfrac 2r0.0 6r0.25354 end fuelfrac
  bunarea  2r0.25 6r0.1985 end bunarea
  eqdiam   2r0.5 6r0.05083 end eqdiam
  hydiam   2r0.5 6r0.06302 end hydiam
  fpinrad  2r0.0 6r0.2435  end fpinrad
  frodrad  2r0.0 6r0.2815  end frodrad
  numfrods 2r0 6r49        end numfrods
  wtfri  2r1.0 6r0.57325   end wtfri
  wtfro  2r1.0 6r0.57325   end wtfro
  lattice_ids  1 2 3 4 5 6 7 8 end lattice_ids

  losscoeffs 7r1.0 end losscoeffs
  losscoeffs_loc 2.325 4.0 5.683 7.358 9.042 10.717 12.392 end losscoeffs_loc
  orificecoeff 45.0 201.4 72.1 10. end orificecoeff
  orificecoeff_ids 1 2 3 4 end orificecoeff_ids
end fuelmech

read burndata
  pres=1050
  burnup=0.0  sm=no xe=no crod_id=1 delbu=0.0 pctpwr=55.7 pctflow=103.3 bypass=13.37
tinlet=530.17 end
  burnup=1.0  sm=eq xe=eq crod_id=1  pctpwr=55.7  pctflow=103.3 bypass=13.37 tinlet=530.17  end
  burnup=253.5  sm=eq xe=eq crod_id=1  pctpwr=55.7  pctflow=103.3 bypass=13.37 tinlet=530.17  end
  burnup=429.9  sm=eq xe=eq crod_id=2  pctpwr=79    pctflow=105.3 bypass=13.67 tinlet=528.80  end
  burnup=714.29 sm=eq xe=eq crod_id=3  pctpwr=76.3  pctflow=70.3  bypass=8.32  tinlet=522.94  end
  burnup=816.80 sm=eq xe=eq crod_id=4  pctpwr=96.1  pctflow=105.1 bypass=13.64 tinlet=528.29  end
  burnup=1113.3 sm=eq xe=eq crod_id=5  pctpwr=99.0  pctflow=103.0 bypass=13.33 tinlet=528.72  end
  burnup=1747.1 sm=eq xe=eq crod_id=6  pctpwr=99.6  pctflow=94.7  bypass=12.06 tinlet=528.34  end
  burnup=2292.8 sm=eq xe=eq crod_id=7  pctpwr=100.0 pctflow=100.6 bypass=12.96 tinlet=527.66  end
  burnup=2816.4 sm=eq xe=eq crod_id=8  pctpwr=99.1  pctflow=98.7  bypass=12.67 tinlet=528.04  end
  burnup=3218.7 sm=eq xe=eq crod_id=9  pctpwr=86.7  pctflow=76.8  bypass=9.31  tinlet=521.77  end
  burnup=3904.4 sm=eq xe=eq crod_id=10 pctpwr=99.3  pctflow=101.3 bypass=13.06 tinlet=529.87  end
  burnup=4810.4 sm=eq xe=eq crod_id=11 pctpwr=99.6  pctflow=101.6 bypass=13.11 tinlet=529.06  end
  burnup=5177.5 sm=eq xe=eq crod_id=12 pctpwr=99.5  pctflow=101.5 bypass=13.09 tinlet=529.30  end
  burnup=5800.3 sm=eq xe=eq crod_id=13 pctpwr=100.0 pctflow=100.6 bypass=12.96 tinlet=529.55  end
  burnup=6217.0 sm=eq xe=eq crod_id=14 pctpwr=99.7  pctflow=103.5 bypass=13.40 tinlet=529.58  end
  burnup=6730.6 sm=eq xe=eq crod_id=15 pctpwr=97.6  pctflow=103.5 bypass=13.40 tinlet=529.61  end
  burnup=7131.9 sm=eq xe=eq crod_id=16 pctpwr=96.3  pctflow=102.8 bypass=13.30 tinlet=529.69  end
  burnup=7716.1 sm=eq xe=eq crod_id=17 pctpwr=50.1  pctflow=48.9  bypass=5.03  tinlet=519.22  end
  burnup=8046.8 sm=eq xe=eq crod_id=18 pctpwr=56.3  pctflow=38.9  bypass=3.50  tinlet=510.62  end
  burnup=8500.9 sm=eq xe=eq crod_id=19 pctpwr=57.2  pctflow=39.4  bypass=3.58  tinlet=512.55  end
  burnup=8928.6 sm=eq xe=eq crod_id=20 pctpwr=56.4  pctflow=39.9  bypass=1.59  tinlet=511.88  end
  burnup=9292.4 sm=eq xe=eq crod_id=21 pctpwr=99.8  pctflow=104.5 bypass=6.76  tinlet=530.10  end
  burnup=9662.8 sm=eq xe=eq crod_id=22 pctpwr=100.0 pctflow=98.7  bypass=6.30  tinlet=528.12  end
  burnup=10246  sm=eq xe=eq crod_id=23 pctpwr=98.8  pctflow=104.1 bypass=6.73  tinlet=530.26  end
  burnup=11133  sm=eq xe=eq crod_id=24 pctpwr=91.1  pctflow=105.8 bypass=6.86  tinlet=526.81  end
end burndata

read geom
' BOUNDARY CONDITIONS
  inner=cyclic
  outer=zero
  up=zero
  down=zero
  orifice_id=117

' BUNDLE PITCHES
  bpitchx=6.0 bpitchy=6.0
```

```
' X/Y/Z meshes
  deltax 34r6.0 end deltax
  deltay 34r6.0 end deltay
  bottomfuelnode=4 topfuelnode=27
  deltaz 3r3.0 24r6.0 3r3.0 end deltaz
  figure  3r6 2r1 6r2 4r3  2r4 6r5 4r1 3r7 end figure

' Rotation for nodal ADF's
  rotation=217

' CRODS
  crload=bottomup
  crbank 1 17
  144 144 144 144
  144 144 24  144 114
  144 144 144 144 144 144
  144 144 114 144 114 144 12
  144 144 144 144 144 144 144 144
  144 24  144 114 144 12  144 114
  144 144 144 144 144 144 144 144
  144 114 144 12  144 114 144 30
  end crbank

  crbank 2 17
  144 144 144 144
  144 144 114 144 102
  144 144 144 144 144 144
  144 144 114 144 102 144 42
  144 144 144 144 144 144 144 144
  144 114 144 102 144 36  144 114
  144 144 144 144 144 144 144 144
  144 102 144 42  144 114 144 42
  end crbank

  crbank 3 17
  144 144 144 144
  144 126 144 120 144
  144 144 144 144 144 144
  144 144 144 114 144 96  144
  144 144 144 144 144 144 144 144
  144 144 114 144 42  144 120 144
  144 144 144 144 144 144 144 144
  144 144 90  144 114 144 48  144
  end crbank

  crbank 4 17
  144 144 144 144
  144 144 90 144  120
  144 144 144 144 144 144
  144 144 120 144 114 144 114
  144 144 144 144 144 144 144 144
  144 90  144 114 144 42  144 114
  144 144 144 144 144 144 144 144
  144 144 144 114 144 114 144 48
  end crbank

  crbank 5 17
  144 144 144 144
  144 144 96  144  120
  144 144 144 144 144 144
  144 144 120 144 102 144 84
  144 144 144 144 144 144 144 144
  144 96  144 114 144 36  144 114
  144 144 144 144 144 144 144 144
```

```
144 120 144 84  144 114 144 42
end crbank

crbank 6 17
144 144 144 144
144 144 96  144 120
144 144 144 144 144 144
144 144 120 144 96  144 60
144 144 144 144 144 144 144 144
144 96  144 96  144 24  144 108
144 144 144 144 144 144 144 144
144 120 144 60  144 108 144 30
end crbank

crbank 7 17
144 144 144 144
144 126 144 78  144
144 144 144 144 144 144
144 102 144 90  144 24  144
144 144 144 132 144 126 144 144
144 144 96  144 24  144 84  144
144 144 144 132 144 120 144 132
144 144 42  144 96  144 18  144
end crbank
crbank 8 17
144 144 144 144
144 114 144 78  144
144 144 144 144 144 144
144 102 144 60  144 18  144
144 144 144 114 144 126 144 144
144 144 78  144 12  144 72  144
144 144 144 132 144 120 144 120
144 144 30  144 96  144 18  144
end crbank

crbank 9 17
144 144 144 144
144 144 60  144 42
144 144 120 144 132 144
144 144 42  144 54  144 24
144 144 120 144 144 144 114 144
144 60  144 54  144 12  144 66
144 144 132 144 114 144 108 144
144 42  144 24  144 66  144 24
end crbank

crbank 10 17
144 144 144 144
144 144 90  144 42
144 144 108 144 114 144
144 144 42  144 36  144 24
144 144 108 144 108 144 114 144
144 90  144 36  144 18  144 36
144 144 114 144 114 144 102 144
144 42  144 24  144 36  144 30
end crbank

crbank 11 17
144 144 144 144
144 114 144 84  144
144 108 144 48  144 18
144 144 144 90  144 114 144
144 108 144 24  144 18  144 48
144 144 72  144 108 144 102 144
```

```
144 96  144 18  144 30  144 36
144 144 30  144 108 144 108 144
end crbank

crbank 12 17
144 144 144 144
144 144 72  144 42
144 144 108 144 114 144
144 144 36  144 30  144 18
144 144 108 144 96  144 102 144
144 72  144 30  144 18  144 30
144 144 114 144 102 144 102 144
144 42  144 18  144 30  144 30
end crbank
crbank 13 17
144 144 144 144
144 144 72  144 42
144 144 108 144 114 144
144 144 36  144 30  144 24
144 144 108 144 102 144 114 144
144 72  144 30  144 18  144 30
144 144 114 144 114 144 102 144
144 42  144 24  144 30  144 36
end crbank

crbank 14 17
144 144 144 144
144 114 144 84  144
144 108 144 42  144 24
144 144 144 84  144 114 144
144 108 144 24  144 24  144 54
144 144 60  144 108 144 102 144
144 90  144 18  144 24  144 36
144 144 30  144 114 144 108 144
end crbank

crbank 15 17
144 144 144 144
144 114 144 84  144
144 108 144 42  144 24
144 144 144 84  144 114 144
144 108 144 30  144 24  144 54
144 144 60  144 108 144 102 144
144 90  144 18  144 24  144 36
144 144 36  144 114 144 108 144
end crbank

crbank 16 17
144 144 144 144
144 114 144 90  144
144 108 144 42  144 24
144 144 144 96  144 114 144
144 108 144 36  144 24  144 60
144 144 60  144 108 144 108 144
144 96  144 18  144 24  144 36
144 144 42  144 120 144 108 144
end crbank

crbank 17 17
144 144 144 144
144 144 36  144 36
144 144 120 144 132 144
144 144 24  144 24  144 12
144 144 120 144 132 144 120 144
```

```
144 36  144 24  144 0   144 12
144 144 132 144 120 144 120 144
144 36  144 12  144 12  144 18
end crbank
crbank 18 17
144 144 144 144
144 144 48  144 66
144 144 126 144 132 144
144 144 60  144 30  144 18
144 144 126 144 132 144 120 144
144 48  144 30  144 24  144 36
144 144 132 144 120 144 120 144
144 66  144 18  144 36  144 48
end crbank

crbank 19 17
144 144 144 144
144 144 54  144 78
144 144 132 144 132 144
144 144 84  144 30  144 30
144 144 132 144 132 144 132 144
144 54  144 30  144 24  144 36
144 144 132 144 132 144 126 144
144 78  144 30  144 36  144 66
end crbank

crbank 20 17
144 144 144 144
144 144 144 114 144
144 102 144 72  144 30
144 144 144 138 144 144 144
144 102 144 36  144 36  144 30
144 144 144 144 126 144 126 144
144 72  144 24  144 48  144 30
144 144 144 144 144 144 132 144
end crbank

crbank 21 17
144 144 144 144
144 144 144 114 144
144 114 144 96  144 60
144 144 144 144 144 144 144
144 108 144 90  144 36  144 96
144 144 144 144 132 144 132 144
144 96  144 36  144 60  144 54
144 144 144 144 144 144 144 144
end crbank
crbank 22 17
144 144 144 144
144 144 144 132 144
144 126 144 108 144 102
144 144 144 144 144 144 144
144 126 144 114 144 54  144 120
144 144 144 144 144 144 144 144
144 114 144 60  144 102 144 54
144 144 144 144 144 144 144 144
end crbank

crbank 23 17
144 144 144 144
144 144 114 144 114
144 144 144 144 144 144
144 144 120 144 108 144 108
144 144 144 144 144 144 144 144
```

```
  144 114 144 108 144 96  144 60
  144 144 144 144 144 144 144 144
  144 114 144 108 144 60  144 78
  end crbank

  crbank 24 17
  144 144 144 144
  144 144 120 144 120
  144 144 144 144 144 144
  144 144 126 144 108 144 120
  144 144 144 144 144 144 144 144
  144 120 144 108 144 108 144 78
  144 144 144 144 144 144 144 144
  144 120 144 120 144 78  144 96
  end crbank
end geom

' FUEL TYPE <0----12><12-----48><48-----72><72--84><84-----120><120---144>
'  1          4          4          4        4         4           4
'  2          3          6          6        3         3           3
'  3          5          7          8        8         7           5

read arrays
ara=1 nux=34 nuy=34 fill
' BOTTOM 12IN ACTIVE FUEL, 120IN to 144IN
' 1 2 3 4 5 6 7 8 9101112131415161718192021222324252627282930
  0 0 0 0 0 0 0 0 0 0 1 1 1 1 1 1 1 1 1 1 1 1 1 1 0 0 0 0 0 0 0 0 0 0
  0 0 0 0 0 0 0 0 0 1 1 1 1 1 1 1 1 1 1 1 1 1 1 1 1 0 0 0 0 0 0 0 0 0
  0 0 0 0 0 0 0 0 1 1 3 3 3 3 3 3 3 3 3 3 3 3 3 3 1 1 0 0 0 0 0 0 0 0
  0 0 0 0 0 0 1 1 1 3 3 4 4 3 3 4 4 3 3 3 4 3 3 3 3 1 1 1 0 0 0 0 0 0
  0 0 0 0 0 1 1 3 3 3 3 3 3 3 3 3 3 3 3 3 3 3 3 3 3 3 3 1 1 0 0 0 0 0
  0 0 0 0 0 1 1 3 4 3 3 4 4 3 3 4 4 3 3 4 4 3 3 4 4 3 3 1 1 0 0 0 0 0
  0 0 0 1 1 1 3 4 4 3 5 4 4 5 5 4 4 5 5 4 4 5 5 4 4 3 4 3 1 1 1 0 0 0
  0 0 1 1 3 3 3 3 3 5 5 5 5 5 5 5 5 5 5 5 5 5 5 5 5 3 3 4 3 3 1 1 0 0
  0 0 1 1 3 3 3 3 5 5 5 5 5 5 5 5 5 5 5 5 5 5 5 5 5 5 3 3 3 3 1 1 0 0
  0 1 1 3 4 3 3 4 4 5 5 4 4 5 5 4 4 5 5 4 4 5 5 4 4 5 5 4 4 3 3 1 1 0
  1 1 3 3 4 3 5 4 4 5 5 4 4 5 5 4 4 5 5 4 4 5 5 4 4 5 5 4 4 3 3 3 1 1
  1 1 3 3 3 3 5 5 5 5 5 5 5 5 5 5 5 5 5 5 5 5 5 5 5 5 5 5 3 3 3 3 1 1
  1 1 3 3 3 3 5 5 5 5 5 5 5 5 5 5 5 5 5 5 5 5 5 5 5 5 5 5 3 3 3 3 1 1
  1 1 3 3 4 3 5 4 4 5 5 4 4 5 5 4 4 5 5 4 4 5 5 4 4 5 5 4 4 3 4 3 1 1
  1 1 3 3 4 3 5 4 4 5 5 4 4 5 5 4 4 5 5 4 4 5 5 4 4 5 5 4 4 3 3 3 1 1
  1 1 3 3 3 3 5 5 5 5 5 5 5 5 5 5 5 5 5 5 5 5 5 5 5 5 5 5 3 3 3 3 1 1
  1 1 3 3 3 3 5 5 5 5 5 5 5 5 5 5 5 5 5 5 5 5 5 5 5 5 5 5 3 3 3 3 1 1
  1 1 3 3 4 3 5 4 4 5 5 4 4 5 5 4 4 5 5 4 4 5 5 4 4 5 5 4 4 3 4 3 1 1
  1 1 3 3 4 3 5 4 4 5 5 4 4 5 5 4 4 5 5 4 4 5 5 4 4 5 5 4 4 3 4 3 1 1
  1 1 3 3 3 3 5 5 5 5 5 5 5 5 5 5 5 5 5 5 5 5 5 5 5 5 5 5 3 3 3 3 1 1
  1 1 3 3 3 3 5 5 5 5 5 5 5 5 5 5 5 5 5 5 5 5 5 5 5 5 5 5 3 3 3 3 1 1
  1 1 3 3 4 3 5 4 4 5 5 4 4 5 5 4 4 5 5 4 4 5 5 4 4 5 5 4 4 3 4 3 1 1
  1 1 3 3 4 3 5 4 4 5 5 4 4 5 5 4 4 5 5 4 4 5 5 4 4 5 5 4 4 3 4 3 1 1
  1 1 3 3 3 3 5 5 5 5 5 5 5 5 5 5 5 5 5 5 5 5 5 5 5 5 5 5 3 3 3 3 1 1
  0 1 1 3 3 3 3 5 5 5 5 5 5 5 5 5 5 5 5 5 5 5 5 5 5 5 5 3 3 3 3 1 1 0
  0 0 1 1 3 4 3 4 4 5 5 4 4 5 5 4 4 5 5 4 4 5 5 4 4 5 3 4 4 3 1 1 0 0
  0 0 1 1 3 3 3 4 4 5 5 4 4 5 5 4 4 5 5 4 4 5 5 4 4 3 3 4 3 3 1 1 0 0
  0 0 0 1 1 1 3 3 3 3 5 5 5 5 5 5 5 5 5 5 5 5 5 5 3 3 3 3 1 1 1 0 0 0
  0 0 0 0 0 1 1 3 4 3 3 3 3 3 3 3 3 3 3 3 3 3 3 3 3 3 3 1 1 0 0 0 0 0
  0 0 0 0 0 1 1 3 3 3 3 4 4 3 3 4 4 3 3 4 4 3 3 4 4 3 3 1 1 0 0 0 0 0
  0 0 0 0 0 0 1 1 1 3 3 3 3 3 3 3 3 3 3 3 3 3 3 3 3 1 1 1 0 0 0 0 0 0
  0 0 0 0 0 0 0 0 1 1 3 3 3 3 3 3 3 3 3 3 3 3 3 3 1 1 0 0 0 0 0 0 0 0
  0 0 0 0 0 0 0 0 0 1 1 1 1 1 1 1 1 1 1 1 1 1 1 1 1 0 0 0 0 0 0 0 0 0
  0 0 0 0 0 0 0 0 0 0 1 1 1 1 1 1 1 1 1 1 1 1 1 1 0 0 0 0 0 0 0 0 0 0 end fill

ara=2 nux=34 nuy=34 fill
' ACTIVE FUEL 12IN to 48IN,
' 1 2 3 4 5 6 7 8 9101112131415161718192021222324252627282930
```

```
  0 0 0 0 0 0 0 0 0 0 1 1 1 1 1 1 1 1 1 1 1 1 1 1 0 0 0 0 0 0 0 0 0 0
  0 0 0 0 0 0 0 0 0 1 1 1 1 1 1 1 1 1 1 1 1 1 1 1 1 1 0 0 0 0 0 0 0 0 0
  0 0 0 0 0 0 0 0 1 1 6 6 6 6 6 6 6 6 6 6 6 6 6 6 1 1 0 0 0 0 0 0 0 0
  0 0 0 0 0 0 1 1 1 6 6 4 4 6 6 4 4 6 6 6 4 6 6 6 6 1 1 1 0 0 0 0 0 0
  0 0 0 0 0 1 1 6 6 6 6 6 6 6 6 6 6 6 6 6 6 6 6 6 6 6 6 1 1 0 0 0 0 0
  0 0 0 0 0 1 1 6 4 6 6 4 4 6 6 4 4 6 6 4 4 6 6 4 4 6 6 1 1 0 0 0 0 0
  0 0 0 1 1 1 6 4 4 6 7 4 4 7 7 4 4 7 7 4 4 7 7 4 4 6 4 6 1 1 1 0 0 0
  0 0 1 1 6 6 6 6 6 7 7 7 7 7 7 7 7 7 7 7 7 7 7 7 7 6 6 4 6 6 1 1 0 0
  0 0 1 1 6 6 6 6 7 7 7 7 7 7 7 7 7 7 7 7 7 7 7 7 7 7 6 6 6 6 1 1 0 0
  0 1 1 6 4 6 6 4 4 7 7 4 4 7 7 4 4 7 7 4 4 7 7 4 4 7 7 4 4 6 6 1 1 0
  1 1 6 6 4 6 7 4 4 7 7 4 4 7 7 4 4 7 7 4 4 7 7 4 4 7 7 4 4 6 6 6 1 1
  1 1 6 6 6 6 7 7 7 7 7 7 7 7 7 7 7 7 7 7 7 7 7 7 7 7 7 7 6 6 6 6 1 1
  1 1 6 6 6 6 7 7 7 7 7 7 7 7 7 7 7 7 7 7 7 7 7 7 7 7 7 7 6 6 6 6 1 1
  1 1 6 6 4 6 7 4 4 7 7 4 4 7 7 4 4 7 7 4 4 7 7 4 4 7 7 4 4 6 4 6 1 1
  1 1 6 6 4 6 7 4 4 7 7 4 4 7 7 4 4 7 7 4 4 7 7 4 4 7 7 4 4 6 6 6 1 1
  1 1 6 6 6 6 7 7 7 7 7 7 7 7 7 7 7 7 7 7 7 7 7 7 7 7 7 7 6 6 6 6 1 1
  1 1 6 6 6 6 7 7 7 7 7 7 7 7 7 7 7 7 7 7 7 7 7 7 7 7 7 7 6 6 6 6 1 1
  1 1 6 6 4 6 7 4 4 7 7 4 4 7 7 4 4 7 7 4 4 7 7 4 4 7 7 4 4 6 4 6 1 1
  1 1 6 6 4 6 7 4 4 7 7 4 4 7 7 4 4 7 7 4 4 7 7 4 4 7 7 4 4 6 4 6 1 1
  1 1 6 6 6 6 7 7 7 7 7 7 7 7 7 7 7 7 7 7 7 7 7 7 7 7 7 7 6 6 6 6 1 1
  1 1 6 6 6 6 7 7 7 7 7 7 7 7 7 7 7 7 7 7 7 7 7 7 7 7 7 7 6 6 6 6 1 1
  1 1 6 6 4 6 7 4 4 7 7 4 4 7 7 4 4 7 7 4 4 7 7 4 4 7 7 4 4 6 4 6 1 1
  1 1 6 6 4 6 7 4 4 7 7 4 4 7 7 4 4 7 7 4 4 7 7 4 4 7 7 4 4 6 4 6 1 1
  1 1 6 6 6 6 7 7 7 7 7 7 7 7 7 7 7 7 7 7 7 7 7 7 7 7 7 7 6 6 6 6 1 1
  0 1 1 6 6 6 6 7 7 7 7 7 7 7 7 7 7 7 7 7 7 7 7 7 7 7 7 6 6 6 6 1 1 0
  0 0 1 1 6 4 6 4 4 7 7 4 4 7 7 4 4 7 7 4 4 7 7 4 4 7 6 4 4 6 1 1 0 0
  0 0 1 1 6 6 6 4 4 7 7 4 4 7 7 4 4 7 7 4 4 7 7 4 4 6 6 4 6 6 1 1 0 0
  0 0 0 1 1 1 6 6 6 6 7 7 7 7 7 7 7 7 7 7 7 7 7 7 6 6 6 6 1 1 1 0 0 0
  0 0 0 0 0 1 1 6 4 6 6 6 6 6 6 6 6 6 6 6 6 6 6 6 6 6 6 1 1 0 0 0 0 0
  0 0 0 0 0 1 1 6 6 6 6 4 4 6 6 4 4 6 6 4 4 6 6 4 4 6 6 1 1 0 0 0 0 0
  0 0 0 0 0 0 1 1 1 6 6 6 6 6 6 6 6 6 6 6 6 6 6 6 6 1 1 1 0 0 0 0 0 0
  0 0 0 0 0 0 0 0 1 1 6 6 6 6 6 6 6 6 6 6 6 6 6 6 1 1 0 0 0 0 0 0 0 0
  0 0 0 0 0 0 0 0 0 1 1 1 1 1 1 1 1 1 1 1 1 1 1 1 1 1 0 0 0 0 0 0 0 0 0
  0 0 0 0 0 0 0 0 0 0 1 1 1 1 1 1 1 1 1 1 1 1 1 1 0 0 0 0 0 0 0 0 0 0 end fill

ara=3 nux=34 nuy=34 fill
' ACTIVE FUEL 48IN to 72IN
' 1 2 3 4 5 6 7 8 9101112131415161718192021222324252627282930
  0 0 0 0 0 0 0 0 0 0 1 1 1 1 1 1 1 1 1 1 1 1 1 1 0 0 0 0 0 0 0 0 0 0
  0 0 0 0 0 0 0 0 0 1 1 1 1 1 1 1 1 1 1 1 1 1 1 1 1 1 0 0 0 0 0 0 0 0 0
  0 0 0 0 0 0 0 0 1 1 6 6 6 6 6 6 6 6 6 6 6 6 6 6 1 1 0 0 0 0 0 0 0 0
  0 0 0 0 0 0 1 1 1 6 6 4 4 6 6 4 4 6 6 6 4 6 6 6 6 1 1 1 0 0 0 0 0 0
  0 0 0 0 0 1 1 6 6 6 6 6 6 6 6 6 6 6 6 6 6 6 6 6 6 6 6 1 1 0 0 0 0 0
  0 0 0 0 0 1 1 6 4 6 6 4 4 6 6 4 4 6 6 4 4 6 6 4 4 6 6 1 1 0 0 0 0 0
  0 0 0 1 1 1 6 4 4 6 8 4 4 8 8 4 4 8 8 4 4 8 8 4 4 6 4 6 1 1 1 0 0 0
  0 0 1 1 6 6 6 6 6 8 8 8 8 8 8 8 8 8 8 8 8 8 8 8 8 6 6 4 6 6 1 1 0 0
  0 0 1 1 6 6 6 6 8 8 8 8 8 8 8 8 8 8 8 8 8 8 8 8 8 8 6 6 6 6 1 1 0 0
  0 1 1 6 4 6 6 4 4 8 8 4 4 8 8 4 4 8 8 4 4 8 8 4 4 8 8 4 4 6 6 1 1 0
  1 1 6 6 4 6 8 4 4 8 8 4 4 8 8 4 4 8 8 4 4 8 8 4 4 8 8 4 4 6 6 6 1 1
  1 1 6 6 6 6 8 8 8 8 8 8 8 8 8 8 8 8 8 8 8 8 8 8 8 8 8 8 6 6 6 6 1 1
  1 1 6 6 6 6 8 8 8 8 8 8 8 8 8 8 8 8 8 8 8 8 8 8 8 8 8 8 6 6 6 6 1 1
  1 1 6 6 4 6 8 4 4 8 8 4 4 8 8 4 4 8 8 4 4 8 8 4 4 8 8 4 4 6 4 6 1 1
  1 1 6 6 4 6 8 4 4 8 8 4 4 8 8 4 4 8 8 4 4 8 8 4 4 8 8 4 4 6 6 6 1 1
  1 1 6 6 6 6 8 8 8 8 8 8 8 8 8 8 8 8 8 8 8 8 8 8 8 8 8 8 6 6 6 6 1 1
  1 1 6 6 6 6 8 8 8 8 8 8 8 8 8 8 8 8 8 8 8 8 8 8 8 8 8 8 6 6 6 6 1 1
  1 1 6 6 4 6 8 4 4 8 8 4 4 8 8 4 4 8 8 4 4 8 8 4 4 8 8 4 4 6 4 6 1 1
  1 1 6 6 4 6 8 4 4 8 8 4 4 8 8 4 4 8 8 4 4 8 8 4 4 8 8 4 4 6 4 6 1 1
  1 1 6 6 6 6 8 8 8 8 8 8 8 8 8 8 8 8 8 8 8 8 8 8 8 8 8 8 6 6 6 6 1 1
  1 1 6 6 6 6 8 8 8 8 8 8 8 8 8 8 8 8 8 8 8 8 8 8 8 8 8 8 6 6 6 6 1 1
  1 1 6 6 4 6 8 4 4 8 8 4 4 8 8 4 4 8 8 4 4 8 8 4 4 8 8 4 4 6 4 6 1 1
  1 1 6 6 4 6 8 4 4 8 8 4 4 8 8 4 4 8 8 4 4 8 8 4 4 8 8 4 4 6 4 6 1 1
  1 1 6 6 6 6 8 8 8 8 8 8 8 8 8 8 8 8 8 8 8 8 8 8 8 8 8 8 6 6 6 6 1 1
  0 1 1 6 6 6 6 8 8 8 8 8 8 8 8 8 8 8 8 8 8 8 8 8 8 8 8 6 6 6 6 1 1 0
  0 0 1 1 6 4 6 4 4 8 8 4 4 8 8 4 4 8 8 4 4 8 8 4 4 8 6 4 4 6 1 1 0 0
```

```
  0 0 1 1 6 6 6 4 4 8 8 4 4 8 8 4 4 8 8 4 4 8 8 4 4 6 6 4 6 6 1 1 0 0
  0 0 0 1 1 1 6 6 6 6 8 8 8 8 8 8 8 8 8 8 8 8 8 8 6 6 6 6 1 1 1 0 0 0
  0 0 0 0 0 1 1 6 4 6 6 6 6 6 6 6 6 6 6 6 6 6 6 6 6 6 6 1 1 0 0 0 0 0
  0 0 0 0 0 1 1 6 6 6 6 4 4 6 6 4 4 6 6 4 4 6 6 4 4 6 6 1 1 0 0 0 0 0
  0 0 0 0 0 0 1 1 1 6 6 6 6 6 6 6 6 6 6 6 6 6 6 6 6 1 1 1 0 0 0 0 0 0
  0 0 0 0 0 0 0 0 1 1 6 6 6 6 6 6 6 6 6 6 6 6 6 6 1 1 0 0 0 0 0 0 0 0
  0 0 0 0 0 0 0 0 0 1 1 1 1 1 1 1 1 1 1 1 1 1 1 1 1 0 0 0 0 0 0 0 0 0
  0 0 0 0 0 0 0 0 0 0 1 1 1 1 1 1 1 1 1 1 1 1 1 1 0 0 0 0 0 0 0 0 0 0 end fill

ara=4 nux=34 nuy=34 fill
' ACTIVE FUEL 72IN to 84IN
' 1 2 3 4 5 6 7 8 910111213141516171819202122232425262728293О
  0 0 0 0 0 0 0 0 0 0 1 1 1 1 1 1 1 1 1 1 1 1 1 1 0 0 0 0 0 0 0 0 0 0
  0 0 0 0 0 0 0 0 0 1 1 1 1 1 1 1 1 1 1 1 1 1 1 1 1 1 0 0 0 0 0 0 0 0 0
  0 0 0 0 0 0 0 0 1 1 3 3 3 3 3 3 3 3 3 3 3 3 3 3 1 1 0 0 0 0 0 0 0 0
  0 0 0 0 0 0 1 1 1 3 3 4 4 3 3 4 4 3 3 3 4 3 3 3 3 1 1 1 0 0 0 0 0 0
  0 0 0 0 0 1 1 3 3 3 3 3 3 3 3 3 3 3 3 3 3 3 3 3 3 3 3 1 1 0 0 0 0 0
  0 0 0 0 0 1 1 3 4 3 3 4 4 3 3 4 4 3 3 4 4 3 3 4 4 3 3 1 1 0 0 0 0 0
  0 0 0 1 1 1 3 4 4 3 8 4 4 8 8 4 4 8 8 4 4 8 8 4 4 3 4 3 1 1 1 0 0 0
  0 0 1 1 3 3 3 3 3 8 8 8 8 8 8 8 8 8 8 8 8 8 8 8 8 3 3 4 3 3 1 1 0 0
  0 0 1 1 3 3 3 3 8 8 8 8 8 8 8 8 8 8 8 8 8 8 8 8 8 8 3 3 3 3 1 1 0 0
  0 1 1 3 4 3 3 4 4 8 8 4 4 8 8 4 4 8 8 4 4 8 8 4 4 8 8 4 4 3 3 1 1 0
  1 1 3 3 4 3 8 4 4 8 8 4 4 8 8 4 4 8 8 4 4 8 8 4 4 8 8 4 4 3 3 3 1 1
  1 1 3 3 3 3 8 8 8 8 8 8 8 8 8 8 8 8 8 8 8 8 8 8 8 8 8 8 3 3 3 3 1 1
  1 1 3 3 3 3 8 8 8 8 8 8 8 8 8 8 8 8 8 8 8 8 8 8 8 8 8 8 3 3 3 3 1 1
  1 1 3 3 4 3 8 4 4 8 8 4 4 8 8 4 4 8 8 4 4 8 8 4 4 8 8 4 4 3 4 3 1 1
  1 1 3 3 4 3 8 4 4 8 8 4 4 8 8 4 4 8 8 4 4 8 8 4 4 8 8 4 4 3 3 3 1 1
  1 1 3 3 3 3 8 8 8 8 8 8 8 8 8 8 8 8 8 8 8 8 8 8 8 8 8 8 3 3 3 3 1 1
  1 1 3 3 3 3 8 8 8 8 8 8 8 8 8 8 8 8 8 8 8 8 8 8 8 8 8 8 3 3 3 3 1 1
  1 1 3 3 4 3 8 4 4 8 8 4 4 8 8 4 4 8 8 4 4 8 8 4 4 8 8 4 4 3 4 3 1 1
  1 1 3 3 4 3 8 4 4 8 8 4 4 8 8 4 4 8 8 4 4 8 8 4 4 8 8 4 4 3 4 3 1 1
  1 1 3 3 3 3 8 8 8 8 8 8 8 8 8 8 8 8 8 8 8 8 8 8 8 8 8 8 3 3 3 3 1 1
  1 1 3 3 3 3 8 8 8 8 8 8 8 8 8 8 8 8 8 8 8 8 8 8 8 8 8 8 3 3 3 3 1 1
  1 1 3 3 4 3 8 4 4 8 8 4 4 8 8 4 4 8 8 4 4 8 8 4 4 8 8 4 4 3 4 3 1 1
  1 1 3 3 4 3 8 4 4 8 8 4 4 8 8 4 4 8 8 4 4 8 8 4 4 8 8 4 4 3 4 3 1 1
  1 1 3 3 3 3 8 8 8 8 8 8 8 8 8 8 8 8 8 8 8 8 8 8 8 8 8 8 3 3 3 3 1 1
  0 1 1 3 3 3 3 8 8 8 8 8 8 8 8 8 8 8 8 8 8 8 8 8 8 8 8 3 3 3 3 1 1 0
  0 0 1 1 3 4 3 4 4 8 8 4 4 8 8 4 4 8 8 4 4 8 8 4 4 8 3 4 4 3 1 1 0 0
  0 0 1 1 3 3 3 4 4 8 8 4 4 8 8 4 4 8 8 4 4 8 8 4 4 3 3 4 3 3 1 1 0 0
  0 0 0 1 1 1 3 3 3 3 8 8 8 8 8 8 8 8 8 8 8 8 8 8 3 3 3 3 1 1 1 0 0 0
  0 0 0 0 0 1 1 3 4 3 3 3 3 3 3 3 3 3 3 3 3 3 3 3 3 3 3 1 1 0 0 0 0 0
  0 0 0 0 0 1 1 3 3 3 3 4 4 3 3 4 4 3 3 4 4 3 3 4 4 3 3 1 1 0 0 0 0 0
  0 0 0 0 0 0 1 1 1 3 3 3 3 3 3 3 3 3 3 3 3 3 3 3 3 1 1 1 0 0 0 0 0 0
  0 0 0 0 0 0 0 0 1 1 3 3 3 3 3 3 3 3 3 3 3 3 3 3 1 1 0 0 0 0 0 0 0 0
  0 0 0 0 0 0 0 0 0 1 1 1 1 1 1 1 1 1 1 1 1 1 1 1 1 1 0 0 0 0 0 0 0 0 0
  0 0 0 0 0 0 0 0 0 0 1 1 1 1 1 1 1 1 1 1 1 1 1 1 0 0 0 0 0 0 0 0 0 0 end fill

ara=5 nux=34 nuy=34 fill
' ACTIVE FUEL 84IN to 120IN
' 1 2 3 4 5 6 7 8 910111213141516171819202122232425262728293О
  0 0 0 0 0 0 0 0 0 0 1 1 1 1 1 1 1 1 1 1 1 1 1 1 0 0 0 0 0 0 0 0 0 0
  0 0 0 0 0 0 0 0 0 1 1 1 1 1 1 1 1 1 1 1 1 1 1 1 1 1 0 0 0 0 0 0 0 0 0
  0 0 0 0 0 0 0 0 1 1 3 3 3 3 3 3 3 3 3 3 3 3 3 3 1 1 0 0 0 0 0 0 0 0
  0 0 0 0 0 0 1 1 1 3 3 4 4 3 3 4 4 3 3 3 4 3 3 3 3 1 1 1 0 0 0 0 0 0
  0 0 0 0 0 1 1 3 3 3 3 3 3 3 3 3 3 3 3 3 3 3 3 3 3 3 3 1 1 0 0 0 0 0
  0 0 0 0 0 1 1 3 4 3 3 4 4 3 3 4 4 3 3 4 4 3 3 4 4 3 3 1 1 0 0 0 0 0
  0 0 0 1 1 1 3 4 4 3 7 4 4 7 7 4 4 7 7 4 4 7 7 4 4 3 4 3 1 1 1 0 0 0
  0 0 1 1 3 3 3 3 3 7 7 7 7 7 7 7 7 7 7 7 7 7 7 7 7 3 3 4 3 3 1 1 0 0
  0 0 1 1 3 3 3 3 7 7 7 7 7 7 7 7 7 7 7 7 7 7 7 7 7 7 3 3 3 3 1 1 0 0
  0 1 1 3 4 3 3 4 4 7 7 4 4 7 7 4 4 7 7 4 4 7 7 4 4 7 7 4 4 3 3 1 1 0
  1 1 3 3 4 3 7 4 4 7 7 4 4 7 7 4 4 7 7 4 4 7 7 4 4 7 7 4 4 3 3 3 1 1
  1 1 3 3 3 3 7 7 7 7 7 7 7 7 7 7 7 7 7 7 7 7 7 7 7 7 7 7 3 3 3 3 1 1
  1 1 3 3 3 3 7 7 7 7 7 7 7 7 7 7 7 7 7 7 7 7 7 7 7 7 7 7 3 3 3 3 1 1
  1 1 3 3 4 3 7 4 4 7 7 4 4 7 7 4 4 7 7 4 4 7 7 4 4 7 7 4 4 3 4 3 1 1
```

```
  1 1 3 3 4 3 7 4 4 7 7 4 4 7 7 4 4 7 7 4 4 7 7 4 4 7 7 4 4 3 3 3 1 1
  1 1 3 3 3 3 7 7 7 7 7 7 7 7 7 7 7 7 7 7 7 7 7 7 7 7 7 7 3 3 3 3 1 1
  1 1 3 3 3 3 7 7 7 7 7 7 7 7 7 7 7 7 7 7 7 7 7 7 7 7 7 7 3 3 3 3 1 1
  1 1 3 3 4 3 7 4 4 7 7 4 4 7 7 4 4 7 7 4 4 7 7 4 4 7 7 4 4 3 4 3 1 1
  1 1 3 3 4 3 7 4 4 7 7 4 4 7 7 4 4 7 7 4 4 7 7 4 4 7 7 4 4 3 4 3 1 1
  1 1 3 3 3 3 7 7 7 7 7 7 7 7 7 7 7 7 7 7 7 7 7 7 7 7 7 7 3 3 3 3 1 1
  1 1 3 3 3 3 7 7 7 7 7 7 7 7 7 7 7 7 7 7 7 7 7 7 7 7 7 7 3 3 3 3 1 1
  1 1 3 3 4 3 7 4 4 7 7 4 4 7 7 4 4 7 7 4 4 7 7 4 4 7 7 4 4 3 4 3 1 1
  1 1 3 3 4 3 7 4 4 7 7 4 4 7 7 4 4 7 7 4 4 7 7 4 4 7 7 4 4 3 4 3 1 1
  1 1 3 3 3 3 7 7 7 7 7 7 7 7 7 7 7 7 7 7 7 7 7 7 7 7 7 7 3 3 3 3 1 1
  0 1 1 3 3 3 3 7 7 7 7 7 7 7 7 7 7 7 7 7 7 7 7 7 7 7 7 3 3 3 3 1 1 0
  0 0 1 1 3 4 3 4 4 7 7 4 4 7 7 4 4 7 7 4 4 7 7 4 4 7 3 4 4 3 1 1 0 0
  0 0 1 1 3 3 3 4 4 7 7 4 4 7 7 4 4 7 7 4 4 7 7 4 4 3 3 4 3 3 1 1 0 0
  0 0 0 1 1 1 3 3 3 3 7 7 7 7 7 7 7 7 7 7 7 7 7 7 3 3 3 3 1 1 1 0 0 0
  0 0 0 0 0 1 1 3 4 3 3 3 3 3 3 3 3 3 3 3 3 3 3 3 3 3 3 1 1 0 0 0 0 0
  0 0 0 0 0 1 1 3 3 3 3 4 4 3 3 4 4 3 3 4 4 3 3 4 4 3 3 1 1 0 0 0 0 0
  0 0 0 0 0 0 1 1 1 3 3 3 3 3 3 3 3 3 3 3 3 3 3 3 3 1 1 1 0 0 0 0 0 0
  0 0 0 0 0 0 0 0 1 1 3 3 3 3 3 3 3 3 3 3 3 3 3 3 1 1 0 0 0 0 0 0 0 0
  0 0 0 0 0 0 0 0 0 1 1 1 1 1 1 1 1 1 1 1 1 1 1 1 1 0 0 0 0 0 0 0 0 0
  0 0 0 0 0 0 0 0 0 0 1 1 1 1 1 1 1 1 1 1 1 1 1 1 0 0 0 0 0 0 0 0 0 0 end fill

ara=6 nux=34 nuy=34 fill
' ACTIVE FUEL 84IN to 120IN
' 1 2 3 4 5 6 7 8 9101112131415161718192021222324252627282930
  0 0 0 0 0 0 0 0 0 0 1 1 1 1 1 1 1 1 1 1 1 1 1 1 0 0 0 0 0 0 0 0 0 0
  0 0 0 0 0 0 0 0 0 1 1 1 1 1 1 1 1 1 1 1 1 1 1 1 1 0 0 0 0 0 0 0 0 0
  0 0 0 0 0 0 0 0 1 1 1 1 1 1 1 1 1 1 1 1 1 1 1 1 1 1 0 0 0 0 0 0 0 0
  0 0 0 0 0 0 1 1 1 1 1 1 1 1 1 1 1 1 1 1 1 1 1 1 1 1 1 1 0 0 0 0 0 0
  0 0 0 0 0 1 1 1 1 1 1 1 1 1 1 1 1 1 1 1 1 1 1 1 1 1 1 1 1 0 0 0 0 0
  0 0 0 0 0 1 1 1 1 1 1 1 1 1 1 1 1 1 1 1 1 1 1 1 1 1 1 1 1 0 0 0 0 0
  0 0 0 1 1 1 1 1 1 1 1 1 1 1 1 1 1 1 1 1 1 1 1 1 1 1 1 1 1 1 1 0 0 0
  0 0 1 1 1 1 1 1 1 1 1 1 1 1 1 1 1 1 1 1 1 1 1 1 1 1 1 1 1 1 1 1 0 0
  0 0 1 1 1 1 1 1 1 1 1 1 1 1 1 1 1 1 1 1 1 1 1 1 1 1 1 1 1 1 1 1 0 0
  0 1 1 1 1 1 1 1 1 1 1 1 1 1 1 1 1 1 1 1 1 1 1 1 1 1 1 1 1 1 1 1 1 0
  1 1 1 1 1 1 1 1 1 1 1 1 1 1 1 1 1 1 1 1 1 1 1 1 1 1 1 1 1 1 1 1 1 1
  1 1 1 1 1 1 1 1 1 1 1 1 1 1 1 1 1 1 1 1 1 1 1 1 1 1 1 1 1 1 1 1 1 1
  1 1 1 1 1 1 1 1 1 1 1 1 1 1 1 1 1 1 1 1 1 1 1 1 1 1 1 1 1 1 1 1 1 1
  1 1 1 1 1 1 1 1 1 1 1 1 1 1 1 1 1 1 1 1 1 1 1 1 1 1 1 1 1 1 1 1 1 1
  1 1 1 1 1 1 1 1 1 1 1 1 1 1 1 1 1 1 1 1 1 1 1 1 1 1 1 1 1 1 1 1 1 1
  1 1 1 1 1 1 1 1 1 1 1 1 1 1 1 1 1 1 1 1 1 1 1 1 1 1 1 1 1 1 1 1 1 1
  1 1 1 1 1 1 1 1 1 1 1 1 1 1 1 1 1 1 1 1 1 1 1 1 1 1 1 1 1 1 1 1 1 1
  1 1 1 1 1 1 1 1 1 1 1 1 1 1 1 1 1 1 1 1 1 1 1 1 1 1 1 1 1 1 1 1 1 1
  1 1 1 1 1 1 1 1 1 1 1 1 1 1 1 1 1 1 1 1 1 1 1 1 1 1 1 1 1 1 1 1 1 1
  1 1 1 1 1 1 1 1 1 1 1 1 1 1 1 1 1 1 1 1 1 1 1 1 1 1 1 1 1 1 1 1 1 1
  1 1 1 1 1 1 1 1 1 1 1 1 1 1 1 1 1 1 1 1 1 1 1 1 1 1 1 1 1 1 1 1 1 1
  1 1 1 1 1 1 1 1 1 1 1 1 1 1 1 1 1 1 1 1 1 1 1 1 1 1 1 1 1 1 1 1 1 1
  1 1 1 1 1 1 1 1 1 1 1 1 1 1 1 1 1 1 1 1 1 1 1 1 1 1 1 1 1 1 1 1 1 1
  1 1 1 1 1 1 1 1 1 1 1 1 1 1 1 1 1 1 1 1 1 1 1 1 1 1 1 1 1 1 1 1 1 1
  0 1 1 1 1 1 1 1 1 1 1 1 1 1 1 1 1 1 1 1 1 1 1 1 1 1 1 1 1 1 1 1 1 0
  0 0 1 1 1 1 1 1 1 1 1 1 1 1 1 1 1 1 1 1 1 1 1 1 1 1 1 1 1 1 1 1 0 0
  0 0 1 1 1 1 1 1 1 1 1 1 1 1 1 1 1 1 1 1 1 1 1 1 1 1 1 1 1 1 1 1 0 0
  0 0 0 1 1 1 1 1 1 1 1 1 1 1 1 1 1 1 1 1 1 1 1 1 1 1 1 1 1 1 1 0 0 0
  0 0 0 0 0 1 1 1 1 1 1 1 1 1 1 1 1 1 1 1 1 1 1 1 1 1 1 1 1 0 0 0 0 0
  0 0 0 0 0 1 1 1 1 1 1 1 1 1 1 1 1 1 1 1 1 1 1 1 1 1 1 1 1 0 0 0 0 0
  0 0 0 0 0 0 1 1 1 1 1 1 1 1 1 1 1 1 1 1 1 1 1 1 1 1 1 1 0 0 0 0 0 0
  0 0 0 0 0 0 0 0 1 1 1 1 1 1 1 1 1 1 1 1 1 1 1 1 1 1 0 0 0 0 0 0 0 0
  0 0 0 0 0 0 0 0 0 1 1 1 1 1 1 1 1 1 1 1 1 1 1 1 1 0 0 0 0 0 0 0 0 0
  0 0 0 0 0 0 0 0 0 0 1 1 1 1 1 1 1 1 1 1 1 1 1 1 0 0 0 0 0 0 0 0 0 0 end fill

ara=7 nux=34 nuy=34 fill
' ACTIVE FUEL 84IN to 120IN
' 1 2 3 4 5 6 7 8 9101112131415161718192021222324252627282930
  0 0 0 0 0 0 0 0 0 0 1 1 1 1 1 1 1 1 1 1 1 1 1 1 0 0 0 0 0 0 0 0 0 0
  0 0 0 0 0 0 0 0 0 1 1 1 1 1 1 1 1 1 1 1 1 1 1 1 1 0 0 0 0 0 0 0 0 0
```

```
  0 0 0 0 0 0 0 0 1 1 2 2 2 2 2 2 2 2 2 2 2 2 2 2 1 1 0 0 0 0 0 0 0 0
  0 0 0 0 0 0 1 1 1 2 2 2 2 2 2 2 2 2 2 2 2 2 2 2 2 1 1 1 0 0 0 0 0 0
  0 0 0 0 0 1 1 2 2 2 2 2 2 2 2 2 2 2 2 2 2 2 2 2 2 2 2 1 1 0 0 0 0 0
  0 0 0 0 0 1 1 2 2 2 2 2 2 2 2 2 2 2 2 2 2 2 2 2 2 2 2 1 1 0 0 0 0 0
  0 0 0 1 1 1 2 2 2 2 2 2 2 2 2 2 2 2 2 2 2 2 2 2 2 2 2 2 1 1 1 0 0 0
  0 0 1 1 2 2 2 2 2 2 2 2 2 2 2 2 2 2 2 2 2 2 2 2 2 2 2 2 2 2 1 1 0 0
  0 0 1 1 2 2 2 2 2 2 2 2 2 2 2 2 2 2 2 2 2 2 2 2 2 2 2 2 2 2 1 1 0 0
  0 1 1 2 2 2 2 2 2 2 2 2 2 2 2 2 2 2 2 2 2 2 2 2 2 2 2 2 2 2 2 1 1 0
  1 1 2 2 2 2 2 2 2 2 2 2 2 2 2 2 2 2 2 2 2 2 2 2 2 2 2 2 2 2 2 2 1 1
  1 1 2 2 2 2 2 2 2 2 2 2 2 2 2 2 2 2 2 2 2 2 2 2 2 2 2 2 2 2 2 2 1 1
  1 1 2 2 2 2 2 2 2 2 2 2 2 2 2 2 2 2 2 2 2 2 2 2 2 2 2 2 2 2 2 2 1 1
  1 1 2 2 2 2 2 2 2 2 2 2 2 2 2 2 2 2 2 2 2 2 2 2 2 2 2 2 2 2 2 2 1 1
  1 1 2 2 2 2 2 2 2 2 2 2 2 2 2 2 2 2 2 2 2 2 2 2 2 2 2 2 2 2 2 2 1 1
  1 1 2 2 2 2 2 2 2 2 2 2 2 2 2 2 2 2 2 2 2 2 2 2 2 2 2 2 2 2 2 2 1 1
  1 1 2 2 2 2 2 2 2 2 2 2 2 2 2 2 2 2 2 2 2 2 2 2 2 2 2 2 2 2 2 2 1 1
  1 1 2 2 2 2 2 2 2 2 2 2 2 2 2 2 2 2 2 2 2 2 2 2 2 2 2 2 2 2 2 2 1 1
  1 1 2 2 2 2 2 2 2 2 2 2 2 2 2 2 2 2 2 2 2 2 2 2 2 2 2 2 2 2 2 2 1 1
  1 1 2 2 2 2 2 2 2 2 2 2 2 2 2 2 2 2 2 2 2 2 2 2 2 2 2 2 2 2 2 2 1 1
  1 1 2 2 2 2 2 2 2 2 2 2 2 2 2 2 2 2 2 2 2 2 2 2 2 2 2 2 2 2 2 2 1 1
  1 1 2 2 2 2 2 2 2 2 2 2 2 2 2 2 2 2 2 2 2 2 2 2 2 2 2 2 2 2 2 2 1 1
  1 1 2 2 2 2 2 2 2 2 2 2 2 2 2 2 2 2 2 2 2 2 2 2 2 2 2 2 2 2 2 2 1 1
  1 1 2 2 2 2 2 2 2 2 2 2 2 2 2 2 2 2 2 2 2 2 2 2 2 2 2 2 2 2 2 2 1 1
  0 1 1 2 2 2 2 2 2 2 2 2 2 2 2 2 2 2 2 2 2 2 2 2 2 2 2 2 2 2 2 1 1 0
  0 0 1 1 2 2 2 2 2 2 2 2 2 2 2 2 2 2 2 2 2 2 2 2 2 2 2 2 2 2 1 1 0 0
  0 0 1 1 2 2 2 2 2 2 2 2 2 2 2 2 2 2 2 2 2 2 2 2 2 2 2 2 2 2 1 1 0 0
  0 0 0 1 1 1 2 2 2 2 2 2 2 2 2 2 2 2 2 2 2 2 2 2 2 2 2 2 1 1 1 0 0 0
  0 0 0 0 0 1 1 2 2 2 2 2 2 2 2 2 2 2 2 2 2 2 2 2 2 2 2 1 1 0 0 0 0 0
  0 0 0 0 0 1 1 2 2 2 2 2 2 2 2 2 2 2 2 2 2 2 2 2 2 2 2 1 1 0 0 0 0 0
  0 0 0 0 0 0 1 1 1 2 2 2 2 2 2 2 2 2 2 2 2 2 2 2 2 1 1 1 0 0 0 0 0 0
  0 0 0 0 0 0 0 0 1 1 2 2 2 2 2 2 2 2 2 2 2 2 2 2 1 1 0 0 0 0 0 0 0 0
  0 0 0 0 0 0 0 0 0 1 1 1 1 1 1 1 1 1 1 1 1 1 1 1 1 0 0 0 0 0 0 0 0 0
  0 0 0 0 0 0 0 0 0 0 1 1 1 1 1 1 1 1 1 1 1 1 1 1 0 0 0 0 0 0 0 0 0 0 end fill

ara=17 nux=34 nuy=34 fill
' CONTROL BLADE CONTROL
' 1 2 3  4  5  6  7  8  9  10 11 12 13 14 15 16 17 18 19 20 21 22 23 24 25 26 27 28 29 30 31 32
3334
0 0 0  0  0  0  0  0  0  0  0  0  0  0  0  0  0  0  0  0  0  0  0  0  0  0  0  0  0  0  0 0
0 0 0  0  0  0  0  0  0  0  0  0  0  0  0  0  0  0  0  0  0  0  0  0  0  0  0  0  0  0  0 0
0 0 0  0  0  0  0  0  0  0  1  1  2  2  3  3  4  4  3  3  2  2  1  1  0  0  0  0  0  0  0 0
0 0 0  0  0  0  0  0  0  0  1  1  2  2  3  3  4  4  3  3  2  2  1  1  0  0  0  0  0  0  0 0
0 0 0  0  0  0  0  0  5  5  6  6  7  7  8  8  9  9  8  8  7  7  6  6  5  5  0  0  0  0  0 0
0 0 0  0  0  0  0  0  5  5  6  6  7  7  8  8  9  9  8  8  7  7  6  6  5  5  0  0  0  0  0 0
0 0 0  0  0  0  10 10 11 11 12 12 13 13 14 14 15 15 14 14 13 13 12 12 11 11 10 10 0  0  0  0  0 0
0 0 0  0  0  0  10 10 11 11 12 12 13 13 14 14 15 15 14 14 13 13 12 12 11 11 10 10 0  0  0  0  0 0
0 0 0  0  16 16 17 17 18 18 19 19 20 20 21 21 22 22 21 21 20 20 19 19 18 18 17 17 16 16 0  0  0 0
0 0 0  0  16 16 17 17 18 18 19 19 20 20 21 21 22 22 21 21 20 20 19 19 18 18 17 17 16 16 0  0  0 0
0 0 23 23 24 24 25 25 26 26 27 27 28 28 29 29 30 30 29 29 28 28 27 27 26 26 25 25 24 24 23 23 0 0
0 0 23 23 24 24 25 25 26 26 27 27 28 28 29 29 30 30 29 29 28 28 27 27 26 26 25 25 24 24 23 23 0 0
0 0 31 31 32 32 33 33 34 34 35 35 36 36 37 37 38 38 37 37 36 36 35 35 34 34 33 33 32 32 31 31 0 0
0 0 31 31 32 32 33 33 34 34 35 35 36 36 37 37 38 38 37 37 36 36 35 35 34 34 33 33 32 32 31 31 0 0
0 0 39 39 40 40 41 41 42 42 43 43 44 44 45 45 46 46 45 45 44 44 43 43 42 42 41 41 40 40 39 39 0 0
0 0 39 39 40 40 41 41 42 42 43 43 44 44 45 45 46 46 45 45 44 44 43 43 42 42 41 41 40 40 39 39 0 0
0 0 47 47 48 48 49 49 50 50 51 51 52 52 53 53 54 54 53 53 52 52 51 51 50 50 49 49 48 48 47 47 0 0
0 0 47 47 48 48 49 49 50 50 51 51 52 52 53 53 54 54 53 53 52 52 51 51 50 50 49 49 48 48 47 47 0 0
0 0 39 39 40 40 41 41 42 42 43 43 44 44 45 45 46 46 45 45 44 44 43 43 42 42 41 41 40 40 39 39 0 0
0 0 39 39 40 40 41 41 42 42 43 43 44 44 45 45 46 46 45 45 44 44 43 43 42 42 41 41 40 40 39 39 0 0
0 0 31 31 32 32 33 33 34 34 35 35 36 36 37 37 38 38 37 37 36 36 35 35 34 34 33 33 32 32 31 31 0 0
0 0 31 31 32 32 33 33 34 34 35 35 36 36 37 37 38 38 37 37 36 36 35 35 34 34 33 33 32 32 31 31 0 0
0 0 23 23 24 24 25 25 26 26 27 27 28 28 29 29 30 30 29 29 28 28 27 27 26 26 25 25 24 24 23 23 0 0
0 0 23 23 24 24 25 25 26 26 27 27 28 28 29 29 30 30 29 29 28 28 27 27 26 26 25 25 24 24 23 23 0 0
0 0 0  0  16 16 17 17 18 18 19 19 20 20 21 21 22 22 21 21 20 20 19 19 18 18 17 17 16 16 0  0  0 0
0 0 0  0  16 16 17 17 18 18 19 19 20 20 21 21 22 22 21 21 20 20 19 19 18 18 17 17 16 16 0  0  0 0
0 0 0  0  0  0  10 10 11 11 12 12 13 13 14 14 15 15 14 14 13 13 12 12 11 11 10 10 0  0  0  0  0 0
```

```
0 0 0  0  0  0  10 10 11 11 12 12 13 13 14 14 15 15 14 14 13 13 12 12 11 11 10 10 0  0  0  0  0 0
0 0 0  0  0  0  0  0  5  5  6  6  7  7  8  8  9  9  8  8  7  7  6  6  5  5  0  0  0  0  0  0  0 0
0 0 0  0  0  0  0  0  5  5  6  6  7  7  8  8  9  9  8  8  7  7  6  6  5  5  0  0  0  0  0  0  0 0
0 0 0  0  0  0  0  0  0  0  1  1  2  2  3  3  4  4  3  3  2  2  1  1  0  0  0  0  0  0  0  0  0 0
0 0 0  0  0  0  0  0  0  0  1  1  2  2  3  3  4  4  3  3  2  2  1  1  0  0  0  0  0  0  0  0  0 0
0 0 0  0  0  0  0  0  0  0  0  0  0  0  0  0  0  0  0  0  0  0  0  0  0  0  0  0  0  0  0  0  0 0
0 0 0  0  0  0  0  0  0  0  0  0  0  0  0  0  0  0  0  0  0  0  0  0  0  0  0  0  0  0  0  0  0 0
end fill

ara=117 nux=34 nuy=34 fill
' Orifice Loss Coeff Array
' 1 2 3 4 5 6 7 8 910111213141516171819202122232425262728293031323334
  0 0 0 0 0 0 0 0 0 0 4 4 4 4 4 4 4 4 4 4 4 4 4 4 0 0 0 0 0 0 0 0 0 0
  0 0 0 0 0 0 0 0 0 4 4 4 4 4 4 4 4 4 4 4 4 4 4 4 4 0 0 0 0 0 0 0 0 0
  0 0 0 0 0 0 0 0 4 4 2 2 2 2 2 2 2 2 2 2 2 2 2 2 4 4 0 0 0 0 0 0 0 0
  0 0 0 0 0 0 4 4 4 2 1 3 3 1 1 3 3 1 1 1 3 1 1 1 2 4 4 4 0 0 0 0 0 0
  0 0 0 0 0 4 4 2 2 1 1 1 1 1 1 1 1 1 1 1 1 1 1 1 1 2 2 4 4 0 0 0 0 0
  0 0 0 0 0 4 4 2 3 1 1 3 3 1 1 3 3 1 1 3 3 1 1 3 3 1 2 4 4 0 0 0 0 0
  0 0 0 4 4 4 2 3 3 1 1 3 3 1 1 3 3 1 1 3 3 1 1 3 3 1 3 2 4 4 4 0 0 0
  0 0 4 4 2 2 1 1 1 1 1 1 1 1 1 1 1 1 1 1 1 1 1 1 1 1 1 3 2 2 4 4 0 0
  0 0 4 4 2 1 1 1 1 1 1 1 1 1 1 1 1 1 1 1 1 1 1 1 1 1 1 1 1 2 4 4 0 0
  0 4 4 2 3 1 1 3 3 1 1 3 3 1 1 3 3 1 1 3 3 1 1 3 3 1 1 3 3 1 2 4 4 0
  4 4 2 1 3 1 1 3 3 1 1 3 3 1 1 3 3 1 1 3 3 1 1 3 3 1 1 3 3 1 1 2 4 4
  4 4 2 1 1 1 1 1 1 1 1 1 1 1 1 1 1 1 1 1 1 1 1 1 1 1 1 1 1 1 1 2 4 4
  4 4 2 1 1 1 1 1 1 1 1 1 1 1 1 1 1 1 1 1 1 1 1 1 1 1 1 1 1 1 1 2 4 4
  4 4 2 1 3 1 1 3 3 1 1 3 3 1 1 3 3 1 1 3 3 1 1 3 3 1 1 3 3 1 3 2 4 4
  4 4 2 1 3 1 1 3 3 1 1 3 3 1 1 3 3 1 1 3 3 1 1 3 3 1 1 3 3 1 1 2 4 4
  4 4 2 1 1 1 1 1 1 1 1 1 1 1 1 1 1 1 1 1 1 1 1 1 1 1 1 1 1 1 1 2 4 4
  4 4 2 1 1 1 1 1 1 1 1 1 1 1 1 1 1 1 1 1 1 1 1 1 1 1 1 1 1 1 1 2 4 4
  4 4 2 1 3 1 1 3 3 1 1 3 3 1 1 3 3 1 1 3 3 1 1 3 3 1 1 3 3 1 3 2 4 4
  4 4 2 1 3 1 1 3 3 1 1 3 3 1 1 3 3 1 1 3 3 1 1 3 3 1 1 3 3 1 3 2 4 4
  4 4 2 1 1 1 1 1 1 1 1 1 1 1 1 1 1 1 1 1 1 1 1 1 1 1 1 1 1 1 1 2 4 4
  4 4 2 1 1 1 1 1 1 1 1 1 1 1 1 1 1 1 1 1 1 1 1 1 1 1 1 1 1 1 1 2 4 4
  4 4 2 1 3 1 1 3 3 1 1 3 3 1 1 3 3 1 1 3 3 1 1 3 3 1 1 3 3 1 3 2 4 4
  4 4 2 1 3 1 1 3 3 1 1 3 3 1 1 3 3 1 1 3 3 1 1 3 3 1 1 3 3 1 3 2 4 4
  4 4 2 1 1 1 1 1 1 1 1 1 1 1 1 1 1 1 1 1 1 1 1 1 1 1 1 1 1 1 1 2 4 4
  0 4 4 2 1 1 1 1 1 1 1 1 1 1 1 1 1 1 1 1 1 1 1 1 1 1 1 1 1 1 2 4 4 0
  0 0 4 4 2 1 1 3 3 1 1 3 3 1 1 3 3 1 1 3 3 1 1 3 3 1 1 3 3 2 4 4 0 0
  0 0 4 4 2 2 1 3 3 1 1 3 3 1 1 3 3 1 1 3 3 1 1 3 3 1 1 3 2 2 4 4 0 0
  0 0 0 4 4 4 2 1 1 1 1 1 1 1 1 1 1 1 1 1 1 1 1 1 1 1 1 2 4 4 4 0 0 0
  0 0 0 0 0 4 4 2 3 1 1 1 1 1 1 1 1 1 1 1 1 1 1 1 1 1 2 4 4 0 0 0 0 0
  0 0 0 0 0 4 4 2 2 1 1 3 3 1 1 3 3 1 1 3 3 1 1 3 3 2 2 4 4 0 0 0 0 0
  0 0 0 0 0 0 4 4 4 2 1 1 1 1 1 1 1 1 1 1 1 1 1 1 2 4 4 4 0 0 0 0 0 0
  0 0 0 0 0 0 0 0 4 4 2 2 2 2 2 2 2 2 2 2 2 2 2 2 4 4 0 0 0 0 0 0 0 0
  0 0 0 0 0 0 0 0 0 4 4 4 4 4 4 4 4 4 4 4 4 4 4 4 4 0 0 0 0 0 0 0 0 0
  0 0 0 0 0 0 0 0 0 0 4 4 4 4 4 4 4 4 4 4 4 4 4 4 0 0 0 0 0 0 0 0 0 0 end fill

ara=217 nux=34 nuy=34 fill
' Rotational XY id
' 1 2 3 4 5 6 7 8 910111213141516171819202122232425262728293031323334
  0 0 0 0 0 0 0 0 0 0 0 0 0 0 0 0 0 0 0 0 0 0 0 0 0 0 0 0 0 0 0 0 0 0
  0 0 0 0 0 0 0 0 0 0 0 0 0 0 0 0 0 0 0 0 0 0 0 0 0 0 0 0 0 0 0 0 0 0
  0 0 0 0 0 0 0 0 0 0 2 3 2 3 2 3 2 3 2 3 2 3 2 3 0 0 0 0 0 0 0 0 0 0
  0 0 0 0 0 0 0 0 0 0 1 0 1 0 1 0 1 0 1 0 1 0 1 0 0 0 0 0 0 0 0 0 0 0
  0 0 0 0 0 0 0 0 2 3 2 3 2 3 2 3 2 3 2 3 2 3 2 3 2 3 0 0 0 0 0 0 0 0
  0 0 0 0 0 0 0 0 1 0 1 0 1 0 1 0 1 0 1 0 1 0 1 0 1 0 0 0 0 0 0 0 0 0
  0 0 0 0 0 0 2 3 2 3 2 3 2 3 2 3 2 3 2 3 2 3 2 3 2 3 2 3 0 0 0 0 0 0
  0 0 0 0 0 0 1 0 1 0 1 0 1 0 1 0 1 0 1 0 1 0 1 0 1 0 1 0 0 0 0 0 0 0
  0 0 0 0 2 3 2 3 2 3 2 3 2 3 2 3 2 3 2 3 2 3 2 3 2 3 2 3 2 3 0 0 0 0
  0 0 0 0 1 0 1 0 1 0 1 0 1 0 1 0 1 0 1 0 1 0 1 0 1 0 1 0 1 0 0 0 0 0
  0 0 2 3 2 3 2 3 2 3 2 3 2 3 2 3 2 3 2 3 2 3 2 3 2 3 2 3 2 3 2 3 0 0
  0 0 1 0 1 0 1 0 1 0 1 0 1 0 1 0 1 0 1 0 1 0 1 0 1 0 1 0 1 0 1 0 0 0
  0 0 2 3 2 3 2 3 2 3 2 3 2 3 2 3 2 3 2 3 2 3 2 3 2 3 2 3 2 3 2 3 0 0
  0 0 1 0 1 0 1 0 1 0 1 0 1 0 1 0 1 0 1 0 1 0 1 0 1 0 1 0 1 0 1 0 0 0
```

```
  0 0 2 3 2 3 2 3 2 3 2 3 2 3 2 3 2 3 2 3 2 3 2 3 2 3 2 3 2 3 2 3 0 0
  0 0 1 0 1 0 1 0 1 0 1 0 1 0 1 0 1 0 1 0 1 0 1 0 1 0 1 0 1 0 1 0 0 0
  0 0 2 3 2 3 2 3 2 3 2 3 2 3 2 3 2 3 2 3 2 3 2 3 2 3 2 3 2 3 2 3 0 0
  0 0 1 0 1 0 1 0 1 0 1 0 1 0 1 0 1 0 1 0 1 0 1 0 1 0 1 0 1 0 1 0 0 0
  0 0 2 3 2 3 2 3 2 3 2 3 2 3 2 3 2 3 2 3 2 3 2 3 2 3 2 3 2 3 2 3 0 0
  0 0 1 0 1 0 1 0 1 0 1 0 1 0 1 0 1 0 1 0 1 0 1 0 1 0 1 0 1 0 1 0 0 0
  0 0 2 3 2 3 2 3 2 3 2 3 2 3 2 3 2 3 2 3 2 3 2 3 2 3 2 3 2 3 2 3 0 0
  0 0 1 0 1 0 1 0 1 0 1 0 1 0 1 0 1 0 1 0 1 0 1 0 1 0 1 0 1 0 1 0 0 0
  0 0 2 3 2 3 2 3 2 3 2 3 2 3 2 3 2 3 2 3 2 3 2 3 2 3 2 3 2 3 2 3 0 0
  0 0 1 0 1 0 1 0 1 0 1 0 1 0 1 0 1 0 1 0 1 0 1 0 1 0 1 0 1 0 1 0 0 0
  0 0 0 0 2 3 2 3 2 3 2 3 2 3 2 3 2 3 2 3 2 3 2 3 2 3 2 3 2 3 0 0 0 0
  0 0 0 0 1 0 1 0 1 0 1 0 1 0 1 0 1 0 1 0 1 0 1 0 1 0 1 0 1 0 0 0 0 0
  0 0 0 0 0 0 2 3 2 3 2 3 2 3 2 3 2 3 2 3 2 3 2 3 2 3 2 3 0 0 0 0 0 0
  0 0 0 0 0 0 1 0 1 0 1 0 1 0 1 0 1 0 1 0 1 0 1 0 1 0 1 0 0 0 0 0 0 0
  0 0 0 0 0 0 0 0 2 3 2 3 2 3 2 3 2 3 2 3 2 3 2 3 2 3 0 0 0 0 0 0 0 0
  0 0 0 0 0 0 0 0 1 0 1 0 1 0 1 0 1 0 1 0 1 0 1 0 1 0 0 0 0 0 0 0 0 0
  0 0 0 0 0 0 0 0 0 0 2 3 2 3 2 3 2 3 2 3 2 3 2 3 0 0 0 0 0 0 0 0 0 0
  0 0 0 0 0 0 0 0 0 0 1 0 1 0 1 0 1 0 1 0 1 0 1 0 0 0 0 0 0 0 0 0 0 0
  0 0 0 0 0 0 0 0 0 0 0 0 0 0 0 0 0 0 0 0 0 0 0 0 0 0 0 0 0 0 0 0 0 0
  0 0 0 0 0 0 0 0 0 0 0 0 0 0 0 0 0 0 0 0 0 0 0 0 0 0 0 0 0 0 0 0 0 0 end fill
end arrays
```

Appendix B – TRITON Memory Management Script

```
#!/bin/bash
# author: David Dixon & Jack Galloway (jack@galloways.net)
# desc:   Used to minimize SCALE IO penalty in cross-section processing

for i in 1 2
do
   CMD=`ps r -A | grep -G "bonami\|pmc\|worker\|centrm" | cut -b 1-5`

   COUNT=0
   MAXCOUNT=1
   MEMTOTALCMD=`cat /proc/meminfo | grep MemTotal | cut -b 13-22`
   MEMCACHECMD=`cat /proc/meminfo | grep -w Cached | cut -b 13-22`
   MEMFREECMD=`cat /proc/meminfo | grep MemFree | cut -b 13-22`
   MEMDISKCMD=`df | grep " /tmp" | cut -b 31-40`

   MEMTEST=$[MEMCACHECMD + MEMFREECMD - MEMDISKCMD]

   for b in $CMD ;
   do
        COUNT=$[COUNT + 1]
        #echo $COUNT $b
   done

   echo MEMTEST: $MEMTEST
   if [ $MEMTEST -gt 500000 ]; then
        MAXCOUNT=$[COUNT + 1]
   fi
   if [ $MAXCOUNT -gt 4 ]; then
        MAXCOUNT=4
   fi

   echo Count: $COUNT
   echo MAXCount: $MAXCOUNT

   if [ $COUNT -gt $MAXCOUNT ]; then
       STPID=`echo $CMD | cut -b 1-5`
   #  echo Stopping $STPID...
       kill -STOP $STPID
   fi

   if [ $COUNT -lt $MAXCOUNT ]; then
       CMD=`ps -A | grep -G "bonami\|pmc\|worker\|centrm" | cut -b 1-5`
       STPID=`echo $CMD | cut -b 1-5`
   #  echo Starting $STPID...
       kill -CONT $STPID
   fi

   sleep 29
done
```

Appendix C – BOC Microscopic Cross-Sections

Parent	Daughter	mt	NESTLE XS	COUPLE XS	% Difference
10010	10020	102	0.048189934	0.0481912	-0.003%
50100	50110	102	0.072464503	0.0724664	-0.003%
50100	40100	103	0.002315805	0.00231579	0.001%
50100	40090	104	0.000273659	0.000300307	-8.874%
50100	30070	107	556.9069	556.921	-0.003%
50110	50100	16	5.33134E-07	5.33129E-07	0.001%
50110	50120	102	0.00073617	0.000736189	-0.003%
50110	40110	103	6.2113E-08	6.21125E-08	0.001%
50110	*40090*	*105*	*7.91264E-07*		
50110	30080	107	9.40079E-06	9.4007E-06	0.001%
70140	70130	16	3.30301E-07	3.30298E-07	0.001%
70140	70150	102	0.010887218	0.0108875	-0.003%
70140	60140	103	0.2767656	0.276772	-0.002%
70140	60130	104	8.22969E-05	8.81014E-05	-6.588%
70140	*60120*	*105*	*0.000214298*		
70140	50110	107	0.023223612	0.0232234	0.001%
80160	80170	102	2.75885E-05	2.75892E-05	-0.003%
80160	70160	103	7.10039E-06	7.10033E-06	0.001%
80160	70150	104	1.45544E-06	1.49007E-06	-2.324%
80160	60130	107	0.002994396	0.00299437	0.001%
320720	320730	102	0.086443953	0.0864379	0.007%
320720	320731	102	0.085985869	0.0859954	-0.011%
320730	320740	102	3.813083	3.81312	-0.001%
320740	320750	102	0.048982367	0.0489854	-0.006%
320740	320751	102	0.024547344	0.0245456	0.007%
320760	320770	102	0.023073409	0.0230729	0.002%
320760	320771	102	0.034500632	0.0345014	-0.002%
330750	330760	102	2.173205	2.17321	0.000%
340760	340770	102	9.280733	9.28099	-0.003%
340760	340771	102	3.244569	3.24463	-0.002%
340770	340780	102	6.597795	6.59795	-0.002%
340780	340790	102	0.021746103	0.0217422	0.018%
340780	340791	102	0.1629004	0.162905	-0.003%
340800	340810	102	0.1007431	0.100748	-0.005%
340800	340811	102	0.018158749	0.0181563	0.013%
340820	340830	102	0.001391649	0.00139099	0.047%

340820	340831	102	0.009216161	0.00921696	-0.009%
350790	350800	102	3.460904	3.46093	-0.001%
350790	350801	102	1.040826	1.04081	0.002%
350810	350820	102	0.1521207	0.152119	0.001%
350810	350821	102	1.516984	1.51698	0.000%
360800	360790	16	2.01209E-05	2.01207E-05	0.001%
360800	360791	16	2.07601E-05	2.07599E-05	0.001%
360800	360810	102	1.976551	1.97656	0.000%
360800	360811	102	1.3008	1.30082	-0.002%
360800	350800	103	0.000181532	0.00018153	0.001%
360800	350801	103	0.000197821	0.00019782	0.001%
360800	350790	104	6.1918E-07	3.29464E-06	-81.206%
360800	350791	104	5.0277E-07	2.67523E-06	-81.206%
360800	*350780*	*105*	*2.09511E-08*		
360800	340780	106	1.81238E-08	1.81237E-08	0.001%
360800	*340770*	*107*	*7.942E-06*		
360800	*340771*	*107*	*1.61246E-05*		
360820	360810	16	7.19562E-05	7.19555E-05	0.001%
360820	360811	16	1.7493E-05	1.74929E-05	0.001%
360820	360830	102	2.790896	2.79091	-0.001%
360820	360831	102	5.589013	5.58907	-0.001%
360820	350820	103	2.29398E-05	2.29396E-05	0.001%
360820	350821	103	2.11752E-05	0.000021175	0.001%
360820	350810	104	4.25411E-07	6.12506E-07	-30.546%
360820	*350800*	*105*	*5.95552E-09*		
360820	*350801*	*105*	*6.66176E-09*		
360820	340800	106	5.04151E-09	5.04146E-09	0.001%
360820	340790	107	1.11762E-06	1.11761E-06	0.001%
360820	340791	107	3.53004E-07	3.53002E-07	0.001%
360830	360820	16	0.001197584	0.00119757	0.001%
360830	360840	102	31.61673	31.6175	-0.002%
360830	350830	103	3.33302E-05	3.33299E-05	0.001%
360830	350820	104	2.38222E-07	2.50245E-07	-4.805%
360830	350821	104	2.16441E-07	2.27365E-07	-4.805%
360830	*350810*	*105*	*1.16989E-07*		
360830	340810	106	8.66891E-10	8.66884E-10	0.001%
360830	340811	106	1.72813E-09	1.72812E-09	0.001%
360830	*340800*	*107*	*2.27879E-06*		
360840	360830	16	0.000116616	0.000116615	0.001%

360840	360831	16	2.88486E-05	2.88484E-05	0.001%
360840	360850	102	0.020142648	0.0201421	0.003%
360840	360851	102	0.08975745	0.0897574	0.000%
360840	350840	103	5.35095E-07	5.3509E-07	0.001%
360840	350841	103	5.79686E-07	5.79681E-07	0.001%
360840	350830	104	1.51738E-07	1.61737E-07	-6.182%
360840	*350820*	*105*	*3.95957E-09*		
360840	*350821*	*105*	*5.0857E-09*		
360840	340820	106	3.01879E-11	3.01876E-11	0.001%
360840	340810	107	9.1699E-09	9.16313E-09	0.074%
360840	340811	107	1.11559E-07	1.11565E-07	-0.005%
360850	360860	102	0.2703112	0.270317	-0.002%
360860	360850	16	0.000158581	0.000158436	0.091%
360860	360851	16	3.96131E-05	3.95769E-05	0.091%
360860	360870	102	0.012700364	0.0127006	-0.002%
360860	350860	103	3.02565E-08	3.02562E-08	0.001%
360860	350850	104	3.94925E-08	4.05574E-08	-2.626%
360860	350840	105	1.71931E-09	1.7193E-09	0.001%
360860	350841	105	1.83748E-09	1.83747E-09	0.001%
370850	370840	16	0.000105307	6.68708E-05	57.478%
370850	370860	102	0.2193295	0.219332	-0.001%
370850	370861	102	0.0301529	0.0301509	0.007%
370850	360850	103	1.46197E-05	1.46195E-05	0.001%
370850	360851	103	4.5884E-06	4.58842E-06	0.000%
370850	360840	104	1.22076E-05	2.35964E-05	-48.265%
370850	*360830*	*105*	*3.42954E-07*		
370850	*360831*	*105*	*1.06583E-07*		
370850	350830	106	1.3273E-09	1.32729E-09	0.001%
370850	350820	107	3.49033E-06	3.49026E-06	0.002%
370850	350821	107	3.52438E-06	3.52438E-06	0.000%
370860	370870	102	1.295108	1.29512	-0.001%
370870	370860	16	0.000101341	0.00010134	0.001%
370870	370861	16	5.28873E-05	5.28868E-05	0.001%
370870	370880	102	0.089409411	0.0894092	0.000%
370870	360870	103	1.1958E-05	1.19579E-05	0.001%
370870	360860	104	3.07341E-06	4.2148E-06	-27.081%
370870	*360850*	*105*	*1.38835E-07*		
370870	*360851*	*105*	*4.27645E-08*		
370870	350850	106	9.03715E-11	9.03707E-11	0.001%

370870	350840	107	1.92791E-06	1.9279E-06	0.000%
370870	350841	107	4.69899E-07	4.69889E-07	0.002%
380840	380850	102	0.1077155	0.107703	0.012%
380840	380851	102	0.3182615	0.318274	-0.004%
380860	380870	102	0.1054967	0.105482	0.014%
380860	380871	102	0.4232619	0.423286	-0.006%
380870	380880	102	4.785339	4.78538	-0.001%
380880	380890	102	0.001488105	0.00148812	-0.001%
380890	380900	102	0.073738948	0.0737404	-0.002%
380900	380910	102	0.1362212	0.136225	-0.003%
390890	390900	102	0.2006462	0.200658	-0.006%
390890	390901	102	0.000377187	0.000370244	1.875%
390900	390910	102	0.4561345	0.456148	-0.003%
390900	390911	102	0.1521935	0.152192	0.001%
390910	390920	102	0.2364995	0.236505	-0.002%
400900	400890	16	2.20458E-05	2.20456E-05	0.001%
400900	400891	16	3.78787E-06	3.78783E-06	0.001%
400900	400910	102	0.010416252	0.0104162	0.000%
400900	390900	103	8.64647E-05	8.64676E-05	-0.003%
400900	390901	103	7.80577E-06	7.80199E-06	0.048%
400900	380870	107	6.92262E-07	6.92256E-07	0.001%
400900	380871	107	3.1968E-07	3.19677E-07	0.001%
400910	400900	16	0.000697101	0.000697108	-0.001%
400910	400901	16	0.000358938	0.000358921	0.005%
400910	400920	102	0.292778	0.292781	-0.001%
400910	390910	103	3.45939E-05	3.45952E-05	-0.004%
400910	390911	103	1.47285E-05	1.47267E-05	0.012%
400910	*380880*	*107*	*6.22833E-05*		
400920	400910	16	0.000360652	0.000360649	0.001%
400920	400930	102	0.052178163	0.0521788	-0.001%
400920	390920	103	9.38847E-06	9.38838E-06	0.001%
400920	*380890*	*107*	*4.96233E-06*		
400930	400940	102	1.062063	1.06207	-0.001%
400940	400930	16	0.000537753	0.000537748	0.001%
400940	400950	102	0.01931259	0.0193127	-0.001%
400940	390940	103	2.48788E-06	2.48786E-06	0.001%
400940	380910	107	1.1704E-06	1.17039E-06	0.001%
400950	400960	102	0.2311645	0.231165	0.000%
400960	400950	16	0.000780481	0.000780474	0.001%

400960	400970	102	0.1497636	0.149762	0.001%
400960	380930	107	8.61179E-07	8.61171E-07	0.001%
410930	410920	16	0.000208333	0.000208177	0.075%
410930	410921	16	8.88672E-05	8.88007E-05	0.075%
410930	410940	102	0.1325809	0.132581	0.000%
410930	410941	102	0.2950305	0.295032	-0.001%
410930	400930	103	0.00013799	0.000137989	0.001%
410930	*390900*	*107*	*1.05925E-05*		
410930	*390901*	*107*	*4.21151E-06*		
410940	410950	102	4.3035	4.30353	-0.001%
410940	410951	102	0.1747302	0.17473	0.000%
410950	410960	102	0.823755	0.823755	0.000%
420920	420930	102	0.041366052	0.0413659	0.000%
420920	420931	102	8.93334E-05	8.92655E-05	0.076%
420920	410920	103	0.000123006	0.00012298	0.021%
420920	410921	103	0.000750285	0.000750303	-0.002%
420920	*400890*	*107*	*1.14782E-05*		
420920	*400891*	*107*	*4.27256E-06*		
420940	420950	102	0.046978448	0.0469781	0.001%
420950	420960	102	4.747674	4.7477	-0.001%
420960	420970	102	0.660292	0.660291	0.000%
420970	420980	102	0.7560235	0.756028	-0.001%
420980	420990	102	0.2068754	0.206874	0.001%
420990	421000	102	0.9744846	0.974484	0.000%
421000	421010	102	0.1406526	0.140652	0.000%
430990	430980	16	0.000382053	0.000382049	0.001%
430990	431000	102	9.475595	9.47561	0.000%
440960	440970	102	0.4162297	0.416227	0.001%
440980	440990	102	1.331122	1.33115	-0.002%
440990	441000	102	4.008308	4.0083	0.000%
441000	441010	102	1.020448	1.02047	-0.002%
441010	441020	102	2.842813	2.8428	0.000%
441020	441030	102	0.2984399	0.298444	-0.001%
441030	441040	102	2.776134	2.77615	-0.001%
441040	441050	102	0.2530403	0.25304	0.000%
441050	441060	102	0.2618212	0.26182	0.000%
441060	441070	102	0.085907519	0.0859075	0.000%
451030	451020	16	0.000102026	0.000102025	0.001%
451030	451021	16	4.88072E-05	4.88067E-05	0.001%

451030	451040	102	43.75417	43.7546	-0.001%
451030	451041	102	3.600037	3.60005	0.000%
451050	451060	102	2302.123	2302.18	-0.002%
451050	451061	102	244.4754	244.481	-0.002%
461020	461030	102	0.9224277	0.922444	-0.002%
461040	461050	102	0.5951329	0.59513	0.000%
461050	461060	102	4.22397	4.224	-0.001%
461060	461070	102	0.2914478	0.291453	-0.002%
461060	461071	102	0.014422944	0.0144167	0.043%
461070	461080	102	3.283981	3.284	-0.001%
461080	461090	102	6.692397	6.6924	0.000%
461080	461091	102	0.1510024	0.150999	0.002%
461100	461110	102	0.2147147	0.214719	-0.002%
461100	461111	102	0.037869439	0.0378635	0.016%
471070	471060	16	0.000113481	0.00011346	0.019%
471070	471061	16	6.92249E-05	6.92115E-05	0.019%
471070	471080	102	7.503272	7.50343	-0.002%
471070	471081	102	0.077076443	0.0770406	0.047%
471070	461070	103	4.54231E-05	4.54237E-05	-0.001%
471070	461071	103	5.13228E-06	5.13117E-06	0.022%
471070	461060	104	7.73533E-06	1.04095E-05	-25.690%
471070	*461050*	*105*	*6.31121E-07*		
471070	451050	106	9.34871E-10	9.34864E-10	0.001%
471070	451051	106	3.01094E-10	3.0109E-10	0.001%
471070	451040	107	2.24877E-06	2.24894E-06	-0.007%
471070	451041	107	9.83255E-07	9.83058E-07	0.020%
471090	471080	16	0.000158148	0.000158067	0.052%
471090	471081	16	9.61742E-05	9.61244E-05	0.052%
471090	471100	102	39.50293	39.503	0.000%
471090	471101	102	1.905684	1.90568	0.000%
471090	461090	103	7.26781E-06	7.26834E-06	-0.007%
471090	461091	103	1.70117E-06	1.70056E-06	0.036%
471090	461080	104	4.07676E-06	4.44989E-06	-8.385%
471090	*461070*	*105*	*2.34455E-07*		
471090	*461071*	*105*	*1.76451E-07*		
471090	451070	106	3.65062E-10	3.65058E-10	0.001%
471090	451060	107	2.04568E-06	2.04569E-06	0.000%
471090	451061	107	1.70743E-06	1.70739E-06	0.003%
471110	471120	102	3.106182	3.10617	0.000%

481060	481070	102	0.4745466	0.474548	0.000%
481080	481090	102	0.3024581	0.302461	-0.001%
481100	481110	102	2.596844	2.59689	-0.002%
481100	481111	102	0.013607627	0.0135941	0.100%
481110	481120	102	4.671438	4.67152	-0.002%
481120	481130	102	0.5772424	0.57727	-0.005%
481120	481131	102	0.087542295	0.0875199	0.026%
481130	481120	16	0.000873243	0.000873235	0.001%
481130	481140	102	6799.146	6799.34	-0.003%
481130	471130	103	1.41529E-06	1.41529E-06	0.000%
481130	471131	103	1.49101E-06	1.49098E-06	0.002%
481130	461100	107	1.17072E-07	1.17071E-07	0.001%
481140	481150	102	0.5290803	0.529078	0.000%
481140	481151	102	0.071098857	0.0710979	0.001%
481160	481170	102	0.063575625	0.0635755	0.000%
481160	481171	102	0.031810384	0.03181	0.001%
491130	491140	102	2.910142	2.91014	0.000%
491130	491141	102	4.034149	4.03415	0.000%
491150	491160	102	40.7686	23.2795	75.127%
491150	491161	102	67.50357	38.5455	75.127%
501120	501130	102	0.7116445	0.711649	-0.001%
501120	501131	102	0.2697019	0.269694	0.003%
501140	501150	102	0.3165502	0.316553	-0.001%
501150	501160	102	7.297351	7.29754	-0.003%
501160	501170	102	0.315666	0.315664	0.001%
501160	501171	102	0.013926281	0.0139261	0.001%
501170	501180	102	0.8346473	0.834653	-0.001%
501180	501190	102	0.1976999	0.197702	-0.001%
501180	501191	102	0.0041513	0.00414819	0.075%
501190	501200	102	0.4135567	0.413565	-0.002%
501200	501210	102	0.059028655	0.0590321	-0.006%
501200	501211	102	0.000725177	0.000721955	0.446%
501220	501230	102	0.000618137	0.000612094	0.987%
501220	501231	102	0.048433226	0.0484397	-0.013%
501230	501240	102	0.095311426	0.0953107	0.001%
501240	501250	102	0.007487495	0.00748733	0.002%
501240	501251	102	0.192766	0.192765	0.001%
501250	501260	102	0.498337	0.498335	0.000%
501260	501270	102	0.014155064	0.0141527	0.017%

501260	501271	102	0.032799616	0.0328031	-0.011%
511210	511220	102	4.40454	4.40453	0.000%
511210	511221	102	0.2965408	0.296538	0.001%
511230	511240	102	3.08853	3.07301	0.505%
511230	511241	102	0.032257728	0.0320879	0.529%
511240	511250	102	1.613233	1.61325	-0.001%
511250	511260	102	0.5369143	0.190407	181.982%
511250	511261	102	0.1200528	0.04257	182.013%
511260	511270	102	1.978724	1.97874	-0.001%
521200	521210	102	0.7950208	0.795117	-0.012%
521200	521211	102	0.1030335	0.102941	0.090%
521220	521230	102	1.47716	1.47716	0.000%
521220	521231	102	0.813584	0.813579	0.001%
521230	521240	102	186.4417	186.442	0.000%
521240	521250	102	1.169976	1.17002	-0.004%
521240	521251	102	0.008747682	0.00872995	0.203%
521250	521260	102	0.8622294	0.86223	0.000%
521260	521270	102	0.3745278	0.374535	-0.002%
521260	521271	102	0.056472931	0.0564671	0.010%
521280	521290	102	0.1050874	0.105089	-0.002%
521280	521291	102	0.008534744	0.00853296	0.021%
521300	521310	102	0.043195903	0.0431983	-0.006%
521300	521311	102	0.007260103	0.0072587	0.019%
521320	521330	102	0.000484152	0.000484357	-0.042%
521320	521331	102	8.25676E-05	8.23674E-05	0.243%
531270	531280	102	4.390788	4.39078	0.000%
531290	531300	102	1.8893	1.88933	-0.002%
531290	531301	102	2.684913	2.68498	-0.002%
531300	531310	102	6.846445	6.84647	0.000%
531310	531320	102	0.3153277	0.315329	0.000%
531310	531321	102	0.005173076	0.00517255	0.010%
531350	531360	102	0.00159133	0.00318273	-50.001%
531350	*531361*	*102*	*0.00159133*		
541240	541230	16	0.000120256	0.00012022	0.030%
541240	541250	102	71.44548	71.4456	0.000%
541240	541251	102	14.63491	14.6349	0.000%
541240	531240	103	8.24261E-06	8.24253E-06	0.001%
541240	531230	104	2.66448E-07	2.4108E-06	-88.948%
541240	*531220*	*105*	*1.43394E-08*		

541240	521220	106	7.76458E-09	7.76451E-09	0.001%
541240	521210	107	3.87099E-06	3.87096E-06	0.001%
541240	521211	107	3.04152E-06	3.04149E-06	0.001%
541260	541250	16	0.000172676	0.000172575	0.058%
541260	541251	16	5.9111E-05	5.90767E-05	0.058%
541260	541270	102	1.244403	1.24441	-0.001%
541260	541271	102	0.1870887	0.187081	0.004%
541260	531260	103	2.15276E-06	2.15274E-06	0.001%
541260	531250	104	1.15866E-07	2.12141E-07	-45.383%
541260	*531240*	*105*	*5.68165E-09*		
541260	521240	106	1.38162E-08	1.3816E-08	0.001%
541260	521230	107	1.14019E-06	1.14018E-06	0.001%
541260	521231	107	8.95883E-07	8.95875E-07	0.001%
541280	541270	16	0.000319674	0.000319198	0.149%
541280	541271	16	6.15346E-05	0.000061443	0.149%
541280	541290	102	0.9218714	0.921904	-0.004%
541280	541291	102	0.1110162	0.111002	0.013%
541280	531280	103	1.09549E-05	1.09548E-05	0.001%
541280	531270	104	6.54041E-08	2.74194E-07	-76.147%
541280	*531260*	*105*	*7.80029E-09*		
541280	521260	106	4.02081E-09	4.02077E-09	0.001%
541280	521250	107	2.7977E-07	2.79767E-07	0.001%
541280	521251	107	2.19842E-07	2.1984E-07	0.001%
541290	541280	16	0.002472497	0.00247175	0.030%
541290	541300	102	8.485444	8.48546	0.000%
541290	531290	103	2.37219E-06	2.37217E-06	0.001%
541290	531280	104	5.40857E-08	1.28976E-07	-58.065%
541290	*531270*	*105*	*2.87381E-08*		
541290	521260	107	3.38607E-06	3.38603E-06	0.001%
541300	541290	16	0.000258034	0.000257347	0.267%
541300	541291	16	0.000187685	0.000187185	0.267%
541300	541310	102	0.8809616	0.880996	-0.004%
541300	541311	102	0.080137879	0.0801258	0.015%
541300	531300	103	8.27173E-07	8.27011E-07	0.020%
541300	531301	103	1.30782E-06	1.30796E-06	-0.011%
541300	531290	104	4.33926E-08	6.7892E-08	-36.086%
541300	*531280*	*105*	*4.23777E-09*		
541300	521270	107	8.70071E-08	8.70061E-08	0.001%
541300	521271	107	6.83867E-08	6.83863E-08	0.001%

541310	541300	16	0.003851215	0.00384982	0.036%
541310	541320	102	35.37563	35.3758	0.000%
541310	531310	103	3.23462E-06	3.23459E-06	0.001%
541310	531300	104	1.15578E-08	1.4424E-08	-19.871%
541310	531301	104	2.1372E-08	2.66745E-08	-19.879%
541310	*531290*	*105*	*3.15975E-08*		
541310	521280	107	1.15935E-06	1.15934E-06	0.001%
541320	541310	16	0.000255956	0.000255073	0.346%
541320	541311	16	0.000365442	0.000364182	0.346%
541320	541330	102	0.1048336	0.104839	-0.005%
541320	541331	102	0.013316823	0.0133125	0.032%
541320	531320	103	5.86849E-07	5.86815E-07	0.006%
541320	531321	103	1.1589E-07	1.15917E-07	-0.023%
541320	531310	104	2.03672E-08	2.4647E-08	-17.365%
541320	*531300*	*105*	*4.04698E-10*		
541320	*531301*	*105*	*1.89507E-09*		
541320	521290	107	2.60758E-08	2.60754E-08	0.001%
541320	521291	107	2.05123E-08	2.05123E-08	0.000%
541330	541340	102	32.35249	32.3532	-0.002%
541330	541341	102	1.363217	1.36318	0.003%
541340	541330	16	0.000467281	0.000465482	0.387%
541340	541331	16	0.000362956	0.000361559	0.386%
541340	541350	102	0.059489004	0.0594938	-0.008%
541340	541351	102	0.000826941	0.000822826	0.500%
541340	531340	103	4.59736E-07	4.59732E-07	0.001%
541340	531341	103	5.9638E-08	5.96371E-08	0.002%
541340	531330	104	1.39038E-08	1.63765E-08	-15.099%
541340	531331	104	6.13367E-10	7.22425E-10	-15.096%
541340	*531320*	*105*	*1.11732E-09*		
541340	*531321*	*105*	*6.64154E-10*		
541340	521310	107	1.32497E-08	1.32494E-08	0.002%
541340	521311	107	1.04346E-08	1.04347E-08	-0.001%
541350	541360	102	421290.8	421303	-0.003%
541360	541350	16	0.000567618	0.000564826	0.494%
541360	541351	16	0.00045605	0.000453807	0.494%
541360	541370	102	0.025146069	0.0251467	-0.003%
541360	531360	103	1.56642E-08	1.56645E-08	-0.002%
541360	531361	103	3.67006E-09	3.66961E-09	0.012%
541360	531350	104	6.85008E-09	7.92787E-09	-13.595%

541360	*531340*	*105*	*9.13669E-10*		
541360	*531341*	*105*	*4.83351E-10*		
541360	521330	107	7.71675E-09	7.7165E-09	0.003%
541360	521331	107	6.0871E-09	6.08722E-09	-0.002%
551330	551320	16	0.000481763	0.000481759	0.001%
551330	551340	102	10.47011	10.4702	-0.001%
551330	551341	102	1.073607	1.07361	0.000%
551330	541330	103	3.72666E-05	3.72663E-05	0.001%
551330	541331	103	3.13825E-05	3.13822E-05	0.001%
551330	531300	107	5.7695E-07	5.76938E-07	0.002%
551330	531301	107	2.94015E-07	2.94018E-07	-0.001%
551340	551350	102	23.72176	23.7223	-0.002%
551340	551351	102	0.095306911	0.0953073	0.000%
551350	551360	102	2.569639	2.56966	-0.001%
551350	551361	102	0.041865673	0.0418645	0.003%
551360	551370	102	1.15117	1.15117	0.000%
551370	551380	102	0.026455818	0.0264564	-0.002%
551370	551381	102	0.002823973	0.00282369	0.010%
561340	561350	102	0.8270382	0.827052	-0.002%
561340	561351	102	0.063964494	0.0639537	0.017%
561350	561360	102	3.23965	3.23965	0.000%
561350	561361	102	0.006889957	0.00688617	0.055%
561360	561370	102	0.1115203	0.111525	-0.004%
561360	561371	102	0.002716322	0.00271233	0.147%
561370	561380	102	0.8181089	0.818128	-0.002%
561380	561370	16	0.000582231	0.000579594	0.455%
561380	561371	16	0.000337215	0.000335688	0.455%
561380	561390	102	0.055936385	0.0559377	-0.002%
561380	551380	103	1.78958E-06	1.78965E-06	-0.004%
561380	551381	103	9.40514E-07	9.40428E-07	0.009%
561380	541350	107	0.000301384	0.000301389	-0.002%
561380	541351	107	0.000140798	0.000140789	0.006%
561400	561410	102	0.5507518	0.550755	-0.001%
571390	571400	102	1.50666	1.50669	-0.002%
571400	571410	102	2.04314	2.04314	0.000%
581400	581410	102	0.093123361	0.0931254	-0.002%
581410	581420	102	4.511943	4.51205	-0.002%
581420	581430	102	0.1558865	0.15589	-0.002%
581430	581440	102	1.905115	1.90513	-0.001%

581440	581450	102	0.1952102	0.195214	-0.002%
591410	591400	16	0.000392666	0.000392411	0.065%
591410	591420	102	1.333434	1.33346	-0.002%
591410	591421	102	0.7118469	0.711858	-0.002%
591410	581410	103	4.09837E-06	4.09833E-06	0.001%
591410	581400	104	9.04626E-07	1.1127E-06	-18.700%
591410	*581390*	*105*	*5.68528E-08*		
591410	*581391*	*105*	*4.29542E-08*		
591410	571390	106	8.02516E-10	8.02509E-10	0.001%
591410	571380	107	4.49937E-05	4.49934E-05	0.001%
591420	591430	102	6.11101	6.11106	-0.001%
591430	591440	102	5.082638	5.08273	-0.002%
591430	591441	102	11.31281	11.313	-0.002%
601420	601430	102	2.736749	2.73682	-0.003%
601430	601420	16	0.005646839	0.00564581	0.018%
601430	601440	102	46.11628	46.1175	-0.003%
601430	591430	103	2.62802E-06	0.000002628	0.001%
601430	591420	104	9.0389E-08	1.41977E-07	-36.335%
601430	591421	104	6.056E-08	9.51198E-08	-36.333%
601430	*591410*	*105*	*2.19092E-07*		
601430	581410	106	8.76918E-10	8.7691E-10	0.001%
601430	*581400*	*107*	*7.76922E-05*		
601440	601450	102	0.6402493	0.640262	-0.002%
601450	601440	16	0.007388257	0.00737738	0.147%
601450	601460	102	11.03297	11.0331	-0.001%
601450	591450	103	8.83468E-07	8.8346E-07	0.001%
601450	591440	104	2.77892E-08	4.53196E-08	-38.682%
601450	591441	104	5.45273E-08	8.89246E-08	-38.681%
601450	*591430*	*105*	*1.34457E-07*		
601450	581430	106	2.36502E-10	2.36499E-10	0.001%
601450	581420	107	4.41261E-05	4.41258E-05	0.001%
601460	601450	16	0.00197865	0.00196337	0.778%
601460	601470	102	0.290017	0.290022	-0.002%
601460	591460	103	1.25845E-07	1.25844E-07	0.001%
601460	591450	104	4.63726E-08	5.93079E-08	-21.810%
601460	*591440*	*105*	*7.17638E-09*		
601460	*591441*	*105*	*1.44773E-08*		
601460	581440	106	1.01719E-10	1.01718E-10	0.001%
601460	581430	107	2.95896E-05	2.95895E-05	0.000%

601470	601480	102	20.22213	20.2222	0.000%
601480	601470	16	0.00217621	0.00214569	1.422%
601480	601490	102	0.8678111	0.867816	-0.001%
601480	591480	103	1.23123E-08	1.23122E-08	0.001%
601480	591481	103	3.25613E-08	3.2561E-08	0.001%
601480	591470	104	2.01449E-08	2.65882E-08	-24.234%
601480	*591460*	*105*	*1.37672E-08*		
601480	581460	106	1.22318E-11	1.22317E-11	0.001%
601480	581450	107	2.04262E-05	2.04261E-05	0.000%
601500	601490	16	0.00216254	0.00212389	1.820%
601500	601510	102	0.5926989	0.5927	0.000%
601500	591500	103	2.88979E-08	2.88977E-08	0.001%
601500	591490	104	1.14324E-08	1.52875E-08	-25.217%
601500	*591480*	*105*	*2.25381E-09*		
601500	*591481*	*105*	*3.99859E-09*		
601500	581470	107	1.24633E-05	1.24633E-05	0.000%
611470	611460	16	0.001857128	0.00184802	0.493%
611470	611480	102	35.42414	35.4243	0.000%
611470	611481	102	31.03626	31.0364	0.000%
611470	601470	103	1.66684E-06	1.66683E-06	0.001%
611470	601460	104	5.48601E-07	7.55788E-07	-27.413%
611470	*601450*	*105*	*2.1787E-07*		
611470	591450	106	2.86894E-10	2.86892E-10	0.001%
611470	591440	107	1.21645E-05	1.21645E-05	0.000%
611470	591441	107	2.46957E-05	2.46955E-05	0.001%
611480	611490	102	1375.379	1375.39	-0.001%
611490	611500	102	208.1731	208.178	-0.002%
611510	611520	102	61.57655	57.6344	6.840%
611510	611521	102	74.1701	69.759	6.323%
621440	621450	102	0.6852851	0.685282	0.000%
621470	621460	16	0.004371258	0.00436726	0.092%
621470	621480	102	26.07682	26.0769	0.000%
621470	611470	103	5.89657E-06	5.89652E-06	0.001%
621470	611460	104	1.82812E-07	4.07603E-07	-55.150%
621470	*611450*	*105*	*1.99794E-07*		
621470	601450	106	1.42826E-09	1.42824E-09	0.001%
621470	*601440*	*107*	*9.74417E-05*		
621480	621490	102	1.151275	1.15128	0.000%
621490	621480	16	0.002852423	0.00284888	0.124%

621490	621500	102	12794.54	12794.9	-0.003%
621490	611490	103	3.57425E-05	3.57422E-05	0.001%
621490	601460	107	3.57425E-05	3.57422E-05	0.001%
621500	621510	102	19.15918	19.1595	-0.002%
621510	621500	16	0.010487607	0.0104747	0.123%
621510	621520	102	1193.938	1193.97	-0.003%
621510	611510	103	9.25379E-07	9.25371E-07	0.001%
621510	611500	104	4.44093E-08	1.13253E-07	-60.788%
621510	*611490*	*105*	*8.57319E-08*		
621510	601490	106	1.03777E-10	1.03776E-10	0.001%
621510	601480	107	3.11355E-05	3.11353E-05	0.001%
621520	621510	16	0.001090355	0.00107875	1.076%
621520	621530	102	85.23193	85.2322	0.000%
621520	611520	103	4.7005E-08	4.50022E-08	4.450%
621520	611521	103	8.35645E-08	8.0004E-08	4.450%
621520	611510	104	3.32963E-08	4.87515E-08	-31.702%
621520	*611500*	*105*	*6.82341E-09*		
621520	601500	106	3.74233E-11	3.74229E-11	0.001%
621520	601490	107	2.461E-05	2.46099E-05	0.001%
621530	621540	102	98.48626	98.4871	-0.001%
621540	621550	102	1.630043	1.63006	-0.001%
631510	631500	16	0.000393053	0.000392487	0.144%
631510	631501	16	0.000317827	0.00031737	0.144%
631510	631520	102	735.5395	735.558	-0.003%
631510	631521	102	386.2953	386.305	-0.003%
631510	621510	103	1.86791E-05	1.86789E-05	0.001%
631510	621500	104	7.73428E-07	7.75397E-07	-0.254%
631510	*621490*	*105*	*2.14379E-07*		
631510	611490	106	8.82569E-09	8.82561E-09	0.001%
631510	611480	107	1.48916E-05	1.48914E-05	0.001%
631510	611481	107	1.87876E-05	1.87874E-05	0.001%
631520	631510	16	0.002602706	0.00259967	0.117%
631520	631530	102	266.9331	266.938	-0.002%
631520	621520	103	5.71319E-05	5.71314E-05	0.001%
631520	621510	104	3.97444E-07	3.9823E-07	-0.197%
631520	*621500*	*105*	*7.19309E-07*		
631520	611500	106	3.32482E-09	3.32479E-09	0.001%
631520	*611490*	*107*	*4.28442E-05*		
631530	631520	16	0.000712492	0.000658389	8.217%

631530	631521	16	0.000309101	0.00028563	8.217%
631530	631540	102	65.80882	65.8095	-0.001%
631530	631541	102	1.070909	1.0709	0.001%
631530	621530	103	2.73565E-06	2.73563E-06	0.001%
631530	621520	104	3.03024E-07	4.7093E-07	-35.654%
631530	*621510*	*105*	*7.01823E-08*		
631530	611510	106	1.55673E-09	1.55672E-09	0.001%
631530	611500	107	2.3218E-05	2.32178E-05	0.001%
631540	631530	16	0.001919396	0.00191829	0.058%
631540	631550	102	413.2274	413.238	-0.003%
631540	621540	103	9.69735E-05	9.69726E-05	0.001%
631540	621530	104	1.41407E-07	1.41483E-07	-0.054%
631540	*621520*	*105*	*2.42506E-07*		
631540	611520	106	4.03327E-10	3.87857E-10	3.989%
631540	611521	106	6.96052E-10	6.69337E-10	3.991%
631540	611510	107	6.20074E-05	6.20069E-05	0.001%
631550	631540	16	0.001099256	0.00109485	0.402%
631550	631541	16	0.000430069	0.000428343	0.403%
631550	631560	102	1461.524	1461.56	-0.002%
631550	621550	103	4.1908E-07	4.19076E-07	0.001%
631550	621540	104	1.13219E-07	2.32014E-07	-51.202%
631550	*621530*	*105*	*3.68195E-08*		
631550	611530	106	1.41643E-11	1.41642E-11	0.001%
631550	611520	107	6.09411E-06	5.83448E-06	4.450%
631550	611521	107	1.0834E-05	1.03724E-05	4.450%
631560	631570	102	97.16634	97.1679	-0.002%
631570	631580	102	53.47796	53.4784	-0.001%
641520	641510	16	0.000822334	0.000822326	0.001%
641520	641530	102	5.330803	10.6616	-50.000%
641520	*641531*	*102*	*5.330803*		
641520	631520	103	3.56043E-06	3.23739E-06	9.978%
641520	631521	103	8.34829E-07	7.59085E-07	9.978%
641520	621490	107	2.72714E-06	2.72712E-06	0.001%
641540	641530	16	0.000405612	0.000811217	-50.000%
641540	*641531*	*16*	*0.000405612*		
641540	641550	102	8.390377	16.781	-50.001%
641540	*641551*	*102*	*8.390377*		
641540	631540	103	3.31745E-06	3.31742E-06	0.001%
641540	631541	103	4.10021E-07	4.10018E-07	0.001%

641540	621510	107	7.82901E-07	7.82894E-07	0.001%
641550	641540	16	0.003933732	0.0039337	0.001%
641550	641560	102	4729.75	4729.88	-0.003%
641550	631550	103	1.21589E-05	1.21588E-05	0.001%
641550	621520	107	2.77354E-06	2.77351E-06	0.001%
641560	641550	16	0.000442806	0.000885604	-50.000%
641560	*641551*	*16*	*0.000442806*		
641560	641570	102	2.81298	2.81296	0.001%
641560	631560	103	5.53088E-06	5.53083E-06	0.001%
641560	621530	107	4.62839E-06	4.62836E-06	0.001%
641570	641560	16	0.004270957	0.00427092	0.001%
641570	641580	102	20347.72	20348.3	-0.003%
641570	631570	103	2.43997E-06	2.43995E-06	0.001%
641570	621540	107	1.20723E-06	1.20722E-06	0.001%
641580	641570	16	0.001197404	0.00119739	0.001%
641580	641590	102	1.627767	1.62776	0.000%
641580	631580	103	7.07997E-07	7.07991E-07	0.001%
641580	621550	107	8.30071E-07	8.30064E-07	0.001%
641600	641590	16	0.002054163	0.00205414	0.001%
641600	641610	102	0.3369885	0.336989	0.000%
641600	631600	103	5.19518E-07	5.19514E-07	0.001%
641600	*621570*	*107*	*5.04791E-07*		
651590	651600	102	14.46117	14.4612	0.000%
651600	651610	102	95.19114	95.1929	-0.002%
661600	661610	102	46.47924	46.4791	0.000%
661610	661620	102	103.2904	103.292	-0.002%
661620	661630	102	81.39048	81.3908	0.000%
661630	661640	102	50.3555	50.3557	0.000%
661640	661630	16	0.001392658	0.00137865	1.016%
661640	661650	102	120.5061	120.509	-0.002%
661640	661651	102	205.1848	205.191	-0.003%
661640	651640	103	6.167E-06	6.16694E-06	0.001%
661640	641610	107	5.07318E-05	5.07313E-05	0.001%
671650	671660	102	25.08161	25.0817	0.000%
671650	671661	102	1.348639	1.34864	0.000%
681660	681670	102	2.032212	2.0322	0.001%
681660	681671	102	6.090317	6.09043	-0.002%
681670	681680	102	272.9089	272.915	-0.002%
711750	711740	16	0.000852005	0.000845072	0.820%

711750	711741	16	0.000365454	0.000362477	0.821%
711750	711760	102	5.859048	5.85902	0.000%
711750	711761	102	11.72891	11.7289	0.000%
711750	701750	103	7.39556E-05	0.00014791	-50.000%
711750	*701751*	*103*	*7.39556E-05*		
711750	691720	107	6.93921E-08	6.93915E-08	0.001%
711760	711750	16	0.004190106	0.00417832	0.282%
711760	711770	102	1017.019	1017.05	-0.003%
711760	711771	102	1.018085	1.01811	-0.002%
711760	701760	103	0.000147911	0.000131279	12.669%
711760	691730	107	6.93921E-08	6.93915E-08	0.001%
731810	731800	16	0.000878398	0.000873715	0.536%
731810	731801	16	0.000548898	0.000545969	0.537%
731810	731820	102	19.28721	19.2679	0.100%
731810	731821	102	0.001621303	0.00161173	0.594%
731810	721810	103	2.31525E-05	2.31523E-05	0.001%
741820	741810	16	0.000856228	0.000854868	0.159%
741820	741830	102	13.11165	13.1116	0.000%
741820	741831	102	1.959982	1.95997	0.001%
741820	731820	103	1.50447E-07	1.41523E-07	6.306%
741820	731821	103	6.51004E-08	6.13002E-08	6.199%
741820	721790	107	5.95872E-08	5.95468E-08	0.068%
741820	721791	107	1.24991E-08	1.24922E-08	0.056%
741830	741820	16	0.003590711	0.00358743	0.091%
741830	741840	102	9.450412	9.45038	0.000%
741830	731830	103	2.42499E-07	2.42497E-07	0.001%
741830	721800	107	7.20555E-08	7.20559E-08	-0.001%
741830	721801	107	3.01735E-11	2.90786E-11	3.765%
741840	741830	16	0.001286517	0.00128193	0.358%
741840	741831	16	0.000197253	0.000196537	0.364%
741840	741850	102	0.690198	0.690209	-0.002%
741840	741851	102	0.001491248	0.00148283	0.568%
741840	721810	107	4.14522E-08	4.14518E-08	0.001%
741860	741850	16	0.00142725	0.00141913	0.572%
741860	741851	16	0.000448258	0.00044569	0.576%
741860	741870	102	16.41164	16.4117	0.000%
751850	751840	16	0.000731188	0.000729212	0.271%
751850	751841	16	0.000174938	0.000174465	0.271%
751850	751860	102	55.888	55.8882	0.000%

751850	751861	102	0.08322531	0.0831025	0.148%
751870	751860	16	0.001167901	0.00115736	0.911%
751870	751861	16	0.000205616	0.000203765	0.908%
751870	751880	102	15.77071	15.7709	-0.001%
751870	751881	102	0.4389825	0.438955	0.006%
791970	791960	16	0.000798855	0.000729248	9.545%
791970	791980	102	44.75188	44.752	0.000%
791970	791981	102	0.04480407	0.0448041	0.000%
791970	781970	103	7.45938E-08	7.44763E-08	0.158%
791970	781971	103	2.6944E-07	2.69555E-07	-0.043%
791970	771940	107	1.09748E-07	1.09746E-07	0.002%
791970	771941	107	4.03116E-09	4.03267E-09	-0.037%
902300	902290	16	0.003849529	0.00383664	0.336%
902300		18	0.052861158	0.0528607	0.001%
902300	902310	102	23.37879	23.3787	0.000%
902320	902310	16	0.003723951	0.00365404	1.913%
902320		18	0.020472635	0.0204724	0.001%
902320	902330	102	3.0609	3.06091	0.000%
912310	912300	16	0.002595159	0.00258861	0.253%
912310		18	0.3292686	0.329266	0.001%
912310	912320	102	68.88335	68.8848	-0.002%
912330	912320	16	0.001065633	0.00104495	1.979%
912330		18	0.1293547	0.129353	0.001%
912330	912340	102	12.16312	12.1631	0.000%
912330	912341	102	12.80866	12.8087	0.000%
922320	922310	16	0.001848025	0.00183516	0.701%
922320		18	19.32417	19.3243	-0.001%
922320	922330	102	14.52327	14.5235	-0.002%
922330	922320	16	0.001322257	0.00132225	0.001%
922330		18	88.54328	88.5452	-0.002%
922330	922340	102	9.928979	9.92915	-0.002%
922340	922330	16	0.000375659	0.000367624	2.186%
922340		18	0.4896477	0.489645	0.001%
922340	922350	102	26.75186	13.3775	99.977%
922350	922340	16	0.00189398	0.00189125	0.144%
922350		18	79.46591	79.4679	-0.003%
922350	922360	102	15.90742	15.9078	-0.002%
922360	922350	16	0.001960768	0.00152871	28.263%
922360		18	0.269853	0.269851	0.001%

922360	922370	102	7.776451	7.77641	0.001%
922380	922370	16	0.003685453	0.0036441	1.135%
922380		18	0.08440721	0.0844065	0.001%
922380	922390	102	0.9160061	0.916012	-0.001%
932370	932360	16	7.28583E-05	7.17876E-05	1.491%
932370	932361	16	0.000267709	0.000263775	1.491%
932370		18	0.4501097	0.450106	0.001%
932370	932380	102	46.04169	46.0425	-0.002%
942380	942370	16	0.000846545	0.000822329	2.945%
942380	942371	16	0.000211309	0.000205264	2.945%
942380		18	3.156241	3.15628	-0.001%
942380	942390	102	63.71869	63.7204	-0.003%
942390	942380	16	0.000789991	0.000788141	0.235%
942390		18	189.4151	189.42	-0.003%
942390	942400	102	104.1363	104.139	-0.003%
942400	942390	16	0.000348305	0.000342549	1.680%
942400		18	0.5124059	0.512401	0.001%
942400	942410	102	233.9092	233.909	0.000%
942410	942400	16	0.005218776	0.00521873	0.001%
942410		18	208.3514	208.357	-0.003%
942410	942420	102	76.66036	76.6624	-0.003%
942420	942410	16	0.001520943	0.00150034	1.373%
942420		18	0.3674031	0.3674	0.001%
942420	942430	102	32.24516	32.245	0.000%
952410	952400	16	0.000287677	0.000282332	1.893%
952410		18	1.33541	1.33543	-0.001%
952410	952420	102	152.6887	152.692	-0.002%
952410	952421	102	13.46145	13.4617	-0.002%
952430	952420	16	7.10456E-05	6.98506E-05	1.711%
952430	952421	16	0.000115802	0.000113854	1.711%
952430		18	0.3617149	0.361712	0.001%
952430	952440	102	3.346284	3.3463	0.000%
952430	952441	102	50.13153	50.1315	0.000%
962420	962410	16	4.20518E-05	4.19221E-05	0.309%
962420		18	0.6903394	0.690348	-0.001%
962420	962430	102	5.975659	5.97569	-0.001%
962430	962420	16	0.002771976	0.00276728	0.170%
962430		18	140.8016	140.804	-0.002%
962430	962440	102	13.62026	13.6204	-0.001%

962440	962430	16	0.000906952	0.00087902	3.178%
962440		18	0.8159229	0.815919	0.000%
962440	962450	102	12.37006	12.37	0.000%

Appendix D – EOC Microscopic Cross-Sections

Parent	Daughter	mt	NESTLE XS	COUPLE XS	% Difference
10010	10020	102	0.029967844	0.0300228	-0.183%
50100	50110	102	0.045071229	0.0451539	-0.183%
50100	40100	103	0.002702696	0.00270186	0.031%
50100	40090	104	0.000346498	0.000381843	-9.256%
50100	30070	107	346.429	347.064	-0.183%
50110	50100	16	7.29827E-07	7.2957E-07	0.035%
50110	50120	102	0.000463388	0.000464212	-0.178%
50110	40110	103	8.50289E-08	8.49989E-08	0.035%
50110	*40090*	*105*	*1.08319E-06*		
50110	30080	107	1.28691E-05	1.28646E-05	0.035%
70140	70130	16	4.52161E-07	4.52002E-07	0.035%
70140	70150	102	0.00677659	0.006789	-0.183%
70140	60140	103	0.1790203	0.179316	-0.165%
70140	60130	104	0.000107642	0.000115549	-6.843%
70140	*60120*	*105*	*0.0002682*		
70140	50110	107	0.027436607	0.0274269	0.035%
80160	80170	102	1.71639E-05	1.71953E-05	-0.183%
80160	70160	103	9.72E-06	9.71657E-06	0.035%
80160	70150	104	1.99241E-06	2.03911E-06	-2.290%
80160	60130	107	0.00366752	0.00366623	0.035%
320720	320730	102	0.061866105	0.0619414	-0.122%
320720	320731	102	0.0613534	0.0614281	-0.122%
320730	320740	102	3.210196	3.21203	-0.057%
320740	320750	102	0.036765009	0.0368024	-0.102%
320740	320751	102	0.018466124	0.0184849	-0.102%
320760	320770	102	0.022592787	0.0225961	-0.015%
320760	320771	102	0.033760782	0.0337657	-0.015%
330750	330760	102	2.125886	2.12599	-0.005%
340760	340770	102	5.844296	5.85467	-0.177%
340760	340771	102	2.043517	2.04714	-0.177%
340770	340780	102	4.36527	4.37202	-0.154%
340780	340790	102	0.020271523	0.0202737	-0.011%
340780	340791	102	0.1514003	0.151417	-0.011%
340800	340810	102	0.077819295	0.0778939	-0.096%
340800	340811	102	0.014067882	0.0140814	-0.096%
340820	340830	102	0.001154056	0.00115482	-0.066%

340820	340831	102	0.007574343	0.00757938	-0.066%
350790	350800	102	3.259799	3.26034	-0.017%
350790	350801	102	0.9805885	0.980751	-0.017%
350810	350820	102	0.2259443	0.225913	0.014%
350810	350821	102	2.252748	2.25244	0.014%
360800	360790	16	2.75443E-05	2.75346E-05	0.035%
360800	360791	16	2.84193E-05	2.84093E-05	0.035%
360800	360810	102	1.716869	1.71766	-0.046%
360800	360811	102	1.129763	1.13028	-0.046%
360800	350800	103	0.000224729	0.000224649	0.035%
360800	350801	103	0.00024481	0.000244724	0.035%
360800	350790	104	8.47667E-07	4.50887E-06	-81.200%
360800	350791	104	6.88213E-07	3.66071E-06	-81.200%
360800	*350780*	*105*	*2.86808E-08*		
360800	340780	106	2.47667E-08	2.47579E-08	0.035%
360800	*340770*	*107*	*9.9375E-06*		
360800	*340771*	*107*	*2.0176E-05*		
360820	360810	16	9.85035E-05	9.84688E-05	0.035%
360820	360811	16	2.39469E-05	2.39384E-05	0.035%
360820	360830	102	2.441984	2.4431	-0.046%
360820	360831	102	4.88996	4.8922	-0.046%
360820	350820	103	2.92338E-05	2.92235E-05	0.035%
360820	350821	103	2.6985E-05	2.69755E-05	0.035%
360820	350810	104	5.82292E-07	8.38125E-07	-30.524%
360820	*350800*	*105*	*8.15274E-09*		
360820	*350801*	*105*	*9.11954E-09*		
360820	340800	106	6.90151E-09	6.89908E-09	0.035%
360820	340790	107	1.45141E-06	1.4509E-06	0.035%
360820	340791	107	4.58412E-07	4.58251E-07	0.035%
360830	360820	16	0.00162659	0.00162602	0.035%
360830	360840	102	21.07614	21.1083	-0.152%
360830	350830	103	4.04956E-05	4.04813E-05	0.035%
360830	350820	104	3.26126E-07	3.42468E-07	-4.772%
360830	350821	104	2.96279E-07	3.11125E-07	-4.772%
360830	*350810*	*105*	*1.60151E-07*		
360830	340810	106	1.18672E-09	1.1863E-09	0.035%
360830	340811	106	2.3657E-09	2.36487E-09	0.035%
360830	*340800*	*107*	*2.82687E-06*		
360840	360830	16	0.000159641	0.000159584	0.035%

360840	360831	16	3.9492E-05	3.94781E-05	0.035%
360840	360850	102	0.01546225	0.0154598	0.016%
360840	360851	102	0.068860047	0.0688491	0.016%
360840	350840	103	7.1741E-07	7.17157E-07	0.035%
360840	350841	103	7.77195E-07	7.76921E-07	0.035%
360840	350830	104	2.0772E-07	2.21332E-07	-6.150%
360840	*350820*	*105*	*5.42041E-09*		
360840	*350821*	*105*	*6.96201E-09*		
360840	340820	106	4.13254E-11	4.13108E-11	0.035%
360840	340810	107	1.31404E-08	1.31358E-08	0.035%
360840	340811	107	1.49866E-07	1.49813E-07	0.035%
360850	360860	102	0.1838482	0.184111	-0.143%
360860	360850	16	0.000217087	0.000216815	0.125%
360860	360851	16	5.42279E-05	5.41598E-05	0.126%
360860	360870	102	0.009671882	0.0096806	-0.090%
360860	350860	103	4.14133E-08	4.13987E-08	0.035%
360860	350850	104	5.40628E-08	5.55015E-08	-2.592%
360860	350840	105	2.35363E-09	2.3528E-09	0.035%
360860	350841	105	2.5154E-09	2.51452E-09	0.035%
370850	370840	16	0.000144159	9.15106E-05	57.532%
370850	370860	102	0.227146	0.227149	-0.001%
370850	370861	102	0.031262048	0.0312625	-0.001%
370850	360850	103	1.94849E-05	1.94781E-05	0.035%
370850	360851	103	6.11744E-06	6.11528E-06	0.035%
370850	360840	104	1.60208E-05	3.14763E-05	-49.102%
370850	*360830*	*105*	*4.69483E-07*		
370850	*360831*	*105*	*1.45906E-07*		
370850	350830	106	1.81699E-09	1.81635E-09	0.035%
370850	350820	107	4.34302E-06	4.34149E-06	0.035%
370850	350821	107	4.37508E-06	4.37354E-06	0.035%
370860	370870	102	1.106403	1.10698	-0.052%
370870	370860	16	0.000138729	0.00013868	0.035%
370870	370861	16	7.23994E-05	7.23739E-05	0.035%
370870	370880	102	0.082674555	0.0826682	0.008%
370870	360870	103	1.51994E-05	1.51941E-05	0.035%
370870	360860	104	4.1316E-06	5.69213E-06	-27.416%
370870	*360850*	*105*	*1.90057E-07*		
370870	*360851*	*105*	*5.8542E-08*		
370870	350850	106	1.23713E-10	1.23669E-10	0.036%

370870	350840	107	2.43262E-06	2.43176E-06	0.035%
370870	350841	107	5.93501E-07	5.93292E-07	0.035%
380840	380850	102	0.1076994	0.107702	-0.002%
380840	380851	102	0.3174772	0.317485	-0.002%
380860	380870	102	0.080080412	0.0801643	-0.105%
380860	380871	102	0.3203703	0.320706	-0.105%
380870	380880	102	3.93386	3.93574	-0.048%
380880	380890	102	0.001267628	0.00126833	-0.055%
380890	380900	102	0.052564673	0.0526291	-0.122%
380900	380910	102	0.087656565	0.0878033	-0.167%
390890	390900	102	0.1305896	0.130796	-0.158%
390890	390901	102	0.000325461	0.000325974	-0.157%
390900	390910	102	0.3230956	0.3235	-0.125%
390900	390911	102	0.107874	0.108009	-0.125%
390910	390920	102	0.1650009	0.165219	-0.132%
400900	400890	16	3.01794E-05	3.01687E-05	0.035%
400900	400891	16	5.18536E-06	5.18353E-06	0.035%
400900	400910	102	0.01127156	0.0112698	0.016%
400900	390900	103	0.00010931	0.000109271	0.035%
400900	390901	103	1.03858E-05	1.03821E-05	0.036%
400900	380870	107	9.33499E-07	9.3317E-07	0.035%
400900	380871	107	4.31077E-07	4.30925E-07	0.035%
400910	400900	16	0.000944862	0.000944528	0.035%
400910	400901	16	0.000489688	0.000489516	0.035%
400910	400920	102	0.2425646	0.242713	-0.061%
400910	390910	103	4.42491E-05	4.42335E-05	0.035%
400910	390911	103	1.91216E-05	1.91148E-05	0.035%
400910	*380880*	*107*	*7.82988E-05*		
400920	400910	16	0.00049371	0.000493536	0.035%
400920	400930	102	0.043562796	0.0435907	-0.064%
400920	390920	103	1.25622E-05	1.25577E-05	0.035%
400920	*380890*	*107*	*6.53796E-06*		
400930	400940	102	1.025863	1.026	-0.013%
400940	400930	16	0.000736151	0.000735892	0.035%
400940	400950	102	0.018871443	0.0188745	-0.016%
400940	390940	103	3.3882E-06	3.38701E-06	0.035%
400940	380910	107	1.58022E-06	1.57966E-06	0.035%
400950	400960	102	0.2281908	0.228207	-0.007%
400960	400950	16	0.001068072	0.0010677	0.035%

400960	400970	102	0.1778334	0.177775	0.033%
400960	380930	107	1.1652E-06	1.16479E-06	0.035%
410930	410920	16	0.000285194	0.000284883	0.109%
410930	410921	16	0.000121654	0.000121521	0.109%
410930	410940	102	0.1245502	0.124577	-0.022%
410930	410941	102	0.2771465	0.277205	-0.021%
410930	400930	103	0.000173528	0.000173467	0.035%
410930	*390900*	*107*	*1.35158E-05*		
410930	*390901*	*107*	*5.46548E-06*		
410940	410950	102	3.805331	3.80658	-0.033%
410940	410951	102	0.1545241	0.154575	-0.033%
410950	410960	102	0.8336084	0.833611	0.000%
420920	420930	102	0.044700153	0.0446917	0.019%
420920	420931	102	9.7636E-05	9.76177E-05	0.019%
420920	410920	103	0.000154622	0.000154567	0.035%
420920	410921	103	0.000921728	0.000921403	0.035%
420920	*400890*	*107*	*1.5168E-05*		
420920	*400891*	*107*	*5.64601E-06*		
420940	420950	102	0.052829444	0.052814	0.029%
420950	420960	102	3.877498	3.87899	-0.038%
420960	420970	102	0.695258	0.695211	0.007%
420970	420980	102	0.7048289	0.70501	-0.026%
420980	420990	102	0.2327592	0.232702	0.025%
420990	421000	102	0.9765254	0.976517	0.001%
421000	421010	102	0.1485885	0.148575	0.009%
430990	430980	16	0.000523007	0.000522822	0.035%
430990	431000	102	6.814414	6.81595	-0.023%
440960	440970	102	0.4574571	0.457345	0.025%
440980	440990	102	0.9159256	0.917182	-0.137%
440990	441000	102	4.072896	4.07246	0.011%
441000	441010	102	0.7330108	0.733897	-0.121%
441010	441020	102	2.832414	2.83203	0.014%
441020	441030	102	0.2436999	0.243871	-0.070%
441030	441040	102	2.554577	2.5552	-0.024%
441040	441050	102	0.2640432	0.264036	0.003%
441050	441060	102	0.2848376	0.284777	0.021%
441060	441070	102	0.087740526	0.0877384	0.002%
451030	451020	16	0.000139668	0.000139619	0.035%
451030	451021	16	6.6814E-05	6.67904E-05	0.035%

451030	451040	102	28.37936	28.4006	-0.075%
451030	451041	102	2.335571	2.33731	-0.074%
451050	451060	102	1443.222	1445.66	-0.169%
451050	451061	102	153.2649	153.524	-0.169%
461020	461030	102	0.6932113	0.693909	-0.101%
461040	461050	102	0.8626544	0.862427	0.026%
461050	461060	102	3.780485	3.78192	-0.038%
461060	461070	102	0.3240355	0.323966	0.021%
461060	461071	102	0.01614612	0.0161427	0.021%
461070	461080	102	2.943955	2.94489	-0.032%
461080	461090	102	6.189281	6.18946	-0.003%
461080	461091	102	0.1397102	0.139714	-0.003%
461100	461110	102	0.2188644	0.218824	0.018%
461100	461111	102	0.038697455	0.0386903	0.018%
471070	471060	16	0.000155349	0.000155266	0.054%
471070	471061	16	9.47646E-05	9.47137E-05	0.054%
471070	471080	102	5.726216	5.73146	-0.091%
471070	471081	102	0.059267137	0.0593215	-0.092%
471070	461070	103	5.55573E-05	5.55378E-05	0.035%
471070	461071	103	6.4203E-06	6.41804E-06	0.035%
471070	461060	104	1.00535E-05	1.37096E-05	-26.668%
471070	*461050*	*105*	*8.54394E-07*		
471070	451050	106	1.27955E-09	1.2791E-09	0.035%
471070	451051	106	4.12409E-10	4.12263E-10	0.035%
471070	451040	107	2.90776E-06	2.90674E-06	0.035%
471070	451041	107	1.30791E-06	1.30745E-06	0.035%
471090	471080	16	0.000216496	0.000216309	0.086%
471090	471081	16	0.000131656	0.000131543	0.086%
471090	471100	102	32.08086	32.0872	-0.020%
471090	471101	102	1.547945	1.54825	-0.020%
471090	461090	103	9.33502E-06	9.33173E-06	0.035%
471090	461091	103	2.25843E-06	2.25763E-06	0.035%
471090	461080	104	5.34343E-06	5.85221E-06	-8.694%
471090	*461070*	*105*	*3.1832E-07*		
471090	*461071*	*105*	*2.40223E-07*		
471090	451070	106	4.99747E-10	4.99571E-10	0.035%
471090	451060	107	2.70677E-06	2.70581E-06	0.035%
471090	451061	107	2.26715E-06	2.26635E-06	0.035%
471110	471120	102	3.302125	3.30155	0.017%

481060	481070	102	0.4593925	0.459446	-0.012%
481080	481090	102	0.2634609	0.263585	-0.047%
481100	481110	102	2.09127	2.09271	-0.069%
481100	481111	102	0.011134622	0.0111423	-0.069%
481110	481120	102	3.505101	3.50866	-0.101%
481120	481130	102	0.4727346	0.472945	-0.044%
481120	481131	102	0.072009273	0.0720413	-0.044%
481130	481120	16	0.001193424	0.001193	0.036%
481130	481140	102	3988.294	3996.5	-0.205%
481130	471130	103	1.92368E-06	0.000001923	0.035%
481130	471131	103	2.03193E-06	2.03122E-06	0.035%
481130	461100	107	1.60264E-07	1.60207E-07	0.035%
481140	481150	102	0.5945149	0.594364	0.025%
481140	481151	102	0.079913661	0.0798934	0.025%
481160	481170	102	0.070692398	0.0706776	0.021%
481160	481171	102	0.03537719	0.0353698	0.021%
491130	491140	102	2.700132	2.70015	-0.001%
491130	491141	102	3.742713	3.74274	-0.001%
491150	491160	102	32.41428	18.5125	75.094%
491150	491161	102	53.66981	30.652	75.094%
501120	501130	102	0.7384626	0.738366	0.013%
501120	501131	102	0.2801018	0.280065	0.013%
501140	501150	102	0.2800231	0.280142	-0.042%
501150	501160	102	4.554486	4.56275	-0.181%
501160	501170	102	0.3635427	0.363437	0.029%
501160	501171	102	0.016059745	0.0160551	0.029%
501170	501180	102	0.7519151	0.752163	-0.033%
501180	501190	102	0.2292246	0.22916	0.028%
501180	501191	102	0.004875224	0.00487384	0.028%
501190	501200	102	0.3004836	0.300832	-0.116%
501200	501210	102	0.060438395	0.0604446	-0.010%
501200	501211	102	0.000788427	0.000788507	-0.010%
501220	501230	102	0.000610255	0.000610553	-0.049%
501220	501231	102	0.041850757	0.0418712	-0.049%
501230	501240	102	0.1079289	0.107897	0.030%
501240	501250	102	0.008264288	0.00826234	0.024%
501240	501251	102	0.2125747	0.212524	0.024%
501250	501260	102	0.5304122	0.530334	0.015%
501260	501270	102	0.009384673	0.00939928	-0.155%

501260	501271	102	0.02164113	0.0216748	-0.155%
511210	511220	102	4.374444	4.37408	0.008%
511210	511221	102	0.2945819	0.294557	0.008%
511230	511240	102	2.311382	2.29979	0.504%
511230	511241	102	0.024257211	0.0241355	0.504%
511240	511250	102	1.346772	1.34758	-0.060%
511250	511260	102	0.5489392	0.194703	181.937%
511250	511261	102	0.1229414	0.043606	181.937%
511260	511270	102	1.806943	1.80745	-0.028%
521200	521210	102	0.7534531	0.753586	-0.018%
521200	521211	102	0.099199295	0.0992169	-0.018%
521220	521230	102	1.500749	1.50058	0.011%
521220	521231	102	0.8266472	0.826553	0.011%
521230	521240	102	156.7702	156.802	-0.020%
521240	521250	102	0.8304397	0.831479	-0.125%
521240	521251	102	0.006428891	0.00643694	-0.125%
521250	521260	102	0.8871008	0.887094	0.001%
521260	521270	102	0.3565866	0.356639	-0.015%
521260	521271	102	0.05386259	0.0538704	-0.014%
521280	521290	102	0.1044148	0.104417	-0.002%
521280	521291	102	0.008509446	0.00850964	-0.002%
521300	521310	102	0.029958518	0.0299969	-0.128%
521300	521311	102	0.005056731	0.00506322	-0.128%
521320	521330	102	0.00042517	0.000425356	-0.044%
521320	521331	102	7.53968E-05	7.54297E-05	-0.044%
531270	531280	102	4.375877	4.37556	0.007%
531290	531300	102	1.345639	1.34737	-0.128%
531290	531301	102	1.912138	1.91459	-0.128%
531300	531310	102	6.359491	6.3608	-0.021%
531310	531320	102	0.3102924	0.310319	-0.009%
531310	531321	102	0.005098115	0.00509855	-0.009%
531350	531360	102	0.001065124	0.00213344	-50.075%
531350	*531361*	*102*	*0.001065124*		
541240	541230	16	0.000164623	0.000164517	0.065%
541240	541250	102	62.51224	62.5178	-0.009%
541240	541251	102	12.80542	12.8065	-0.008%
541240	531240	103	1.05179E-05	1.05141E-05	0.036%
541240	531230	104	3.63358E-07	3.26646E-06	-88.876%
541240	*531220*	*105*	*1.96298E-08*		

541240	521220	106	1.01707E-08	1.01671E-08	0.035%
541240	521210	107	4.85873E-06	4.85702E-06	0.035%
541240	521211	107	3.81759E-06	3.81625E-06	0.035%
541260	541250	16	0.000236382	0.000236164	0.092%
541260	541251	16	8.09193E-05	8.08445E-05	0.093%
541260	541270	102	1.260978	1.26091	0.005%
541260	541271	102	0.1897245	0.189714	0.006%
541260	531260	103	2.78863E-06	2.78765E-06	0.035%
541260	531250	104	1.58613E-07	2.90024E-07	-45.310%
541260	*531240*	*105*	*7.77783E-09*		
541260	521240	106	1.80569E-08	1.80505E-08	0.035%
541260	521230	107	1.45882E-06	1.4583E-06	0.036%
541260	521231	107	1.14624E-06	1.14583E-06	0.035%
541280	541270	16	0.000437614	0.000436813	0.183%
541280	541271	16	8.4237E-05	8.40828E-05	0.183%
541280	541290	102	0.6107427	0.611459	-0.117%
541280	541291	102	0.073747188	0.0738337	-0.117%
541280	531280	103	1.40944E-05	1.40895E-05	0.035%
541280	531270	104	8.92812E-08	3.74973E-07	-76.190%
541280	*531260*	*105*	*1.06781E-08*		
541280	521260	106	5.38945E-09	5.38755E-09	0.035%
541280	521250	107	3.61696E-07	3.61569E-07	0.035%
541280	521251	107	2.84213E-07	2.84113E-07	0.035%
541290	541280	16	0.003330269	0.00332811	0.065%
541290	541300	102	8.113688	8.1144	-0.009%
541290	531290	103	3.04047E-06	3.0394E-06	0.035%
541290	531280	104	7.38909E-08	1.7635E-07	-58.100%
541290	*531270*	*105*	*3.92931E-08*		
541290	521260	107	4.25731E-06	4.25581E-06	0.035%
541300	541290	16	0.000353233	0.000352171	0.301%
541300	541291	16	0.00025693	0.000256157	0.302%
541300	541310	102	0.5872959	0.588195	-0.153%
541300	541311	102	0.053603023	0.0536851	-0.153%
541300	531300	103	1.08641E-06	1.08603E-06	0.035%
541300	531301	103	1.66619E-06	1.6656E-06	0.035%
541300	531290	104	5.89379E-08	9.24444E-08	-36.245%
541300	*531280*	*105*	*5.80125E-09*		
541300	521270	107	1.15076E-07	1.15035E-07	0.035%
541300	521271	107	9.04409E-08	9.0409E-08	0.035%

541310	541300	16	0.005104597	0.00510094	0.072%
541310	541320	102	27.55169	27.5599	-0.030%
541310	531310	103	4.08316E-06	4.08172E-06	0.035%
541310	531300	104	1.5846E-08	1.97914E-08	-19.935%
541310	531301	104	2.89894E-08	3.62072E-08	-19.935%
541310	*531290*	*105*	*4.28443E-08*		
541310	521280	107	1.48201E-06	1.48149E-06	0.035%
541320	541310	16	0.000350388	0.000349059	0.381%
541320	541311	16	0.000500268	0.000498371	0.381%
541320	541330	102	0.088719316	0.088765	-0.051%
541320	541331	102	0.011333395	0.0113392	-0.051%
541320	531320	103	7.71354E-07	7.71082E-07	0.035%
541320	531321	103	1.47944E-07	1.47892E-07	0.035%
541320	531310	104	2.78384E-08	3.36857E-08	-17.358%
541320	*531300*	*105*	*5.54007E-10*		
541320	*531301*	*105*	*2.59423E-09*		
541320	521290	107	3.5193E-08	3.51806E-08	0.035%
541320	521291	107	2.76761E-08	2.76663E-08	0.035%
541330	541340	102	22.91019	22.9381	-0.122%
541330	541341	102	0.9659269	0.967103	-0.122%
541340	541330	16	0.000639679	0.000636997	0.421%
541340	541331	16	0.000496865	0.000494781	0.421%
541340	541350	102	0.048314445	0.0483458	-0.065%
541340	541351	102	0.000723725	0.000724194	-0.065%
541340	531340	103	5.90006E-07	5.89799E-07	0.035%
541340	531341	103	7.65427E-08	7.65158E-08	0.035%
541340	531330	104	1.89574E-08	2.23341E-08	-15.119%
541340	531331	104	8.39466E-10	9.88993E-10	-15.119%
541340	*531320*	*105*	*1.52955E-09*		
541340	*531321*	*105*	*9.09185E-10*		
541340	521310	107	1.81186E-08	1.81123E-08	0.035%
541340	521311	107	1.42605E-08	1.42555E-08	0.035%
541350	541360	102	254980.8	255506	-0.206%
541360	541350	16	0.000776612	0.000772525	0.529%
541360	541351	16	0.000624056	0.000620773	0.529%
541360	541370	102	0.016642421	0.0166681	-0.154%
541360	531360	103	2.07179E-08	2.07106E-08	0.035%
541360	531361	103	4.9305E-09	4.92876E-09	0.035%
541360	531350	104	9.37224E-09	1.0844E-08	-13.572%

541360	*531340*	*105*	*1.25076E-09*		
541360	*531341*	*105*	*6.61677E-10*		
541360	521330	107	1.05685E-08	1.05647E-08	0.036%
541360	521331	107	8.32815E-09	8.32521E-09	0.035%
551330	551320	16	0.000659504	0.000659272	0.035%
551330	551340	102	8.293414	8.29586	-0.029%
551330	551341	102	0.8504203	0.850671	-0.029%
551330	541330	103	4.63825E-05	4.63662E-05	0.035%
551330	541331	103	3.9059E-05	3.90453E-05	0.035%
551330	531300	107	7.56771E-07	7.56505E-07	0.035%
551330	531301	107	3.84506E-07	3.8437E-07	0.035%
551340	551350	102	16.43814	16.4599	-0.132%
551340	551351	102	0.066063181	0.0661505	-0.132%
551350	551360	102	2.234746	2.23565	-0.040%
551350	551361	102	0.036429189	0.0364439	-0.040%
551360	551370	102	1.013479	1.01338	0.010%
551370	551380	102	0.022100374	0.0221122	-0.053%
551370	551381	102	0.002363286	0.00236455	-0.053%
561340	561350	102	0.6276463	0.627821	-0.028%
561340	561351	102	0.048672322	0.0486858	-0.028%
561350	561360	102	3.24993	3.24993	0.000%
561350	561361	102	0.006975388	0.00697539	0.000%
561360	561370	102	0.102437	0.10248	-0.042%
561360	561371	102	0.002550672	0.00255174	-0.042%
561370	561380	102	0.5545812	0.555393	-0.146%
561380	561370	16	0.000797039	0.000793156	0.490%
561380	561371	16	0.000461627	0.000459378	0.490%
561380	561390	102	0.03738578	0.0374418	-0.150%
561380	551380	103	2.34397E-06	2.34314E-06	0.035%
561380	551381	103	1.24842E-06	1.24798E-06	0.035%
561380	541350	107	0.00036324	0.000363112	0.035%
561380	541351	107	0.000171217	0.000171157	0.035%
561400	561410	102	0.5089836	0.509119	-0.027%
571390	571400	102	1.034862	1.03627	-0.136%
571400	571410	102	2.107116	2.10691	0.010%
581400	581410	102	0.063511431	0.0636016	-0.142%
581410	581420	102	2.960243	2.96493	-0.158%
581420	581430	102	0.1064706	0.106621	-0.141%
581430	581440	102	1.721374	1.72195	-0.033%

581440	581450	102	0.1479977	0.148143	-0.098%
591410	591400	16	0.000537535	0.000537002	0.099%
591410	591420	102	0.960219	0.961361	-0.119%
591410	591421	102	0.5126635	0.513273	-0.119%
591410	581410	103	5.1275E-06	5.12585E-06	0.032%
591410	581400	104	1.23718E-06	1.50412E-06	-17.747%
591410	*581390*	*105*	*7.78294E-08*		
591410	*581391*	*105*	*5.88001E-08*		
591410	571390	106	1.09859E-09	1.09821E-09	0.035%
591410	571380	107	4.89932E-05	4.89833E-05	0.020%
591420	591430	102	5.361551	5.36361	-0.038%
591430	591440	102	3.660426	3.66458	-0.113%
591430	591441	102	8.147219	8.15647	-0.113%
601420	601430	102	1.714446	1.71753	-0.180%
601430	601420	16	0.007385881	0.00738194	0.053%
601430	601440	102	28.94723	28.9998	-0.181%
601430	591430	103	3.42066E-06	3.41945E-06	0.035%
601430	591420	104	1.23527E-07	1.93172E-07	-36.054%
601430	591421	104	8.31131E-08	1.29973E-07	-36.054%
601430	*591410*	*105*	*2.99924E-07*		
601430	581410	106	1.20045E-09	1.20002E-09	0.036%
601430	*581400*	*107*	*8.88355E-05*		
601440	601450	102	0.4539701	0.454521	-0.121%
601450	601440	16	0.009602142	0.00958396	0.190%
601450	601460	102	8.519893	8.52521	-0.062%
601450	591450	103	1.16754E-06	1.16713E-06	0.035%
601450	591440	104	3.80291E-08	6.19765E-08	-38.639%
601450	591441	104	7.4657E-08	1.21669E-07	-38.639%
601450	*591430*	*105*	*1.84063E-07*		
601450	581430	106	3.23756E-10	3.23642E-10	0.035%
601450	581420	107	4.9534E-05	4.95223E-05	0.024%
601460	601450	16	0.002684255	0.00266242	0.820%
601460	601470	102	0.2287924	0.228988	-0.085%
601460	591460	103	1.71551E-07	1.71491E-07	0.035%
601460	591450	104	6.34812E-08	8.1161E-08	-21.784%
601460	*591440*	*105*	*9.82141E-09*		
601460	*591441*	*105*	*1.98212E-08*		
601460	581440	106	1.39246E-10	1.39197E-10	0.036%
601460	581430	107	3.21827E-05	3.21763E-05	0.020%

601470	601480	102	18.40439	18.4076	-0.017%
601480	601470	16	0.002958953	0.00291617	1.467%
601480	601490	102	0.8038428	0.804053	-0.026%
601480	591480	103	1.68433E-08	1.68373E-08	0.035%
601480	591481	103	4.45679E-08	4.45522E-08	0.035%
601480	591470	104	2.75771E-08	3.63852E-08	-24.208%
601480	*591460*	*105*	*1.88465E-08*		
601480	581460	106	1.67446E-11	1.67387E-11	0.035%
601480	581450	107	2.20956E-05	2.20913E-05	0.019%
601500	601490	16	0.002944177	0.00289027	1.865%
601500	601510	102	0.5903103	0.590339	-0.005%
601500	591500	103	3.95498E-08	3.95358E-08	0.035%
601500	591490	104	1.56503E-08	2.09205E-08	-25.192%
601500	*591480*	*105*	*3.08532E-09*		
601500	*591481*	*105*	*5.47383E-09*		
601500	581470	107	1.3445E-05	1.34425E-05	0.019%
611470	611460	16	0.002521038	0.0025077	0.532%
611470	611480	102	26.18852	26.198	-0.036%
611470	611481	102	22.94418	22.9525	-0.036%
611470	601470	103	2.17876E-06	2.17799E-06	0.035%
611470	601460	104	7.50698E-07	1.01903E-06	-26.332%
611470	*601450*	*105*	*2.9825E-07*		
611470	591450	106	3.92741E-10	3.92602E-10	0.035%
611470	591440	107	1.33543E-05	1.33515E-05	0.021%
611470	591441	107	2.71116E-05	0.000027106	0.021%
611480	611490	102	1015.107	1015.7	-0.058%
611490	611500	102	132.6324	132.862	-0.173%
611510	611520	102	44.95403	42.3542	6.138%
611510	611521	102	53.24929	50.1697	6.138%
621440	621450	102	0.7297807	0.72966	0.017%
621470	621460	16	0.005780772	0.00577331	0.129%
621470	621480	102	24.65683	24.6604	-0.014%
621470	611470	103	7.20814E-06	7.20596E-06	0.030%
621470	611460	104	2.50258E-07	5.50912E-07	-54.574%
621470	*611450*	*105*	*2.73506E-07*		
621470	601450	106	1.9552E-09	1.95451E-09	0.035%
621470	*601440*	*107*	*0.000111147*		
621480	621490	102	1.103476	1.10362	-0.013%
621490	621480	16	0.003780492	0.00377434	0.163%

621490	621500	102	7738.909	7754.7	-0.204%
621490	611490	103	4.50059E-05	0.00004499	0.035%
621490	601460	107	4.50059E-05	0.00004499	0.035%
621500	621510	102	10.70981	10.7254	-0.145%
621510	621500	16	0.013461783	0.0134395	0.166%
621510	621520	102	741.8434	743.233	-0.187%
621510	611510	103	1.21173E-06	1.2113E-06	0.035%
621510	611500	104	6.07936E-08	1.54896E-07	-60.752%
621510	*611490*	*105*	*1.17362E-07*		
621510	601490	106	1.42064E-10	1.42014E-10	0.036%
621510	601480	107	3.46066E-05	3.45988E-05	0.022%
621520	621510	16	0.001492277	0.00147588	1.111%
621520	621530	102	76.09412	76.1087	-0.019%
621520	611520	103	6.37147E-08	6.0979E-08	4.486%
621520	611521	103	1.13271E-07	1.08407E-07	4.486%
621520	611510	104	4.55805E-08	6.67149E-08	-31.679%
621520	*611500*	*105*	*9.34082E-09*		
621520	601500	106	5.12301E-11	5.12121E-11	0.035%
621520	601490	107	2.65707E-05	2.65656E-05	0.019%
621530	621540	102	79.79788	79.8349	-0.046%
621540	621550	102	1.458131	1.4587	-0.039%
631510	631500	16	0.000537944	0.000536986	0.178%
631510	631501	16	0.000435042	0.000434267	0.178%
631510	631520	102	471.2856	472.18	-0.189%
631510	631521	102	247.5112	247.981	-0.189%
631510	621510	103	2.39566E-05	2.39482E-05	0.035%
631510	621500	104	1.04929E-06	1.05163E-06	-0.222%
631510	*621490*	*105*	*2.92837E-07*		
631510	611490	106	1.15147E-08	1.15106E-08	0.035%
631510	611480	107	1.80745E-05	1.80682E-05	0.035%
631510	611481	107	2.28034E-05	2.27953E-05	0.035%
631520	631510	16	0.003484611	0.00347926	0.154%
631520	631530	102	184.9835	185.19	-0.112%
631520	621520	103	7.08003E-05	0.000070776	0.034%
631520	621510	104	5.41974E-07	5.42863E-07	-0.164%
631520	*621500*	*105*	*9.79153E-07*		
631520	611500	106	4.41954E-09	4.41799E-09	0.035%
631520	*611490*	*107*	*5.20775E-05*		
631530	631520	16	0.000975358	0.000900984	8.255%

631530	631521	16	0.000423141	0.000390875	8.255%
631530	631540	102	53.86635	53.8963	-0.056%
631530	631541	102	0.8768358	0.877324	-0.056%
631530	621530	103	3.48724E-06	3.48601E-06	0.035%
631530	621520	104	4.11859E-07	6.33271E-07	-34.963%
631530	*621510*	*105*	*9.58095E-08*		
631530	611510	106	2.09475E-09	2.09401E-09	0.035%
631530	611500	107	2.76388E-05	2.76294E-05	0.034%
631540	631530	16	0.002593478	0.00259108	0.093%
631540	631550	102	252.5487	253	-0.178%
631540	621540	103	0.000121954	0.000121911	0.035%
631540	621530	104	1.93384E-07	1.93421E-07	-0.019%
631540	*621520*	*105*	*3.30916E-07*		
631540	611520	106	5.44776E-10	5.23623E-10	4.040%
631540	611521	106	9.43001E-10	9.06387E-10	4.040%
631540	611510	107	7.55088E-05	7.54822E-05	0.035%
631550	631540	16	0.001502881	0.00149633	0.438%
631550	631541	16	0.000587982	0.000585418	0.438%
631550	631560	102	1029.089	1030.75	-0.161%
631550	621550	103	5.53224E-07	5.53029E-07	0.035%
631550	621540	104	1.54989E-07	3.13149E-07	-50.506%
631550	*621530*	*105*	*5.04037E-08*		
631550	611530	106	1.93901E-11	1.93832E-11	0.035%
631550	611520	107	6.59069E-06	6.3087E-06	4.470%
631550	611521	107	1.17168E-05	1.12155E-05	4.469%
631560	631570	102	69.92597	69.9966	-0.101%
631570	631580	102	41.98035	42.003	-0.054%
641520	641510	16	0.001125724	0.00112533	0.035%
641520	641530	102	5.356253	10.7116	-49.996%
641520	*641531*	*102*	*5.356253*		
641520	631520	103	4.45359E-06	4.04803E-06	10.019%
641520	631521	103	1.04428E-06	9.49189E-07	10.019%
641520	621490	107	3.39361E-06	3.39241E-06	0.035%
641540	641530	16	0.000555258	0.00111013	-49.983%
641540	*641531*	*16*	*0.000555258*		
641540	641550	102	6.640119	13.2922	-50.045%
641540	*641551*	*102*	*6.640119*		
641540	631540	103	4.15107E-06	4.1496E-06	0.035%
641540	631541	103	5.13053E-07	5.12872E-07	0.035%

641540	621510	107	9.84098E-07	9.83751E-07	0.035%
641550	641540	16	0.005213897	0.00521206	0.035%
641550	641560	102	2902.37	2908.27	-0.203%
641550	631550	103	1.50423E-05	0.000015037	0.035%
641550	621520	107	3.45572E-06	3.4545E-06	0.035%
641560	641550	16	0.000606174	0.00121192	-49.982%
641560	*641551*	*16*	*0.000606174*		
641560	641570	102	2.839528	2.83887	0.023%
641560	631560	103	6.96012E-06	6.95766E-06	0.035%
641560	621530	107	5.68502E-06	5.68316E-06	0.033%
641570	641560	16	0.005649049	0.00564706	0.035%
641570	641580	102	12430.9	12456.5	-0.206%
641570	631570	103	3.04441E-06	3.04334E-06	0.035%
641570	621540	107	1.52093E-06	1.5204E-06	0.035%
641580	641570	16	0.001639088	0.00163851	0.035%
641580	641590	102	1.773745	1.77352	0.013%
641580	631580	103	9.03922E-07	9.03604E-07	0.035%
641580	621550	107	1.04913E-06	1.04876E-06	0.036%
641600	641590	16	0.002784492	0.00278351	0.035%
641600	641610	102	0.3285295	0.328564	-0.011%
641600	631600	103	6.71795E-07	6.71558E-07	0.035%
641600	*621570*	*107*	*6.46153E-07*		
651590	651600	102	14.2524	14.2525	-0.001%
651600	651610	102	65.71337	65.7937	-0.122%
661600	661610	102	47.14385	47.14	0.008%
661610	661620	102	73.07912	73.1635	-0.115%
661620	661630	102	59.16326	59.1828	-0.033%
661630	661640	102	45.47741	45.4888	-0.025%
661640	661630	16	0.001901843	0.00188202	1.053%
661640	661650	102	73.12783	73.2739	-0.199%
661640	661651	102	124.5136	124.762	-0.199%
661640	651640	103	7.5655E-06	7.56283E-06	0.035%
661640	641610	107	6.0946E-05	6.09245E-05	0.035%
671650	671660	102	22.91874	22.9232	-0.019%
671650	671661	102	1.232509	1.23275	-0.020%
681660	681670	102	1.630482	1.63164	-0.071%
681660	681671	102	4.884365	4.88782	-0.071%
681670	681680	102	192.4919	192.805	-0.162%
711750	711740	16	0.00116419	0.0011543	0.857%

711750	711741	16	0.000499864	0.000495619	0.857%
711750	711760	102	5.641776	5.6413	0.008%
711750	711761	102	11.29268	11.2917	0.009%
711750	701750	103	8.72452E-05	0.000174429	-49.982%
711750	*701751*	*103*	*8.72452E-05*		
711750	691720	107	9.49935E-08	9.496E-08	0.035%
711760	711750	16	0.005549005	0.00553097	0.326%
711760	711770	102	609.7243	610.935	-0.198%
711760	711771	102	0.6103866	0.611599	-0.198%
711760	701760	103	0.00017449	0.000154828	12.700%
711760	691730	107	9.49935E-08	9.496E-08	0.035%
731810	731800	16	0.001199556	0.00119273	0.572%
731810	731801	16	0.000749937	0.000745672	0.572%
731810	731820	102	19.07114	19.0496	0.113%
731810	731821	102	0.001864175	0.00186207	0.113%
731810	721810	103	2.7505E-05	2.74953E-05	0.035%
741820	741810	16	0.001172048	0.00116978	0.194%
741820	741830	102	12.6814	12.6805	0.007%
741820	741831	102	1.895831	1.8957	0.007%
741820	731820	103	2.11762E-07	1.9983E-07	5.971%
741820	731821	103	8.33092E-08	7.86152E-08	5.971%
741820	721790	107	8.17437E-08	8.16648E-08	0.097%
741820	721791	107	1.6938E-08	1.69217E-08	0.096%
741830	741820	16	0.004740659	0.00473455	0.129%
741830	741840	102	9.585461	9.58405	0.015%
741830	731830	103	3.31966E-07	3.31849E-07	0.035%
741830	721800	107	9.86063E-08	9.85716E-08	0.035%
741830	721801	107	7.451E-11	7.44838E-11	0.035%
741840	741830	16	0.001748553	0.00174166	0.396%
741840	741831	16	0.000269962	0.000268899	0.395%
741840	741850	102	0.6568779	0.656989	-0.017%
741840	741851	102	0.001521304	0.00152156	-0.017%
741840	721810	107	5.67454E-08	5.67254E-08	0.035%
741860	741850	16	0.001928172	0.00191639	0.615%
741860	741851	16	0.000608372	0.000604655	0.615%
741860	741870	102	15.25823	15.2603	-0.014%
751850	751840	16	0.000999779	0.000996731	0.306%
751850	751841	16	0.000239242	0.000238513	0.306%
751850	751860	102	48.68159	48.6877	-0.013%

751850	751861	102	0.073874146	0.0738834	-0.013%
751870	751860	16	0.001585509	0.00157054	0.953%
751870	751861	16	0.000278413	0.000275784	0.953%
751870	751880	102	12.86525	12.8738	-0.066%
751870	751881	102	0.3585259	0.358764	-0.066%
791970	791960	16	0.001093528	0.000997898	9.583%
791970	791980	102	36.29241	36.2997	-0.020%
791970	791981	102	0.036337126	0.0363444	-0.020%
791970	781970	103	1.10115E-07	1.10076E-07	0.036%
791970	781971	103	3.5285E-07	3.52725E-07	0.035%
791970	771940	107	1.46068E-07	1.46016E-07	0.035%
791970	771941	107	5.32344E-09	5.32156E-09	0.035%
902300	902290	16	0.005087272	0.00506789	0.382%
902300		18	0.062061138	0.0620393	0.035%
902300	902310	102	18.22257	18.2209	0.009%
902320	902310	16	0.004944139	0.00484677	2.009%
902320		18	0.024239741	0.0242312	0.035%
902320	902330	102	2.882125	2.88255	-0.015%
912310	912300	16	0.003432912	0.00342278	0.296%
912310		18	0.3822138	0.382084	0.034%
912310	912320	102	49.10868	49.1783	-0.142%
912330	912320	16	0.00142072	0.00139192	2.069%
912330		18	0.1525507	0.152497	0.035%
912330	912340	102	9.823501	9.82371	-0.002%
912330	912341	102	10.34351	10.3437	-0.002%
922320	922310	16	0.002486693	0.00246824	0.748%
922320		18	16.34706	16.3548	-0.047%
922320	922330	102	10.9821	10.9906	-0.077%
922330	922320	16	0.001711328	0.00171072	0.036%
922330		18	59.04896	59.1329	-0.142%
922330	922340	102	6.96851	6.97617	-0.110%
922340	922330	16	0.000506203	0.000495032	2.257%
922340		18	0.5350578	0.534955	0.019%
922340	922350	102	20.48722	10.2513	99.850%
922350	922340	16	0.00243748	0.00243291	0.188%
922350		18	50.67509	50.7629	-0.173%
922350	922360	102	10.99472	11.0095	-0.134%
922360	922350	16	0.002601837	0.00202615	28.413%
922360		18	0.2811828	0.281093	0.032%

922360	922370	102	6.095541	6.09442	0.018%
922380	922370	16	0.004846874	0.00478862	1.217%
922380		18	0.099601716	0.0995666	0.035%
922380	922390	102	0.8393278	0.839572	-0.029%
932370	932360	16	9.75064E-05	9.60078E-05	1.561%
932370	932361	16	0.000358283	0.000352776	1.561%
932370		18	0.5290936	0.528911	0.035%
932370	932380	102	34.66672	34.7061	-0.113%
942380	942370	16	0.001146837	0.0011133	3.012%
942380	942371	16	0.000286292	0.000277921	3.012%
942380		18	2.660327	2.66205	-0.065%
942380	942390	102	40.40479	40.4783	-0.182%
942390	942380	16	0.00102508	0.0010222	0.282%
942390		18	111.2493	111.461	-0.190%
942390	942400	102	60.35876	60.4724	-0.188%
942400	942390	16	0.000465583	0.000457545	1.757%
942400		18	0.5648819	0.564696	0.033%
942400	942410	102	75.74758	75.7907	-0.057%
942410	942400	16	0.006603442	0.00660111	0.035%
942410		18	126.6093	126.839	-0.181%
942410	942420	102	46.08841	46.1731	-0.183%
942420	942410	16	0.002018144	0.00198925	1.453%
942420		18	0.4349743	0.434821	0.035%
942420	942430	102	20.22614	20.223	0.016%
952410	952400	16	0.000384872	0.000377425	1.973%
952410		18	1.06885	1.06954	-0.065%
952410	952420	102	95.20266	95.354	-0.159%
952410	952421	102	8.395115	8.40846	-0.159%
952430	952420	16	9.45116E-05	0.000092844	1.796%
952430	952421	16	0.000154059	0.00015134	1.796%
952430		18	0.4278771	0.427726	0.035%
952430	952440	102	2.627115	2.62724	-0.005%
952430	952441	102	39.34027	39.3421	-0.005%
962420	962410	16	5.62553E-05	5.60585E-05	0.351%
962420		18	0.5854609	0.585823	-0.062%
962420	962430	102	5.480319	5.48163	-0.024%
962430	962420	16	0.003549141	0.0035415	0.216%
962430		18	100.424	100.53	-0.105%
962430	962440	102	10.3966	10.4048	-0.079%

962440	962430	16	0.001213867	0.00117523	3.288%
962440		18	0.9178864	0.917675	0.023%
962440	962450	102	13.79674	13.7939	0.021%

7 Vita

Jack Galloway was born in Morgan Hill, CA, to the parents of Gary and Jennie Galloway. He is the younger of two children, Julie Lorraine Galloway Lanford his sister. He attended elementary school and early junior high school in Morgan Hill, California before moving from the Bay Area to Wilmington, North Carolina where he finished junior high school and attended high school at Hoggard High School in Wilmington. After graduation Jack chose to attend North Carolina State University, choosing to major in nuclear engineering. After obtaining a Bachelor of Science degree from N.C. State University in May 2004 in nuclear engineering, and after a brief stint working at Global Nuclear Fuels (GNF) in Wilmington, North Carolina, he left to attend graduate school at the University of Cincinnati pursuant of a Masters of Science degree in nuclear engineering, which he received in December of 2006. Subsequently, following his advising professor Dr. G. Ivan Maldonado to the University of Tennessee, Knoxville, Jack continued his educational pursuits towards a Doctor of Philosophy in nuclear engineering with the research focusing on a joint project between the University of Tennessee, Knoxville and Oak Ridge National Laboratory. Jack graduated with his Ph. D. in the summer of 2010. He is beginning his professional life with a postdoctoral fellowship at Los Alamos National Laboratory in Los Alamos, New Mexico.